SYNTHESIS OF REACTIVE POLYMERS AND STUDY OF THEIR POLYMER-POLYMER REACTIONS

HIROO IWATA

TABLE OF CONTENTS

INTRODUCTION

A large number of experimental and theoretical studies have been carried out on polymer-polymer reactions such as termination of radical polymerization[1], gelation of polymers[2], and condensation polymerization[3]. Hydrolysis of polymeric substrates with enzymes and renaturation of DNA in the biochemistry also belong to the polymer-polymer reactions.

Recently a few investigators have been attracted to the polymer-polymer reactions from the somewhat different point of view, since studies of these reactions may provide valuable information with respect to the static and dynamic states of polymer chains in solution[4,5,6]. In addition, the polymer-polymer condensation reaction has proved to be effective for modifying the polymers[7], particularly preparing block and graft copolymers[8,9]. Nevertheless, not so many studies have been dedicated from these points of view. This may be due to lack of appropriate reaction systems for quantitative kinetic studies of polymer-polymer reactions as well as for synthesis and modification of polymers with these reactions.

Thus the present studies are aimed to develop the simple preparation methods of reactive polymers, to fallow kinetics of chemically controlled polymer-polymer reactions, and to apply these reactions to modification of polymers.

Chapters 1 to 3 describe the synthetic methods of polymers reactive for the coupling reactions and chapters 4 to 10 deal with studies of polymer-polymer reactions and some physico-chemical properties of resultant polymers.

In chapter 1 is discussed the radical chain transfer in catalytic radical polymerization which is one of the simplest methods to prepare polymers having reactive group on one polymer chain end. When the chain transfer reaction takes place to an added chain transfer agent, each transfer makes one molecule of the transfer agent to be incorporated in the polymer[10]. There have been published only few papers[11] which analyze the content of transfer agent fragments on the basis of kinetics of the transfer reaction, except for the telomerization. The content of reactive transfer agent fragments in one polymer molecule is an important factor in their polymer-polymer reactions. Therefore, in Chapter 1 the fraction of polymer molecules containing the transfer agent fragment is determined with a thin-layer chromatographic method which is becoming a powerful tool in polymer characterization[12] and compared with the values predicted from the kinetic treatment.

Chapter 2 discusses the synthesis of polymers carrying terminal functional groups by radiation polymerization. When the chain transfer constant of the agent having the desired functional group is small or vigorous degradative chain

transfer occurs, the catalytic radical polymerization is not useful to introduce the functional group to polymer. This is because the conversion of monomer may be low even after consumption of most of initiators if the vigorous degradative chain transfer occurs. On the contrary, active species can be generated in radiation-induced radical polymerizations in an amount sufficiently enough to increase the monomer conversion to a satisfactory extent. If the added compound has a low chain transfer constant but is highly sensitive to radiation, the initiation may start from the active species formed on the additive by irradiation, resulting in incorporation of the additive fragment in the end of polymer chain.

There are many other methods to prepare reactive polymers than those mentioned above. Chapter 3 describes another example of synthetic method which utilizes modification of a conventional polymer. When Poly(vinyl alcohol)(PVA) is oxidized by ceric ion, Ce(IV), in aqueous HNO_3 medium, the 1, 2-glycol units existing in PVA are selectively oxidized to yield aldehyde or carboxyl groups at the chain ends.

The remaining chapters deal with the polymer-polymer reactions and some properties of resultant polymers. In the reaction of polymeric reactants the rate of reaction has been assumed to be independent on the degree of polymerization[3]. However, it is likely that in the dilute solution of a good solvent the mutual interpenetration of randomly coiled chains

may take place not freely but restrictedly, as the large second virial coefficient suggests. Indeed, the rate constant of polymer-polymer reaction in dilute solution has been observed to depend more or less on the molecular weight of polymeric reactants, the polymer concentration, and the solvating power of the solvent. In addition, Vollmert and his coworkers have reported that even in concentrated polymer solutions of Θ solvent the yield of polymer-polymer reaction depends on the polymer concentration and does not become so high as expected from the reaction of low-molecular-weight analogues[13].

In Chapter 4 the rate constant of polymer-polymer reactions is interpreted in terms of statistical thermodynamics of dilute polymer solutions. Based on a simple model Morawetz and his cosorkers[4] have predicted that the rate constant of polymer-polymer reaction, where the rate-determining step is not a diffusion-controlled but a chemical process, is smaller than that of the low-molecular-weight model compound in the dilute solution from a good solvent medium. However, they did not attempt to relate the kinetic parameters of the polymer-polymer reactions to the physical parameters such as second virial coefficient of dilute polymer solution. In this chapter, the influence of long-range interaction of polymer chains on the reaction rate is theoretically evaluated using more appropriate models and the relation between the kinetic parameter and the second virial coefficient is

discussed.

Experimental results on polymer-polymer reactions are presented in Chapter 5. Inter- and intramolecular acetalizations of PVA carrying one or two terminal aldehyde groups are carried out in aqueous solution as well as in dimethylsulfoxide solution over a wide range of the polymer concentration. The rate constants observed for the intermolecular reaction are compared with those for the acetalization of PVA with low-molecular-weight aldehyde analogues and further with those predicted from dilute polymer solution theories treated in Chapter 4.

In Chapter 6 is studied gelation of PVA by acetalization through aldehyde groups attached to both chain ends. Gelation does not occur even when the reaction proceeds to extents significantly higher than the theoretical extent of reaction at gel point[14]. The reason for this discrepancy is discussed by taking into consideration the facts that polymer coils interpenetrate rather freely with each other and that the reactivity of both terminal aldehyde groups remains unvaried in a wide range of polymer concentration, regardless of the extent of reaction, as confirmed experimentally and theoretically in the two preceding chapters.

Chapters 7 and 8 describe synthetic methods of block and graft copolymers by polymer-polymer reactions. These types of copolymers have been generally synthesized either by

polymerization of monomer A initiated by active sites on polymer B which then functions as a macromolecular initiator, or by coupling reaction between reactive polymers A and B. It is known that radical polymerization is simple, but yiels copolymers with the chemical structure which is controll- - - ed with difficulty. On the other hand, the copolymer A-B with tailor-made structure can be produced by the coupling reaction of polymers prepared by anionic living polymerization[15], though the possible combination of prepolymers A and B giving copolymers is limited and a skillful technique is requied. In contrast, a condensation reaction between polymer A having functional groups and polymer B having the interacting groups does not require such special experimental procedures and the chemical structure is controlled with ease.

Chapter 7 describes a condensation coupling through acetalization between hydroxyl groups on PVA and aldehyde groups attached to a chain end of Poly(vinyl acetate)(PVAc) to produce PVA-PVAc graft copolymers. A method effective for determining the fraction of PVAc having a terminal aldehyde is also presented in this chapter.

Chapter 8 describes another synthetic method of graft and block copolymers by a polymer-polymer coupling reaction, which takes place between a terminal acyl chroride group of polystyrene and a terminal amino group or pendant amino groups of PVAc. This coupling reaction proceeds under

formation of amide linkages with much higher rates than that of acetalization coupling.

The surface chemical properties of polymeric materials are very important from both academic and technological viewpoints. The graft and block copolymers which are constructed of two chemically different and incompatible sequences, exhibit particularly interesting surface chemical properties. For instance, if added in a small proportion to a physical blend of the corresponding homopolymers, the graft or block copolymer molecule will be located at the interface between the two domains, resulting in emulsification[16,17].

Chapter 9 is thus concerned with monolayers of graft and block copolymers, some of which have been synthesized by the coupling reaction described in Chapter 8. Surface pressure-area isotherms for monolayers provide useful information on the surface chemical properties of block and graft copolymers.

In recent years, synthetic polymers have attracted much attention as promising material for medical and related application because of wide variation in their property; for instance, hydrophilic and hydrophobic, ionic and nonionic, water soluble and insoluble, rigid and flexible. In addition, they can be easily manufactured to a desired form. However when the polymeric materials are implanted in body for a long term, foreign body reactions occur. For example,

when a polymer composite comes in contact with blood, thrombus is formed sooner or later on the polymer surface. Application of the polymer-polymer reaction for preparing nonthrombogenic surface is described in Chapter 10. In this reaction, functional groups are introduced on polymer surfaces, followed by a coupling reaction with biopolymers.

mbus
tion
nic
c-
l by

REFERENCES

1. A. M. North, "Progress in High Polymers", Vol. 2, J. C. Robb and F. W. Peaker, Ed., Iliffe, London, 1968, p.95, and references therein.
2. I. Sakurada and Y. Ikada, Bull. Inst. Chem. Res., Kyoto Univ., 40, 25 (1962); 41, 103 (1963); 42, 22 (1964).
3. P. J. Flory, "Principles of Polymer Chemistry", Cornell University Press, Ithaca, N.Y., 1953.
4. H. Morawetz, J.-R. Cho, and P. J. Gans, Macromolecules, 6, 624 (1973).
5. B. Vollmert and H. Stutz, "Colloidal and Morphological Behavior of Block and Graft Copolymers", G. E. Molau, Ed., Plenum Press, 1971.
6. K. Horie and I. Mita, Kobunshi, 27, 637 (1978), and references therein.
7. H. F. Hixson, Jr. and E. P. Goldberg, Ed., "Polymer Grafts in Biochemistry", Marcel Dekker, Inc., New York and Basel, 1976.
8. H. W. Melville, F. W. Peaker, and R. L. Vale, Makromol. Chem., 28, 140 (1958).
9. A. G. DeBoos and G. Allen, Polymer, 16, 38 (1975).
10. J. W. Breitenback and A. Maschin, Z. Physik. Chem., Leipzig, A187, 175 (1940).

11. T. Maekawa, M. Matsuo, H. Yoshida, K. Hayashi and S. Okamura, Polymer, 11, 342 (1970); 11, 351 (1970).
12. H. Inagaki, Adv. Polym. Sci., 24, 189 (1977).
13. B. Vollmert and H. Stutz, Angew. Makromol. Chem., 3, 182 (1968); 20, 71 (1971). B. Vollmert, H. Stutz, and J. Stemper, Angew. Makromol. Chem., 25, 187 (1972).
14. O. Saito, Polymer Engineering and Science, 19, 234 (1979).
15. M. Szwarc, "Carbanions Living Polymers, and Electron-Transfer Processes", Interscience Publ., New York, 1968.
16. G. Molau Ed., Colloidal and Morphological Behavior of Block and Graft Copolymers, Plenum Press, New York, 1971.
17. F. Horii, Ph. D. Thesis, Kyoto Univ., Kyoto, Japan, 1974.

Chapter 1

Chain Transfer in Radical Polymerizations and Endgroup Content of Resultant Polymers

INTRODUCTION

When transfer reaction takes place to an added chain transfer agent, each transfer causes one molecule of the transfer agent to become incorporated in polymer.[1] Although factors influencing the chain transfer and effects of the chain transfer agent on reduction in polymer chain length have been extensively investigated, there have been published few papers[2,3] which analyze the content of transfer agent fragments based on kinetics of the transfer reaction, except for the telomerization.

The objects of the present study on radical polymerizations in the presence of chain transfer agents are determination of the endgroups of the resultant polymer by thin layer chromatography, comparison of the endgroup content with the theoretical values from the kinetic treatment, and preparation of polymers bearing terminal functional groups to be used for polymer-polymer coupling reactions.

This chapter describes a radical polymerization of styrene in the presence of trichloroacetyl chloride (TCAC) and that of methyl methacrylate (MMA) in the presence of 2-aminoethanethiol hydrochloride (AET·HCl). Both are reported to be reactive chain transfer agents.[4,5] It is expected that polystyrene (PS) with an acyl chloride endgroup and PMMA with an amino endgroup will be produced as a result of these chain transfer polymerizations.

EXPERIMENT

Reagents. Styrene and MMA monomers were purified by the conventional method. 2-Aminoethanethiol (AET) was synthesized in our laboratory from ethyleneimine and hydrogen sulfide[6] and purified by sublimation immediately before use. AET·HCl was obtained by addition of hydrochloric acid to AET in an aqueous solution. TCAC and other reagents were all commercial materials, which were purified by distillation before use.

Polymerization. Styrene-TCAC mixtures containing a given quantity of 2,2'-azobisisobutyronitrile (AIBN) as initiator were degassed by freezing-thawing cycle and sealed under a pressure of 10^{-5} mmHg. In the case of MMA-AET·HCl, methanol was added to the monomer mixtures by 50 vol% to dissolve the proper amount of AET·HCl in MMA and then degassed without freezing. In both cases polymerization was carried out at 60 ^{o}C until a maximum of 10 % conversion had taken place. After the polymerization, the contents were poured into plenty of methanol to precipitate the polymers. By the contact with methanol the acyl chloride end-groups attached to PS molecules were directly converted to methyl ester. On the other hand, a portion of styrene polymerization mixtures was evaporated to dryness and the polymer was dissolved in dioxane followed by addition of water by 50 % to convert the acyl chloride into carboxyl groups. The styrene and MMA polymers were purified by repeated precipitation from their solutions and dried at reduced pressure to a constant weight. The rate of polymerization was deduced from the weight of the

polymer formed.

The number-average degrees of polymerization $\overline{P}_n$ of the polymers were determined from intrinsic viscosities at 25 °C using the following equations derived with osmometry.

$$[\eta] = 33.5 \times 10^{-4}\overline{P}^{0.73} \quad \text{(PS, in benzene)}^{7} \qquad (1)$$

$$[\eta] = 17.3 \times 10^{-4}\overline{P}^{0.71} \quad \text{(PMMA, in acetone)}^{8} \qquad (2)$$

Thin Layer Chromatography. Silica gels precoated to a thickness of 0.25 mm on glass plates were used for the thin layer chromatography. The coated gel was washed by developing with methanol followed by activating at 110 °C for 1 hr just prior to use. 10 μl of 0.1 % chloroform solutions of polymer was deposited on the plate and then the development was done at room temperature with benzene for PS and with ethyl acetate for PMMA. For comparison, the thin layer chromatography was also carried out for the polymers after converting their polar end-groups -COOH and $-NH_2 \cdot HCl$ to $-COOCH_3$ and $-NHCOCH_3$, respectively. The weight fraction of polymers carrying the polar endgroups was determined by densitometry of the chromatograms after staining the developed (upper spot, $R_f = 1$) and undeveloped (lower spot, $R_f = 0$) portions with 10 % perchloric acid aqueous solution for PS and 10 % methanol solution of I_2 for PMMA. Transmitted white light was used for the densitometry of PS and reflected light with a scanning wave length of 420 nm for that of PMMA.

RESULTS and DISCUSSION

Equations Necessary to Evaluate the Number of Transfer Agent

Fragments per Polymer Molecule. The polymerization of vinyl monomers in the presence of chain transfer agent SX would give rise to formation of three kinds of polymer which are different in the number of the transfer agent fragment X attached to the chain ends. In the present chain transfer polymerizations X must have a reactive functional group; acyl chloride or amino group. The polymer with terminal X groups at both chain ends will be designated as XPX, the polymer with a terminal X at one chain end as PX, and the polymer without terminal X as P. The weight fractions of each polymer type, w_{XPX}, w_{PX}, and w_P can be calculated, provided that the polymerization involves the following elementary reactions which are conventionally accepted.

Initiation	$I \longrightarrow 2I\cdot$	R_i	(i)
	$I\cdot + M \longrightarrow M\cdot$		(ii)
Propagation	$M\cdot + M \longrightarrow M\cdot$	$k_p[M\cdot][M]$	(iii)
	$XM\cdot + M \longrightarrow XM\cdot$	$k_p[XM\cdot][M]$	(iv)
Chain transfer	$M\cdot + SX \longrightarrow P + X\cdot$	$k_{tr}[M\cdot][SX]$	(v)
	$XM\cdot + SX \longrightarrow PX + X\cdot$	$k_{tr}[XM\cdot][SX]$	(vi)
Re-initiation	$X\cdot + M \longrightarrow XM\cdot$	$k_1[X\cdot][M]$	(vii)
Termination	$M\cdot + M\cdot \longrightarrow P + P$	$k_{t,d}[M\cdot]^2$	(viii)
	$M\cdot + M\cdot \longrightarrow P$	$k_{t,c}[M\cdot]^2$	(ix)
	$XM\cdot + M\cdot \longrightarrow PX + P$	$k_{t,d}[XM\cdot][M\cdot]$	(x)
	$XM\cdot + M\cdot \longrightarrow PX$	$k_{t,c}[XM\cdot][M\cdot]$	(xi)
	$XM\cdot + XM\cdot \longrightarrow PX + PX$	$k_{t,d}[XM\cdot]^2$	(xii)
	$XM\cdot + XM\cdot \longrightarrow XPX$	$k_{t,c}[XM\cdot]^2$	(xiii)
	$M\cdot + X\cdot \longrightarrow PX$	$k_2[M\cdot][X\cdot]$	(xiv)

$$XM\cdot + X\cdot \longrightarrow XPX \qquad k_2[XM\cdot][X\cdot] \qquad (xv)$$

$$X\cdot + X\cdot \longrightarrow X\text{-}X \qquad k_3[X\cdot]^2 \qquad (xvi)$$

In this scheme the symbols have the conventional meaning and transfer reactions to monomer, polymer, initiator, and methanol were all neglected because of their low possibility compared with that to the added transfer agents. The last three reactions xiv - xvi are involved to account for the reduction in overall rate of polymerization.

As will be discussed later, the present thin layer chromatography cannot distinguish between PX and XPX, but between P and (PX + XPX) and hence enables to determine the w_P value. Considering that the polymer P is produced through the reactions v, viii, ix, or x, we can derive the expression for the w_P as a function of the concentrations of the monomer [M] and the chain transfer agent [SX]:

$$w_P = \frac{(R_i k_t)^{1/2}\left[\left\{\frac{k_1 k_t}{k_2}[M] + k_{tr}[SX] + (R_i k_t)^{1/2}\right\}\left\{k_{tr}[SX](k_{tr}[SX] + (R_i k_t)^{1/2}) + R_i k_t\right\} + \frac{\lambda k_1 k_t k_{tr}}{k_2}[SX][M](R_i k_t)^{1/2}\right]}{\left\{k_{tr}[SX] + (R_i k_t)^{1/2}\right\}^3\left\{\frac{k_1 k_t}{k_2}[M] + (R_i k_t)^{1/2}\right\}} \qquad (3)$$

where k_t and λ are $(k_{t,d} + k_{t,c})$ and $k_{t,d}/k_t$, respectively. The derivation of eq 3 is given in Appendix A, together with that for w_{PX} and w_{XPX}. In the derivation, k_2 is assumed to be equal to $(k_3 k_t)^{1/2}$ as Allen and coworkers postulated.[9]

Among the rate constants in eq 3, k_p, $k_{t,c}$, and $k_{t,d}$ have been reported, and R_i is also available if such an initiator is

used as the decomposition rate constant k_d and the initiator efficiency f are known. Other rate constants, k_{tr}, k_1, and k_2 can be evaluated from R_p and $\overline{P}_n$ which are represented by

$$\frac{1}{R_p} = \frac{k_{tr}}{k_p(R_i/k_t)^{1/2}\left\{(R_i k_t)^{1/2} + \frac{k_1 k_t}{k_2}[M]\right\}} \cdot \frac{[X]}{[M]} + \frac{1}{k_p[M](R_i/k_t)^{1/2}} \quad (4)$$

$$\frac{1}{\overline{P}_n} = \frac{1}{\overline{P}_{n,o}} + \frac{k_{tr}}{k_p} \cdot \frac{[SX]}{[M]}\left[1 + \frac{(1-\lambda)(R_i k_t)^{1/2}}{2\left\{\frac{k_1 k_t}{k_2}[M] + k_{tr}[SX] + (R_i k_t)^{1/2}\right\}}\right] \quad (5)$$

$$\frac{1}{\overline{P}_{n,o}} = \frac{(1+\lambda)(R_i k_t)^{1/2}}{2k_p[M]} \qquad \left(\text{for } \frac{[SX]}{[M]} = 0\right) \quad (6)$$

These equations are derived from the above polymerization scheme (see Appendix A). Strictly, one cannot know separatedly the values of k_1 and k_2, but merely the ratio k_1/k_2. It is of interest to note that the well-known Mayo's linear relation between $1/\overline{P}_n$ and $[SX]/[M]$ is realized only when λ is unity or k_2 is zero.

The eq 3 - 6 are valid for the generalized polymerization. If the transfer reaction is not of degradative type, that is, the reactions xiv - xvi can be neglected, the kinetic expressions become simple. In addition, the weight fractions w_p of polymers carrying no terminal functional groups X can be expressed as a function of $\overline{P}_n$ or $\overline{P}_{n,o}/\overline{P}_n$ (= r) as follows:

$$w_p = \frac{2[\{(1+\lambda)(r-1)+2\}^3 + 2(\lambda^2-1)(r-1)]}{(1+\lambda)(r-1)+2^3} \quad (7)$$

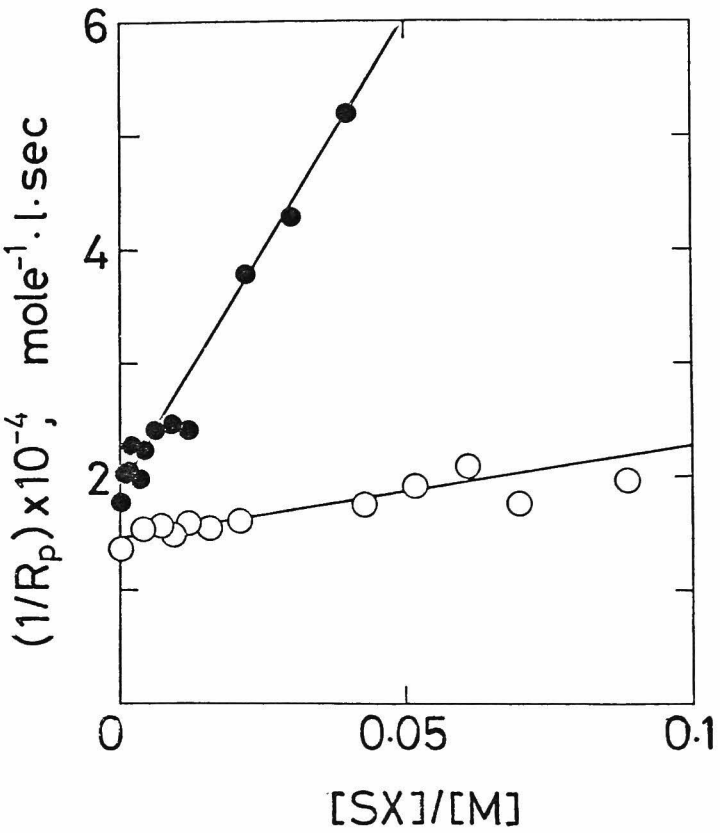

Fig. 1. Overall rates of polymerization R_p in styrene-trichloroacetyl chloride and MMA-2-aminoethanethiol hydrochloride polymerizations at 60 °C: (o) styrene ([AIBN] = 8.72 x 10^{-3} mole·l^{-1}); (•) MMA ([AIBN] = 1.42 x 10^{-3} mole·l^{-1}, [methanol] = 50 vol%); (——) calculated according to eq 4 with kinetic data.

The derivation is given in Appendix B. Therefore, one can calculate w_P only from the data on $\overline{P}_n$, if the transfer reaction is assumed to be not of degradative type.

Polymerization. The reciprocals of the overall rate of polymerization and $\overline{P}_n$ are plotted against [SX]/[M] in Figures 1 and 2, respectively.

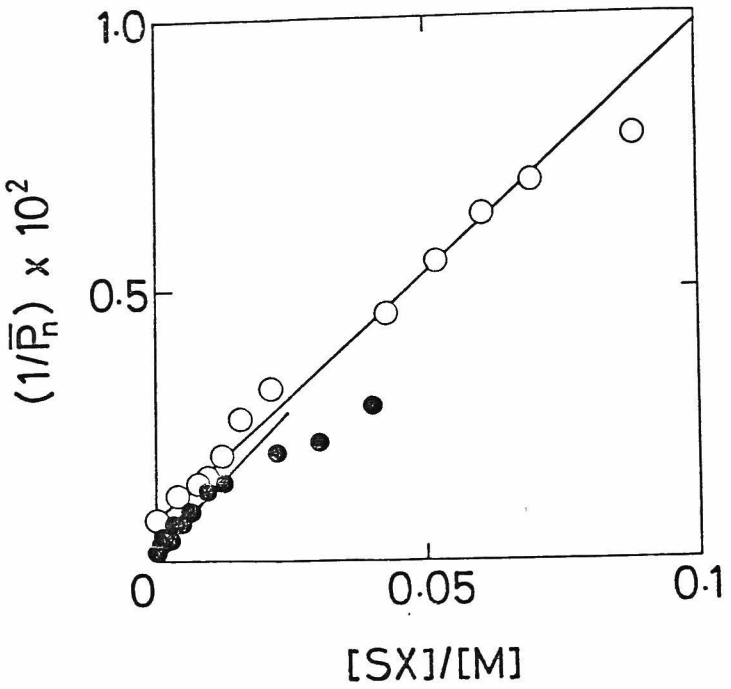

Fig. 2. Number-average degrees of polymerization $\overline{P}_n$ in styrene-trichloroacetyl chloride and MMA-2-aminoethanethiol hydrochloride polymerizations at 60 °C: (o) styrene ([AIBN] = 8.72×10^{-3} mole·l^{-1}); (●) MMA ([AIBN] = 1.42×10^{-3} mole·l^{-1}, [methanol] = 50 vol%); (——) calculated according to eq 5 with kinetic data.

The initial concentrations of AIBN are 8.72×10^{-3} mole·l^{-1} for styrene and 1.42×10^{-3} mole·l^{-1} for MMA. As can be seen, the linearity approximately holds between $1/R_p$ and [SX]/[M] as well as between $1/\overline{P}_n$ and [SX]/[M]. The evaluation of k_{tr} and k_1/k_2 from these results requires the knowledge of k_p, k_t, and λ. As it is known that the styrene polymerization terminates almost exclusively by coupling, while disproportionation is predominant in MMA,[10] we assume for simplicity λ to be zero for styrene and unity for MMA. This assumption can be applied without serious

error, since the transfer reaction predominates in the present polymerizations. As for R_i, k_p, and k_t, we adopt the data of Matheson and coworkers for styrene[11] ($R_i = 1.47 \times 10^{-7}$ mole·l^{-1}·sec^{-1}, $k_p = 176$ l·mole^{-1}·sec^{-1}, and $k_t = 7.2 \times 10^7$ l·mole^{-1}·sec^{-1}) and the data of O'Brien and Gornick for MMA[12] ($R_i = 1.38 \times 10^{-8}$ mole·l^{-1}·sec^{-1}, $k_p = 573$ l·mole^{-1}·sec^{-1}, and $k_t = 2.78 \times 10^7$ l·mole^{-1}·sec^{-1}). By fitting these rate constants, and eq 4 and 5 to Figures 1 and 2, values of k_{tr} and k_1/k_2 were finally obtained. Full lines given in Figures 1 and 2 were drawn on the basis of eq 4 and 5 with a set of the following kinetic constants.

Styrene-TCAC polymerization:

$$k_{tr} = 15.4 \text{ l·mole}^{-1}\text{·sec}^{-1}, \quad k_1/k_2 = 4.5 \times 10^{-8}$$

MMA-AET·HCl polymerization:

$$k_{tr} = 60.2 \text{ l·mole}^{-1}\text{·sec}^{-1}, \quad k_1/k_2 = 3.9 \times 10^{-8}$$

The chain transfer constants C_s are then calculated to be 0.093 for styrene-TCAC and 0.11 for MMA-AET·HCl. The increase in $1/R_p$ with [SX]/[M] shown in Figure 1 indicates that styrene-TCAC and, particularly, MMA-AET·HCl accompany a degradative chain transfer reaction in the polymerizations. The observed plots of $1/\bar{P}_n$ against [SX]/[M] are practically also in agreement with the theoretical curves which would be obtained in the case of non-degradative transfer reactions (The theoretical curves are not given in Figure 2 because of close overlapping with the full lines).

It is noteworthy that no appreciable chain transfer reaction took place when free AET ($HSC_2H_4NH_2$) was used as chain transfer agent instead of hydrochloride salt of AET.

Thin Layer Chromatography. Typical thin layer chromatograms of PS specimen are given in Figure 3.
The symbols H and Me denote that the PS carries carboxyl and methyl ester endgroups, respectively. $\overline{P}_n$ is 100 for Sample 22 and 840 for Sample 34. Sample 35 was obtained by polymerization at [SX]/[M] = 0 and has $\overline{P}_n$ of 1340. The chromatograms for 22-Me and 34-Me demonstrate that their rate of flow is the same as that of the developer, similar to the standard PS from Pressure Chemical Co. (1-S) which bears no functional endgroup. In the case of 22-H and 34-H, however, a portion of polymers remains

1-S 22-H 22-Me 34-H 34-Me 35-H 35-Me

Fig. 3. Examples of thin layer chromatograms of PS specimen (gel, silica; developer, benzene; indicator, perchloric acid). See the text for the code of specimen.

undeveloped on the deposited point, so that these polymers are identified to be a mixture of polymers with and without a functional group, the former being strongly adsorbed on the silica gel owing to the polar carboxyl group attached to the polymer. It is reasonable that no difference in the chromatogram is detected between 35-H and 35-Me, because these polymers, obtained by a polymerization without chain transfer agent, have no functional endgroups at all. The above results afford an evidence that at least a fraction of the intact PS molecules formed by the radical polymerization in the presence of TCAC carry(an) acyl chloride group at the chain end. It follows that the fraction of PS developed in the chromatogram should be exactly equal to the weight fraction w_P of PS carrying no functional endgroups. To examine the accuracy of the densitometry, mixtures from 22-H and the standard PS (1-S) were applied to thin layer chromatography. The result is given in Figure 4, where the ratio of amount of the polymer developed (upper spot in the chromatogram) to the sum of amount of the polymer undeveloped (lower spot in the chromatogram) and developed is plotted against the weight fraction of 22-H in the polymer mixture.
The good linearity found in Figure 4 indicates the densitometry to be feasible for the evaluation of the w_P.

Figure 5 shows the thin layer chromatograms of all the PMMA specimen.
The amount of each polymer deposited is 10 μg. The fraction of

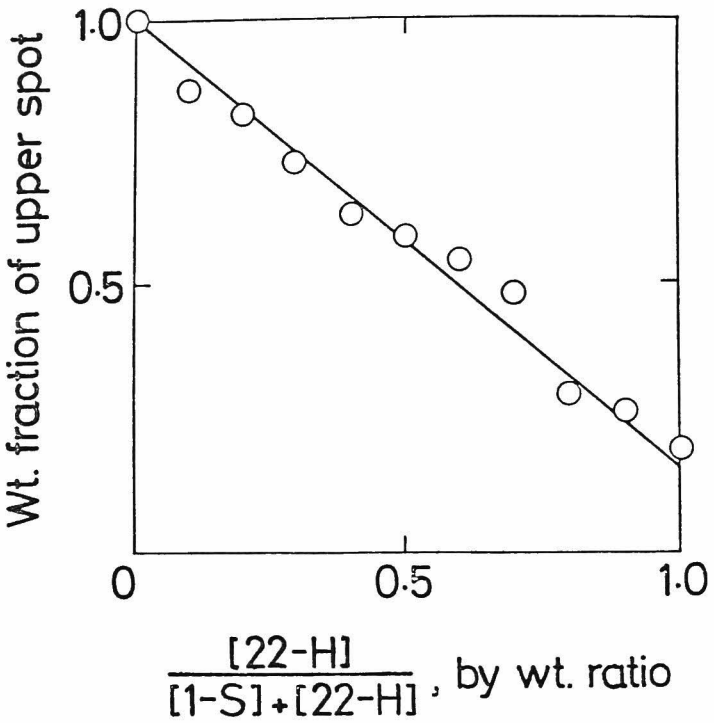

Fig. 4. Weight fraction of upper spot in the thin layer chromatogram determined by a densitometer for mixtures of a PS specimen (22-H) and the standard PS (1-S).

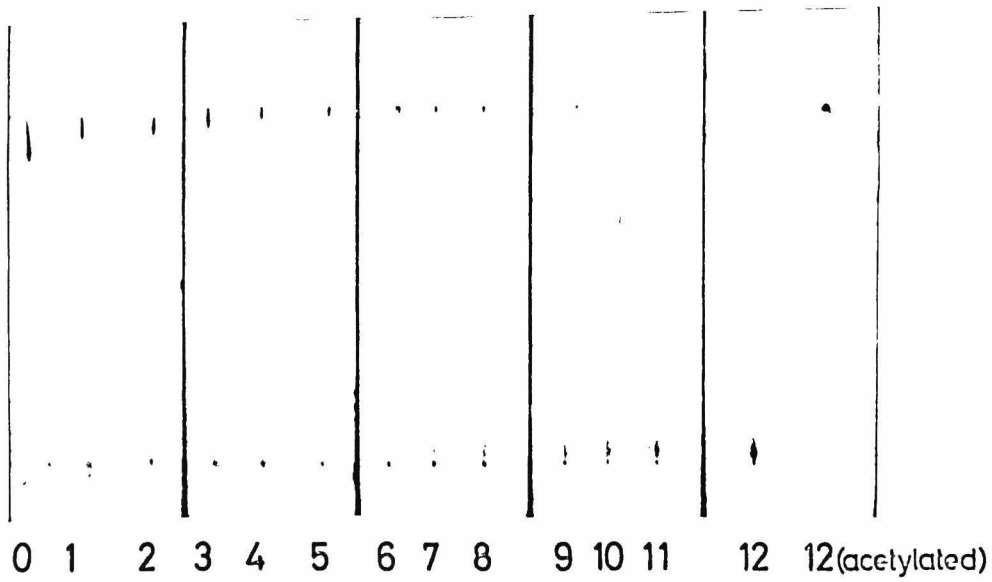

Fig. 5. Thin layer chromatograms of PMMA specimen (gel, silica; developer, ethyl acetate; indicator, I_2). The sample number corresponds to the [SX]/[M] mole ratio as follows: 0 (0); 1 (0.0005); 2 (0.001); 3 (0.002); 4 (0.003); 5 (0.004); 6 (0.006); 7 (0.009); 8 (0.012); 9 (0.016); 10 (0.022); 11 (0.036); 12 (0.040).

lower spot increases, as the sample number, i.e., [SX]/[M] in the polymerization mixture becomes larger. This fact suggests that the MMA polymer has a larger content of polar functional endgroups at higher [SX]/[M] ratio. A strong evidence for the functional endgroup to be an amino group is provided by the chromatogram of the PMMA reacted with acetyl chloride prior to the chromatographic development, as is seen for the PMMA of number 12 in Figure 5. The lower spot which is observed for the polymer before the reaction with acetyl chloride disappears as a consequence of blocking the amino group.

To determine the weight fraction of the polymer developed, the amount of the upper spot of PMMA was measured by a densitometer for varying amounts of the deposited polymer. One example is given in Figure 6, together with that for a standard PMMA possessing no amino group.

The integrated area indicated by the densitometer is proportional to the amount of the deposited PMMA. The ratio of the slope of the linear curve for the PMMA specimen to that of the standard PMMA gives the w_P value.

Comparison of Observed and Calculated w_P Values. As described earlier, the whole polymer must be a mixture of three kinds of polymer different in the number of functional endgroups (P, PX, and XPX). Though we made an additional chromatographic experiment with other developers than benzene and ethyl acetate, it was not successful to separate distinctly PX and XPX, and we could determine merely the fraction of upper spot which corre-

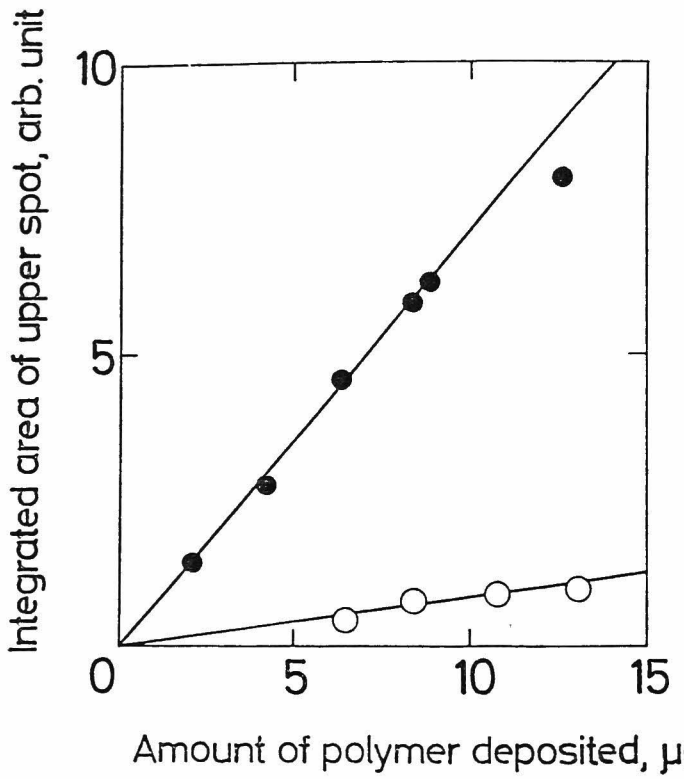

Fig. 6. Relationship between the integrated area of upper spot and the amount of polymer deposited: (o) PMMA, sample number 11; (•) the standard PMMA.

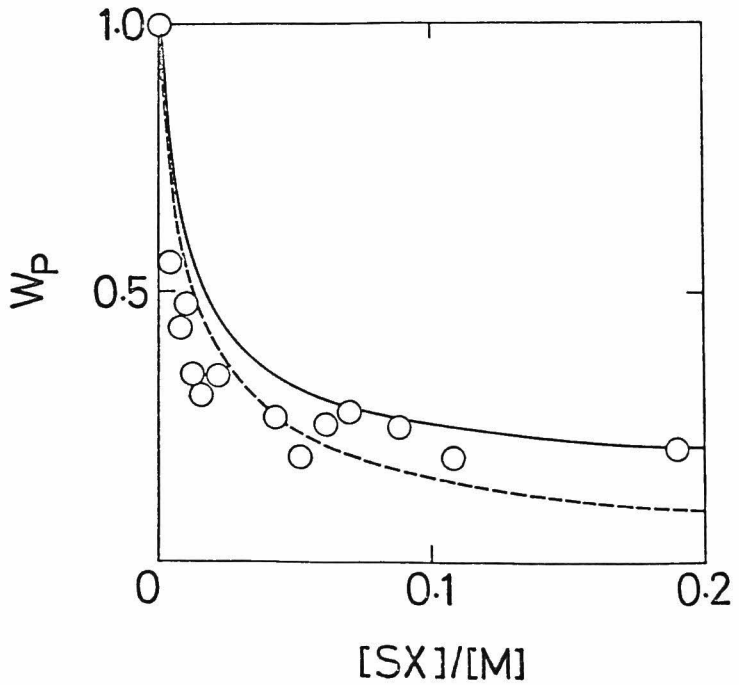

Fig. 7. Plots of weight fraction w_p of PS carrying no transfer agent fragment X against [SX]/[M]: (o) observed values; (——) calculated according to eq 3; (-----) calculated according to eq B1 which is valid for non-degradative transfer.

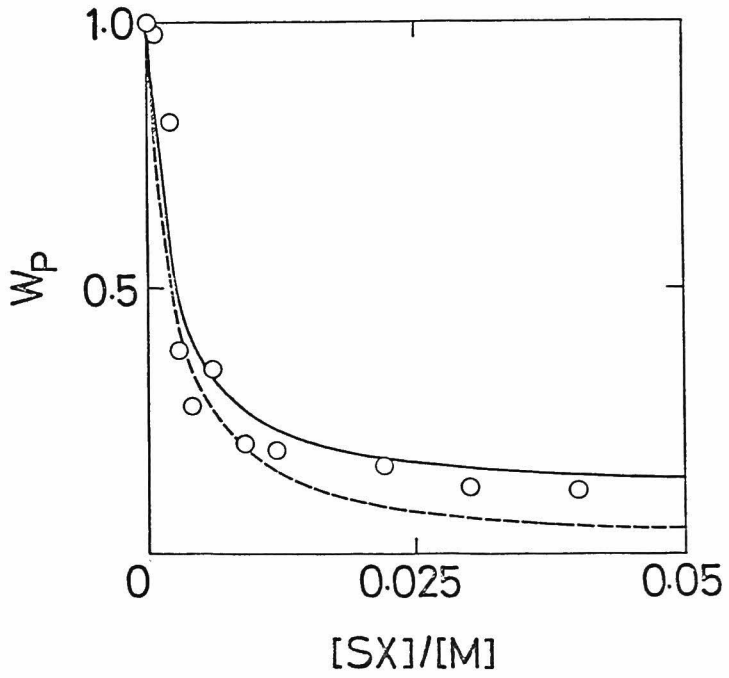

Fig. 8. Plots of weight fraction w_p of PMMA carrying no transfer agent fragment X against [SX]/[M]: (o) observed values; (——) calculated according to eq 3; (-----) calculated according to eq B1 which is valid for non-degradative transfer.

sponds to the fraction w_p of the polymer bearing no functional endgroup.

The observed w_p values are plotted against [SX]/[M] in Figure 7 for PS and in Figure 8 for PMMA.
The solid curves represent the values calculated according to eq 3 with the kinetic data and the broken curves those calculated under the assumption of non-degradative transfer (eq B1 in Appendix B). Initially both the observed and calculated w_p fall off very rapidly as [SX]/[M] increases, but subsequently they flatten out. The observed values are close to the calculated within the limits of experimental error. As is apparent from Figures 9 and 10, a similar agreement between the observed and calculated values is seen in the plots of w_p against $\overline{P}_n/\overline{P}_{n,o}$.

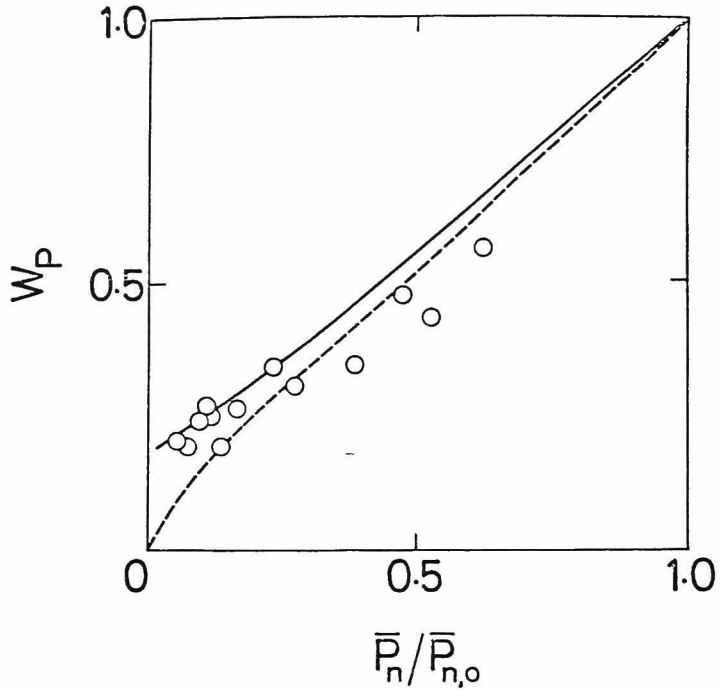

Fig. 9. Plots of weight fraction w_p of PS carrying no transfer agent fragment X against $\overline{P}_n/\overline{P}_{n,o}$: (o) observed values; (——) calculated according to eq 7; (-----) calculated according to eq B7 which is valid for non-degradative transfer.

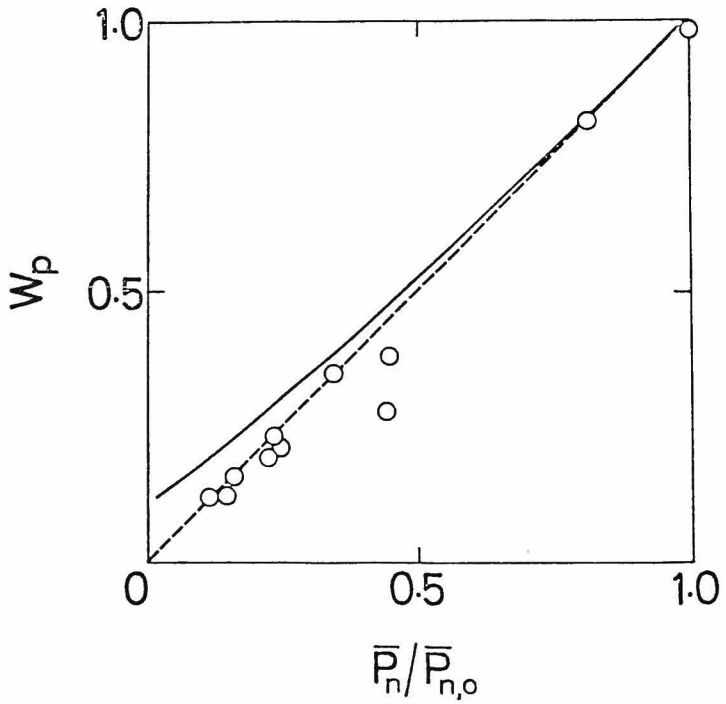

Fig. 10. Plots of weight fraction w_p of PMMA carrying no transfer agent fragment X against $\overline{P}_n/\overline{P}_{n,o}$: (o) observed values; (——) calculated according to eq 7; (-----) calculated according to eq B7 which is valid for non-degradative transfer.

The theoretical curves for non-degradative transfer reaction are different from those for degradative transfer to an appreciable extent, but the reproducibility of the present chromatographic data was not good enough to indicate the transfer to be of degradative type. Inspection of Figures 7 to 10 leads to a conclusion that one may roughly estimate the w_P value from the theory which is valid for the non-degradative chain transfer polymerization, even if the transfer reaction is of a degradative type.

It seems to be very difficult to determine experimentally the w_{PX} and w_{XPX}. Therefore, we estimated them with use of eq A11 and A12 in Appendix A. The w_{PX} and w_{XPX} values, shown in Figure 11, were calculated for the MMA polymerization from the kinetic data under an assumption of disproportionation termination, similar to w_P.

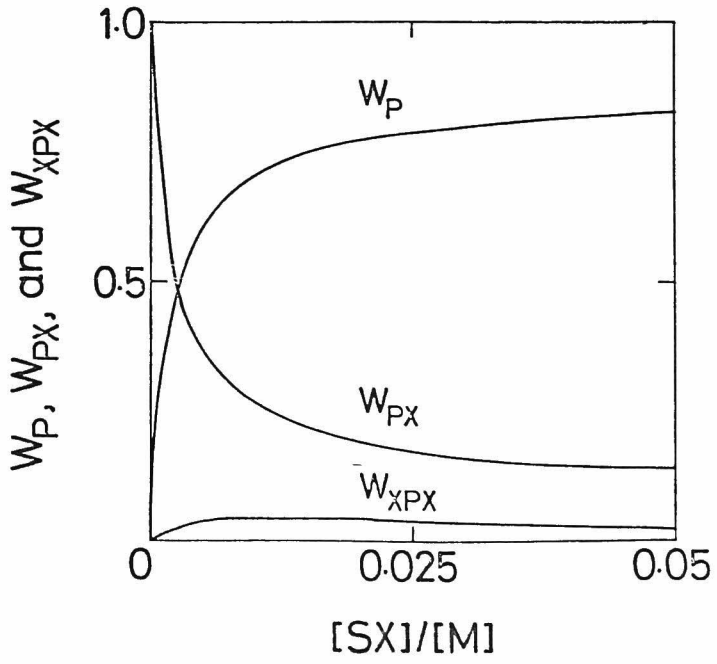

Fig. 11. w_P, w_{PX}, and w_{XPX} values for PMMA calculated according to eq A10, A11, and A12.

It is seen that w_{XPX} amounts to a definite value, though much lower than the w_{PX}. According to the proposed polymerization scheme, the polymer XPX would result from the radical combination reaction(xv) between XP· and X·.

Finally, the distribution of the functional endgroups in the polymer was studied with PMMA prepared at [SX]/[M] = 0.0109. This was fractionated into 11 fractions and the thin layer chromatography was run on each fraction. In contrast to the finding of De Boos[5], it was found that the fractions exhibited no significant difference in w_P.

The satisfactory agreement between the observed and calculated w_P suggests that the thin layer chromatography proves to be a method feasible for determining a functional endgroup, even in case that the molecular weight of the polymer is too high to be determined by the conventional chemical analytical method. For instance, the molecular weight of PMMA in Figure 8 is 2.5×10^5 at [SX]/[M] = 0.002 and 1.0×10^5 at [SX]/[M] = 0.006. Another advantage of the thin layer chromatography is that this method does not require careful removal of all traces of adsorbed material from polymers prior to endgroup analysis. Recently Min and coworkers also have pointed out the usefulness of thin layer chromatography for endgroup analysis.[13]

Coupling reactions of the polymers carrying these reactive endgroups will be described.

APPENDIX

A. Degradative Transfer. From the definition the weight fractions w_P, w_{PX}, and w_{XPX} can be expressed as,

$$w_P = \frac{k_{tr}[M\cdot][SX] + \lambda k_t[M\cdot]^2 + \lambda k_t[XM\cdot][M\cdot] + (1-\lambda)k_t[M\cdot]^2}{k_{tr}[M\cdot][SX]+k_{tr}[XM\cdot][SX]+\lambda k_t([M\cdot]+[XM\cdot])^2+(1-\lambda)k_t([M\cdot]+[XM\cdot])^2+k_2[M\cdot][X\cdot]+k_2[XM\cdot][X\cdot]} \quad (A1)$$

$$w_{PX} = \frac{k_{tr}[XM\cdot][SX] + \lambda k_t[XM\cdot][M\cdot]+2(1-\lambda)k_t[XM\cdot][M\cdot]+\lambda k_t[XM\cdot]^2+k_2[M\cdot][X\cdot]}{k_{tr}[M\cdot][SX]+k_{tr}[XM\cdot][SX]+\lambda k_t([M\cdot]+[XM\cdot])^2+(1-\lambda)k_t([M\cdot]+[XM\cdot])^2+k_2[M\cdot][X\cdot]+k_2[XM\cdot][X\cdot]} \quad (A2)$$

$$w_{XPX} = \frac{(1-\lambda)k_t[XM\cdot]^2 + k_2[XM\cdot][X\cdot]}{k_{tr}[M\cdot][SX]+k_{tr}[XM\cdot][SX]+\lambda k_t([M\cdot]+[XM\cdot])^2+(1-\lambda)k_t([M\cdot]+[XM\cdot])^2+k_2[M\cdot][X\cdot]+k_2[XM\cdot][X\cdot]} \quad (A3)$$

If the usual steady-state assumptions with respect to the concentrations of radicals may be applied and k_2 is assumed to be equal to $(k_1k_3)^{1/2}$, the stationary radical concentrations [M·], [XM·], and [X·] can be obtained from eq A4-A6.

$$R_i = k_{tr}[M\cdot][SX] + k_t[M\cdot]^2 + k_t[XM\cdot][M\cdot] + k_2[M\cdot][X\cdot] \quad (A4)$$

$$k_1[X\cdot][M] = k_{tr}[XM\cdot][SX] + k_t[XM\cdot][M\cdot] + k_t[XM\cdot]^2 + k_2[XM\cdot][X\cdot] \quad (A5)$$

$$k_{tr}[M\cdot][SX] + k_{tr}[XM\cdot][SX] = k_1[X\cdot][M] + k_2[M\cdot][X\cdot] + k_2[XM\cdot][X\cdot] + \frac{k_2^2}{k_t}[X\cdot]^2 \quad (A6)$$

Hence, the concentrations are given by

$$[M\cdot] = \frac{R_i}{k_{tr}[SX] + (R_i k_t)^{1/2}} \tag{A7}$$

$$[XM\cdot] = \frac{\frac{k_1 k_{tr}}{k_2}(R_i k_t)^{1/2}[M][SX]}{\left\{k_{tr}[SX] + (R_i k_t)^{1/2}\right\}\left\{\frac{k_1 k_t}{k_2}[M] + k_{tr}[SX] + (R_i k_t)^{1/2}\right\}} \tag{A8}$$

$$[X\cdot] = \frac{\frac{k_{tr}}{k_2}(R_i k_t)^{1/2}[SX]}{\frac{k_1 k_t}{k_2}[M] + k_{tr}[SX] + (R_i k_t)^{1/2}} \tag{A9}$$

Substitution of these concentrations into eq A1-A3 leads to the following expressions for each fraction as functions of the concentrations of the monomer [M] and the chain transfer agent [SX].

$$w_P = \frac{(R_i k_t)^{1/2}[\{(k_1 k_t/k_2)[M] + k_{tr}[SX] + (R_i k_t)^{1/2}\}\{k_{tr}[SX](k_{tr}[SX] + (R_i k_t)^{1/2}) + R_i k_t\} + (\lambda k_1 k_t k_{tr}/k_2)[SX][M](R_i k_t)^{1/2}]}{\{k_{tr}[SX] + (R_i k_t)^{1/2}\}^3\{(k_1 k_t/k_2)[M] + (R_i k_t)^{1/2}\}} \tag{A10}$$

$$w_{PX} = \frac{k_{tr}[SX][\{k_{tr}[SX] + (R_i k_t)^{1/2}\}\{(k_1 k_t k_{tr}/k_2)[SX][M] + R_i k_t\}\{(k_1 k_t/k_2)[M] + k_{tr}[SX] + (R_i k_t)^{1/2}\} + (2-\lambda)R_i k_t(k_1 k_t/k_2)[M]\{(k_1 k_t/k_2)[M] + k_{tr}[SX] + (R_i k_t)^{1/2}\} + \lambda\{(k_1 k_t/k_2)[M]\}^2 k_{tr}[SX](R_i k_t)^{1/2}]}{\{k_{tr}[SX] + (R_i k_t)^{1/2}\}^3\{(k_1 k_t/k_2)[M] + (R_i k_t)^{1/2}\}\{(k_1 k_t/k_2)[M] + k_{tr}[SX] + (R_i k_t)^{1/2}\}} \tag{A11}$$

$$w_{XPX} = 1 - w_P - w_{PX} = \frac{(k_1 k_t k_{tr}^2/k_2)(R_i k_t)^{1/2}[M][SX]^2\{(1-\lambda)(k_1 k_t/k_2)[M] + k_{tr}[SX] + (R_i k_t)^{1/2}\}}{\{k_{tr}[SX] + (R_i k_t)^{1/2}\}^3\{(k_1 k_t/k_2)[M] + (R_i k_t)^{1/2}\}\{(k_1 k_t/k_2)[M] + k_{tr}[SX] + (R_i k_t)^{1/2}\}} \tag{A12}$$

According to the definition, R_p and $\overline{P}_n$ are represented by

$$\frac{1}{R_p} = \frac{1}{k_p[M]([M\cdot] + [XM\cdot])} \tag{A13}$$

$$\frac{1}{\overline{P}_n} = \frac{R_{tr} + R_t}{R_p}$$

$$= \frac{k_{tr}[M\cdot][SX] + k_{tr}[XM\cdot][SX] + \lambda k_t([M\cdot]+[XM\cdot])^2 + \frac{(1-\lambda)}{2}k_t([M\cdot]+[XM\cdot])^2 + k_2[M\cdot][X\cdot] + k_2[XM\cdot][X\cdot]}{k_p[M]([M\cdot]+[XM\cdot])} \qquad (A14)$$

where R_t and R_{tr} are the rate of termination and transfer, respectively. Substituting the concentrations given by eq A7-A9 into eq A13 and A14, one obtains eq 4, 5, and 6.

B. Non-degradative Transfer. When the transfer reaction can be regarded non-degradative, we can discard the reactions xiv - xvi in the polymerization scheme. Thus the limit $k_2 = 0$ in eq A10-A12 gives the values of w_P, w_{PX}, w_{XPX} in the case of non-degradative transfer:

$$w_P = \frac{(R_i k_t)^{1/2}\left\{k_{tr}[SX] + (R_i k_t)^{1/2}\right\}^2 + (\lambda - 1)k_{tr}[SX]R_i k_t}{\left\{k_{tr}[SX] + (R_i k_t)^{1/2}\right\}^3} \qquad (B1)$$

$$w_{PX} = \frac{k_{tr}^2[SX]^2\left\{(1+\lambda)(R_i k_t)^{1/2} + k_{tr}[SX]\right\} + (2-\lambda)k_{tr}[SX]R_i k_t}{\left\{k_{tr}[SX] + (R_i k_t)^{1/2}\right\}^3} \qquad (B2)$$

$$w_{XPX} = \frac{(1-\lambda)k_{tr}^2[SX]^2(R_i k_t)^{1/2}}{\left\{k_{tr}[SX] + (R_i k_t)^{1/2}\right\}^3} \qquad (B3)$$

In addition, these weight fractions can be expressed as a function of $\overline{P}_n$ of the polymer, if the transfer occurs non-degradatively. In this case the stationary concentrations of $[M\cdot]$ and $[XM\cdot]$ are readily shown to be

$$[M\cdot] = \frac{R_i}{k_{tr}[SX] + (R_i k_t)^{1/2}} \tag{B4}$$

$$[XM\cdot] = \frac{k_{tr}[SX](R_i k_t)^{1/2}}{k_t k_{tr}[SX] + k_t(R_i k_t)^{1/2}} \tag{B5}$$

Since w_P is given by

$$w_P = \frac{k_{tr}[M\cdot][SX] + k_t[M\cdot]^2 + k_t[XM\cdot][M\cdot]}{k_{tr}[SX]([M\cdot] + [XM\cdot]) + k_t([M\cdot] + [XM\cdot])^2} \tag{B6}$$

substitution of eq B4 and B5 into eq B6 leads to

$$w_P = \frac{2[\{(1 + \lambda)(r - 1) + 2\}^2 + 2(\lambda^2 - 1)(r - 1)]}{\{(1 + \lambda)(r - 1) + 2\}^3} \tag{B7}$$

where r is $\overline{P}_{n,o}/\overline{P}_n$. $\overline{P}_{n,o}$ denotes $\overline{P}_n$ of the polymer generated by polymerization in the absence of chain transfer agent. Similarly, one can get

$$w_{PX} = \frac{(1 + \lambda)^3(r + 1)(r - 1)^2 + 4(2 - \lambda)(1 + \lambda)(r - 1)}{\{(1 + \lambda)(r - 1) + 2\}^3} \tag{B8}$$

$$w_{XPX} = \frac{2(1 - \lambda)(1 + \lambda)^2(1 - r)^2}{\{(1 + \lambda)(r - 1) + 2\}^3} \tag{B9}$$

The thin layer chromatography provides the weight fractions,,,, while the endgroup determinations by conventional chemical analysis give us the number fractions. Therefore, it seems also important to derive the expressions for each number fraction x_P, x_{PX}, and x_{XPX}. Considering that these fractions are represented by

$$x_P = \frac{k_{tr}[M\cdot][SX] + \lambda k_t[M\cdot]^2 + \frac{1}{2}(1-\lambda)k_t[M\cdot]^2 + \lambda k_t[XM\cdot][M\cdot]}{k_{tr}[M\cdot][SX]+k_{tr}[XM\cdot][SX]+\lambda k_t([M\cdot]+[XM\cdot])^2+\frac{1}{2}(1-\lambda)k_t([M\cdot]+[XM\cdot])^2} \quad (B10)$$

$$x_{PX} = \frac{k_{tr}[XM\cdot][SX] + \lambda k_t[XM\cdot][M\cdot] + (1-\lambda)k_t[M\cdot][XM\cdot] + \lambda k_t[XM\cdot]^2}{k_{tr}[M\cdot][SX]+k_{tr}[XM\cdot][SX]+\lambda k_t([M\cdot]+[XM\cdot])^2+\frac{1}{2}(1-\lambda)k_t([M\cdot]+[XM\cdot])^2} \quad (B11)$$

$$x_{XPX} = \frac{\frac{1}{2}(1-\lambda)k_t[XM\cdot]^2}{k_{tr}[M\cdot][SX]+k_{tr}[XM\cdot][SX]+\lambda k_t([M\cdot]+[XM\cdot])^2+\frac{1}{2}(1-\lambda)k_t([M\cdot]+[XM\cdot])^2} \quad (B12)$$

and through the algebraic manipulation similar to w_P, w_{PX}, and w_{XPX}, we finally find the following expressions as functions of [M] and [SX]:

$$x_P = \frac{(R_i k_t)^{1/2}\left\{k_{tr}^2[SX]^2 + (1+\lambda)k_{tr}[SX](R_i k_t)^{1/2} + \frac{1}{2}(1+\lambda)R_i k_t\right\}}{\left\{k_{tr}[SX] + (R_i k_t)^{1/2}\right\}^2\left\{k_{tr}[SX] + \frac{1}{2}(1+\lambda)(R_i k_t)^{1/2}\right\}} \quad (B13)$$

$$x_{PX} = \frac{k_{tr}[SX]\left[\left\{k_{tr}[SX] + (R_i k_t)^{1/2}\right\}^2 + (\lambda-1)k_{tr}[SX](R_i k_t)^{1/2}\right]}{\left\{k_{tr}[SX] + (R_i k_t)^{1/2}\right\}^2\left\{k_{tr}[SX] + \frac{1}{2}(1+\lambda)(R_i k_t)^{1/2}\right\}} \quad (B14)$$

$$x_{XPX} = \frac{\frac{1}{2}(1-\lambda)k_{tr}^2[SX]^2(R_i k_t)^{1/2}}{\left\{k_{tr}[SX] + (R_i k_t)^{1/2}\right\}^2\left\{k_{tr}[SX] + \frac{1}{2}(1+\lambda)(R_i k_t)^{1/2}\right\}} \quad (B15)$$

and as a function of r ($= \overline{P}_{n,o}/\overline{P}_n$):

$$x_P = \frac{2\{(1+\lambda)(r^2-1)+2\}}{r\{(1+\lambda)(r-1)+2\}^2} \quad (B16)$$

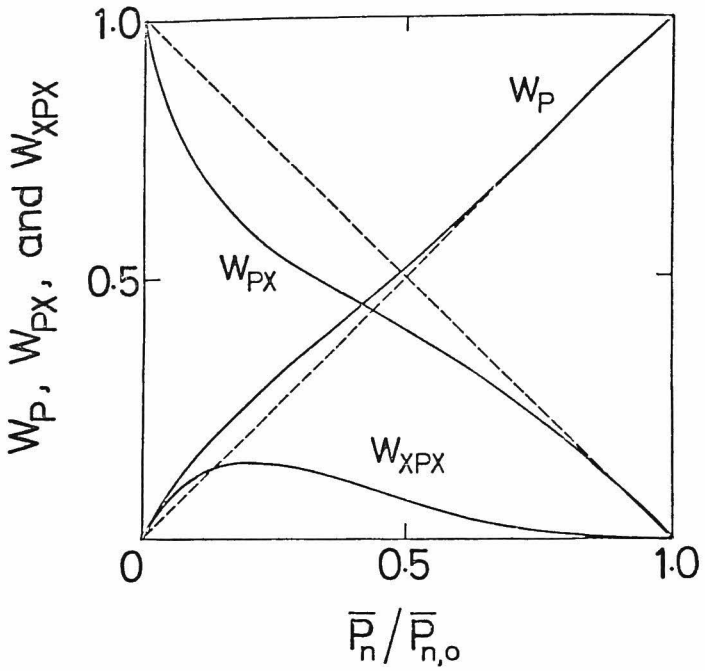

Fig. 12. w_P, w_{PX}, and w_{XPX} values in the case of non-degradative transfer as a function of $\overline{P}_n/\overline{P}_{n,o}$: (——) $\lambda = 0$ (coupling termination); (-----) $\lambda = 1$ (disproportionation termination).

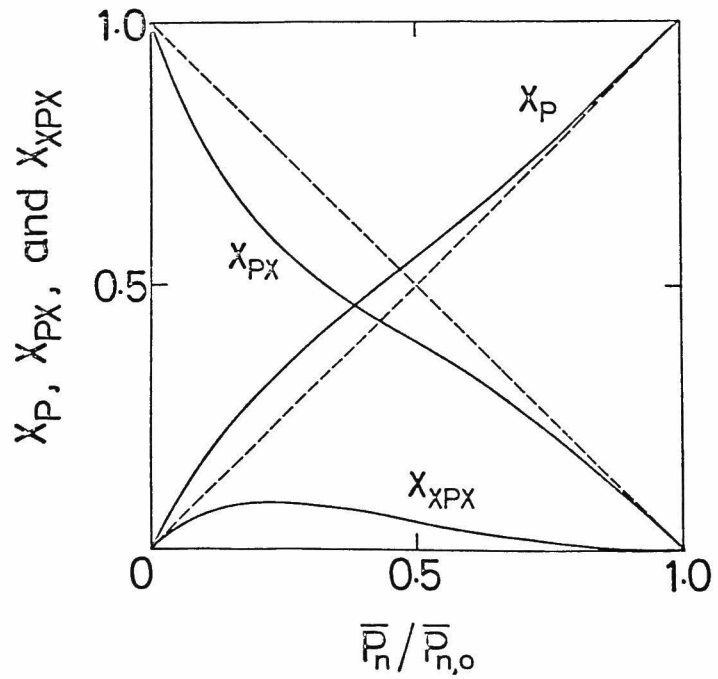

Fig. 13. x_P, x_{PX}, and x_{XPX} values in the case of non-degradative transfer as a function of $\overline{P}_n/\overline{P}_{n,o}$: (——) $\lambda = 0$ (coupling termination); (-----) λ 1 (disproportionation termination).

$$x_{PX} = \frac{(r-1)[\{(1+\lambda)(r-1)+2\}^2 - 2(1-\lambda^2)(r-1)]}{r\{(1+\lambda)(r-1)+2\}^2} \qquad (B17)$$

$$x_{XPX} = \frac{(1-\lambda^2)(r-1)^2}{r\{(1+\lambda)(r-1)+2\}^2} \qquad (B18)$$

The dependence of each fraction on $\bar{P}_n/\bar{P}_{n,0}$ is given in Figures 12 and 13 for the cases of $\lambda = 0$ and $\lambda = 1$.

As is apparent from eq B9 and B18, the w_{XPX} and x_{XPX} values vanish when $\lambda = 1$ (disproportionation termination).

REFEPENCES

1. J. W. Breitenbach and A. Maschin, Z. Physik. Chem. Leipzig, A187, 175 (1940).
2. T. Maekawa, M. Matsuo, H. Yoshida, K. Hayashi, and S. Okamura, Polymer, 11, 342 (1970).
3. T. Maekawa, M. Matsuo, H. Yoshida, K. Hayashi, and S. Okamura, Polymer, 11, 351 (1970).
4. Y. Ikada and T. Kawahara, Report of Japan Atomic Energy Research Institute, No. 5, 93 (1973).
5. A. G. De Boos, Polymer, 14, 587 (1973).
6. T. C. Owen, J. Chem. Soc. C (Org.), 1967, 1373.
7. C. E. H. Bawn, R. F. J. Freeman, and A. R. Kamaliddin, Trans. Faraday Soc., 46, 1107 (1950).
8. W. R. Moore and R. J. Fort, J. Polym. Sci. A, 1, 929 (1963).
9. P. W. Allen, F. M. M. Merrett, and J. Scanlan, Trans. Faraday Soc., 51, 95 (1955).
10. J. C. Bevington, Radical Polymerization, Academic Press, London and New York, 1961.
11. M. S. Matheson, E. E. Auer, E. B. Bevilacqua, and E. J. Hart, J. Amer. Chem. Soc., 73, 1700 (1951).
12. J. L. O'Brien and F. Gornick, J. Amer. Chem. Soc., 77, 4757 (1955).
13. T. I. Min, T. Miyamoto, and H. Inagaki, Bull. Inst. Chem. Res., Kyoto Univ., 53, 381 (1975).

CHAPTER 2.

Synthesis of Polymers with Terminal Functional Groups by Radiation Polymerization

INTPODUCTION

In chapter 1, based on a polymerization kinetics we have calculated the functional end-group content of polymers formed in polymerizations where the chain transfers occur predominantly and compared it with the experimentally determined end-group content in the case of catalytic radical polymerizations . In the present work we will describe radiation polymerizations of styrene in the presence of acid chlorides and of vinyl acetate(VAc) in the presence of carbon tetrachloride (CCl_4), which were performed mainly in an attempt to synthesize polymers with terminal functional groups.

EXPERIMENTAL

Polymerization

VAc was purified by distillation after its partial polymerization.[1] Styrene, acetyl chloride(AC), trichloroacetyl chloride(TCAC), CCl_4 and other chemicals were once distilled

just prior to use. Radiation polymerizations were carried out with gamma rays from Co-60 on monomer-solvent mixtures after degassing by a freeze-thaw method followed by sealing. The temperature and the dose rate employed for the polymerization are tabulated in Table I. Polystyrene(PS) was recovered from the polymerization mixture either by pouring it into n-hexane containing AC(or TCAC) or by evaporating the residual monomer and the solvent. When poly(vinyl acetate) (PVAc) was obtained as viscous, oil-like telomer, it was recovered by allowing the VAc and CCl_4 to evaporate at room temperature with an aspirator. Even VAc telomer with the degree of telomerization of one [CCl_3-CH_2-CH(OCOCH$_3$)-Cl] was reported to remain undistilled under this mild evaporation[2].

TABLE I EXPERIMENTAL CONDITIONS OF POLYMERIZATION

MONOMER	SOLVENT	TEMPERATURE °C	DOSE RATE RAD·SEC^{-1}
STYRENE	AC	25	50
STYRENE	TCAC	50	0.06
VAc	CCL_4	0	7.8
VAc	CCL_4	40	11

End-Group Determination

For determination of COCl end-groups of PS it was dissolved in tetrahydrofuran containing excess cyclohexylamine (CHA) to convert COCl to $CONH_2$-C_6H_{11}. The amount of COCl was calculated from the decrease of the added CHA, which

was titrated potentiometrically with hydrochloric acid[3]. The terminal CHO group attached to poly(vinyl alcohol) (PVA), which was formed as a result of the hydrolysis of PVAc, was determined with 3-methyl-2-benzothiazolone hydrazine hydrochloride in the aqueous solution[4]. The calibration curve for the CHO determination was provided using a conventional PVA, the 1, 2-glycol linkages of which were partially oxidized with a known amount of sodium periodate to aldehyde. The chlorine and oxygen contents of PVA derived from PVAc were determined by elemental analysis.

Determination of Molecular Weight

Molecular weights of PS were determined by vapor-pressure osmometry in chloroform at 29.5°C with the use of Hitachi Perkin-Elmer 115-type Vapor Pressure Osmometer or by viscosimetry in benzene at 25°C. Prior to the osmometry all the COCl end-groups were converted tc amide with CHA. The degree of polymerization based on the viscosimetry, here designated as $\bar{P}_v$, was calculated under the assumption of a most probable molecular weight distribution and with the help of the following empirical formula which is valid for fractionated PS's[5].

$$[\eta] = 5.8 \times 10^{-3} \bar{P}_v^{0.66} \qquad (7)$$

For the vapor-pressure osmometry of PVAc the intact PVAc was hydrolyzed to PVA in alkaline media followed by reacetylation in a acetic anhydride-pyridine mixture. The degree of

telomerization $\bar{n}$ of VAc telomers was evaluated from the conductivity titration of the aqueous solutions resulted from the alkaline hydrolysis of the telomers (see the reaction (10)).

Gel permeation chromatography was conducted using tetrahydrofuran as solvent at 30°C with a HLC-802UR-type apparatus manufactured by Toyōsoda, Ltd.

RESULTS

Polymerization of Styrene

The observed number of COCl end-groups in one PS molecule is shown in Table II, together with the number-average molecular weight $\bar{M}_n$. It appears that the number of COCl groups in one molecule ranges between 1 and 2 for PS formed in the presence of AC and between 0.5 and 1 for PS formed in the

TABLE II COCL END-GROUP DETERMINATION OF POLYSTYRENE

SOLVENT	MOLE FRACTION OF STYRENE	$\bar{M}_N$	COCL	
			PER GRAM POLYMER	PER MOLECULE
AC	0.36	6.46×10^3	1.94×10^{-4}	1.25
	0.50	5.19 〃	2.09 〃	1.08
	0.85	7.71 〃	1.69 〃	1.30
	0.95	9.74 〃	1.23 〃	1.20
TCAC	0.66	3.10×10^3	1.88×10^{-4}	0.583
	0.83	5.91 〃	1.47 〃	0.869
	0.91	5.29 〃	1.34 〃	0.709
	0.95	7.54 〃	1.02 〃	0.769
	0.95	11.7 〃	0.512 〃	0.599

presence of TCAC. Based only upon determination of the end-group and the molecular weight, however, we cannot give any explanation on this difference by about two times in the COCl content observed between two different PS's. In this connection a kinetic analysis may afford some useful information.

Figs. 1 and 2 show the observed and theoretical ratios of the rates of polymerization R_p of mixture to that of bulk

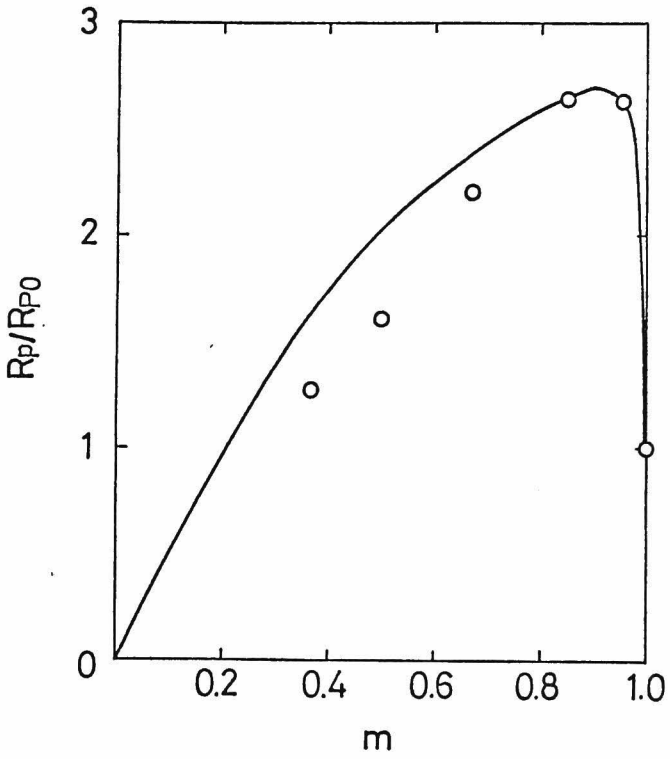

Figure 1 Relative rates of polymerization R_p/R_{p0} of styrene in the presence of acetylchloride(AC) as a function of the mole fraction of monomer m (dose rate=50 rad·sec^{-1}, temp.=25°C). o observed, —— theoretical according to eq. (A1) with ϕ_{rel}=8 and P_{rel}=65.

polymerization R_{p0} as a function of the monomer fraction m in the mixture for the polymerization of styrene-AC and styrene-TCAC, respectively. The theoretical calculation of R_p is based on the kinetics common to the polymerization of binary mixtures and on the initiation characteristic to the radiation polymerization in which energy transfer may take place between the monomer and solvent molecules raised to an excited state

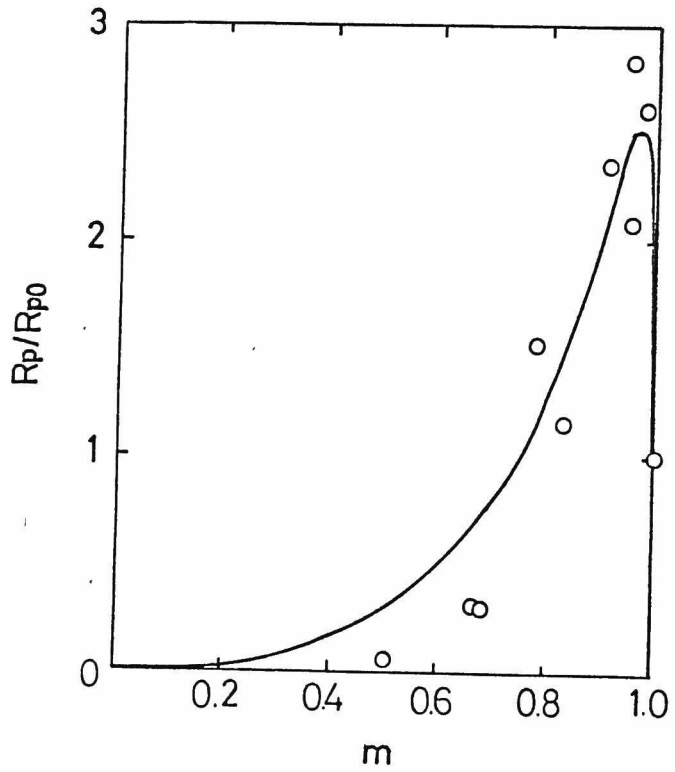

Figure 2 Relative rates of polymerization R_p/R_{p0} of styrene in the presence of trichloacetyl chloride(TCAC) as a function of the mole fraction of monomer m (dose rate =0.06 rad·sec^{-1}, temp.=50°C). o observed, —— theoretical according to eqs.(A3) and (A11) with ϕ_{rel}=20 and P_{rel}=30.

by radiation (the kinetic method how to calculate R_p is given in Appendix). The chain transfer constant C_s was found to be virtually zero for AC and 0.12 for TCAC from the familiar Mayo's plot between [S]/[M] and the reciprocal of $\bar{P}_v$. Fig. 3 shows the $\bar{P}_v$ values.

In Fig. 1, the theoretical R_p was calculated according to eq.(A1), that is, eqs.(A3) and (A11) with $k_{tr}=0$ and assuming the well-known parameters, ϕ_{rel} and P_{rel}, to be 8 and 65, respectively. A small discrepancy between the observed and the calculated R_p/R_{p0} may be attributed mainly to insufficient recovery of the polymer, resulting in a somewhat lower R_p.

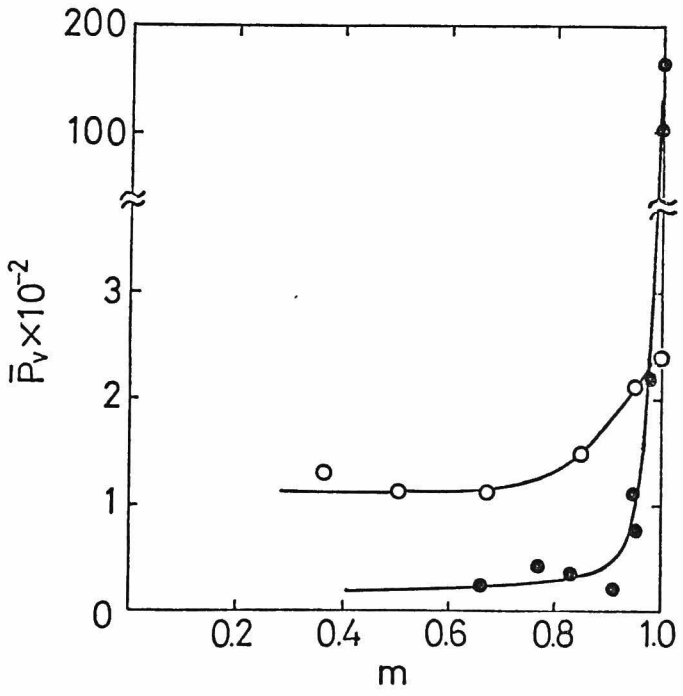

Figure 3 $\bar{P}_v$ of polystyrene as a function of the mole fraction of monomer m. o styrene-acetyl chloride(AC), • styrene-trichloroacetyl chloride(TCAC).

In the case of styrene-TCAC polymerization where C_s has a markedly high value, a degradative chain transfer seems to occur to a significant extent . Thus, the calculation of R_p was made by taking into consideration the degradative chain transfer. ϕ_{rel} and P_{rel} were assumed to be 20 and 30, respectively.

Contribution of active species from the solvent molecule to the initiation can be calculated using the following equation.

$$\alpha_s = \frac{\phi_{rel} P_{rel} [S]/[M]}{1+\phi_{rel} P_{rel} [S]/[M]} \qquad (8)$$

where α_s is the fraction of the initiation rate due to the radical from the solvent molecule. The α_s value is plotted against the monomer fraction in Fig. 4 for the styrene-AC polymerization. Clearly, α_s is close to unity unless the concentration of the solvent is not very low, suggesting

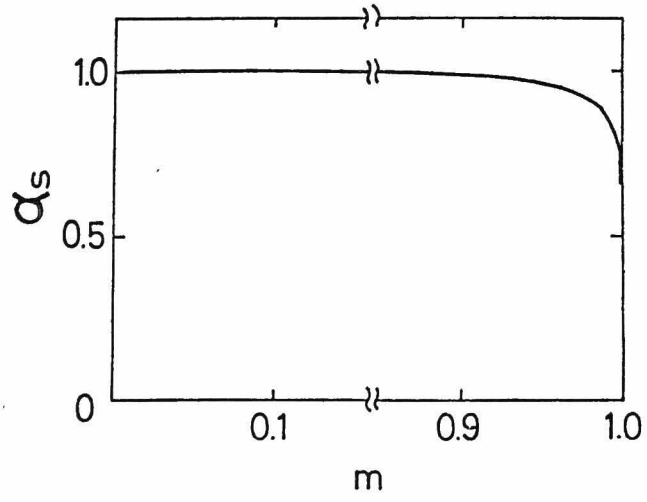

Figure 4. Fraction α_s of rate of initiation by solvent radicals as a function of the mole fraction of monomer m (solvent:acetyl cloride).....

that the chain propagation may start mostly from solvent radicals. Similarly, in the polymerization of styrene-TCAC, the solvent radicals are responsible for the propagation, although they are to be formed as a result of strong chain transfer, not of energy transfer.

Polymerization of VAc

It has been reported that the polymerization of VAc in the presence of CCl_4 gives rise to formation of a VAc polymer or telomer carrying a CCl_3 group at one chain-end and a Cl group at another[6].

$$nVAc + CCl_4 \longrightarrow Cl_3C\text{-}(CH_2\text{-}\underset{\underset{OCOCH_3}{|}}{CH})_n\text{-}Cl \qquad (9)$$

This is believed to be a consequence of vigorous chain transfer with CCl_4. Hydrolysis of this PVAc produces PVA with a terminal CHO group as follows:

$$m\ Cl_3C\text{-}(CH_2\text{-}\underset{\underset{OCOCH_3}{|}}{CH})_n\text{-}Cl \xrightarrow{H_2O} m\ Cl_2C{=}CH\text{-}\underset{\underset{OH}{|}}{CH}\text{-}(CH_2\text{-}\underset{\underset{OH}{|}}{CH})_{n-2}\text{-}CH_2\text{-}CHO + nmCH_3COOH + 2mHCl \qquad (10)$$

Thus reacetylation of this PVA gives PVAc with a terminal CHO group. As the above reaction suggests, a quantitative analysis of CHO, CH_3COOH and HCl in the hydrolyzed mixture allows us to determine the end-group structure of the VAc polymer as well as the n value.

In Table III are tabulated R_p, $\bar{P}_n$ and the end-group content for the VAc polymerization carried out at 40°C in the presence of CCl_4 of fairly low concentrations. It is seen that even an addition of very small amounts of CCl_4 reduces both of R_p and $\bar{P}_n$, indicating occurrence of marked degradative chain transfer. The C_s value is calculated to be 0.58 from the dependence of $\bar{P}_n$ on $[CCl_4]/[VAc]$. The finding that the numbers of CHO and Cl groups in one PVA molecule obtained from PVAc are roughly around unity and in the range of 2 to 5, resp., seems to accord rather well with the prediction from the reaction (10), if we take into consideration the eventual loss of PVA of lower molecular weights during its recovery operation from the hydrolyzed product. The error in determining the molecular weight of the reacetylated

TABLE III
END-GROUP DETERMINATION OF PVA OBTAINED FROM PVAc
(DOSE RATE=11 RAD·SEC^{-1}, TEMP.=40°C)

MOLE FRACTION OF CCl_4	$R_p \times 10^4$ MOL·L^{-1}·SEC^{-1}	$\bar{P}_N$	CHO PER MOLECULE	Cl PER MOLECULE
0	7.41	7340 [a]	0	0
4.76×10^{-3}	7.32	131	0.84	1.67
9.00×10^{-3}	6.31	105	0.94	2.62
1.92×10^{-2}	7.29	100	1.24	3.84
4.34×10^{-2}	3.72	83	1.35	5.38

a. viscosity-average degree of polymerization

PVA might also influence the estimation of the number of end-groups. It is noteworthy that the intact PVAc recovered from the polymerization mixture by evaporation of the monomer became colored on standing, while the reacetylated PVA did not undergo such coloration any more.

As demonstrated above, the polymerization of VAc in the presence of CCl_4 surely leads to formation of PVAc containing chlorine, but further discussion would be difficult because of the above-mentioned uncertainty in determining the end-groups. For this reason the following polymerizations were attempted with CCl_4 of higher concentrations. It may be anticipated that an addition of CCl_4 to the monomer by much higher concentrations than those in Table III would give VAc telomers, the end-groups of which can be determined with good accuracy.

The degree of telomerization $\bar{n}$ determined by different methods is given in Table IV. It is seen that the $\bar{n}$ estimated from the elemental analysis on chlorine and oxygen in the hydrolyzed PVAc is close to that from the titration of the intact PVAc. This accordance of $\bar{n}$ values determined with two independent methods affords a strong evidence for production of PVAc with such a chain-end structure as predicted in the reaction (10). Since, in the telomerization, $\bar{n}$ is readily shown to be given by

TABLE IV
DEGREE OF TELOMERIZATION $\bar{N}$ OF VAc TELOMERS CALCULATED FROM ELEMENTAL ANALYSIS AND TITRATION (DOSE RATE=7.8 RAD.SEC^{-1}, TEMP.=0°C)

MOLE FRACTION OF VAc	$\bar{N}$ FROM			
	Cl%	O%	TITRATION	AVERAGE
0.90	13.2	15.9	18.8	16.0
0.81	8.1	9.5	5.2	7.6
0.75	6.7	8.2	5.0	6.6
0.60	4.8	4.2	3.8	4.3
0.51	4.2	3.8	4.0	4.0
0.34	3.2	3.2	2.6	3.0

$$\bar{n} \fallingdotseq \frac{d[M]}{d[S]} = 1 + \frac{1}{C_s} \frac{[M]}{[S]} \qquad (11)$$

C_s is evaluated as 0.45 from the data in Table IV. It is interesting to note that we can regard the polymerization of VAc as telomerization, even if [S]/[M] is so low as 0.1. In Fig. 5 the gel permeation chromatograph is illustrated for the PVAc obtained by polymerization at 0°C with [S]/[M] of 1.92. The three peaks from left to right seem to correspond to degree of telomerizations n of 3, 2 and 1, respectively.

Fig. 6 gives the R_p/R_{p0} ratio observed in the polymerization at 0°C. In determining the R_p from the telomer yield

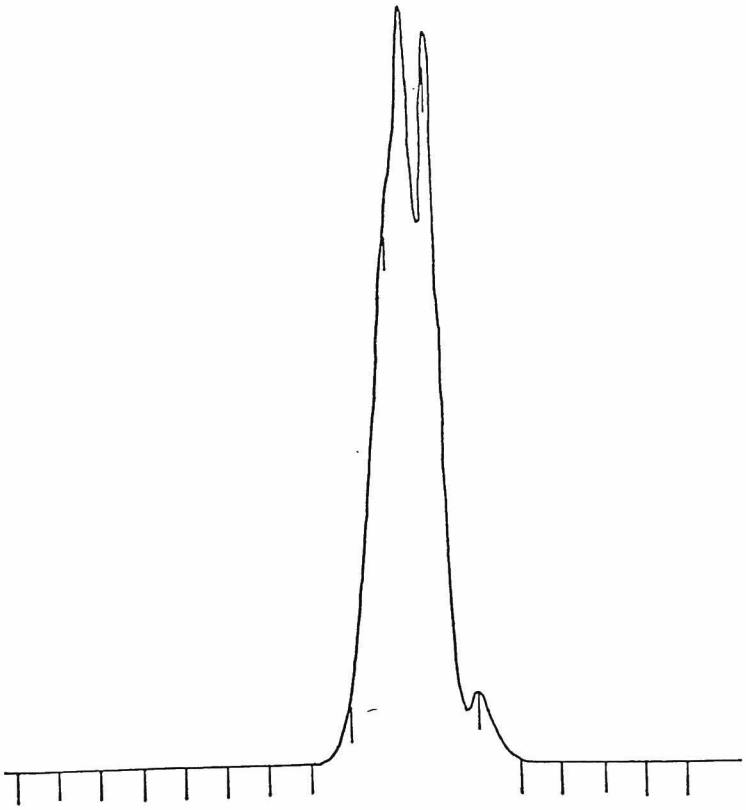

Figure 5 A gel permeation chromatograph of the vinyl acetate telomer obtained by polymerization at [S]/[M]=1.92.

a correction was made for contribution of the chlorine group to the weight of the VAc telomer. It is apparent that with decreasing monomer fraction in the mixture the observed and calculated ratioes of R_p/R_{p0} decrease monotonously without passing a maximum, in marked contrast to the styrene poly-

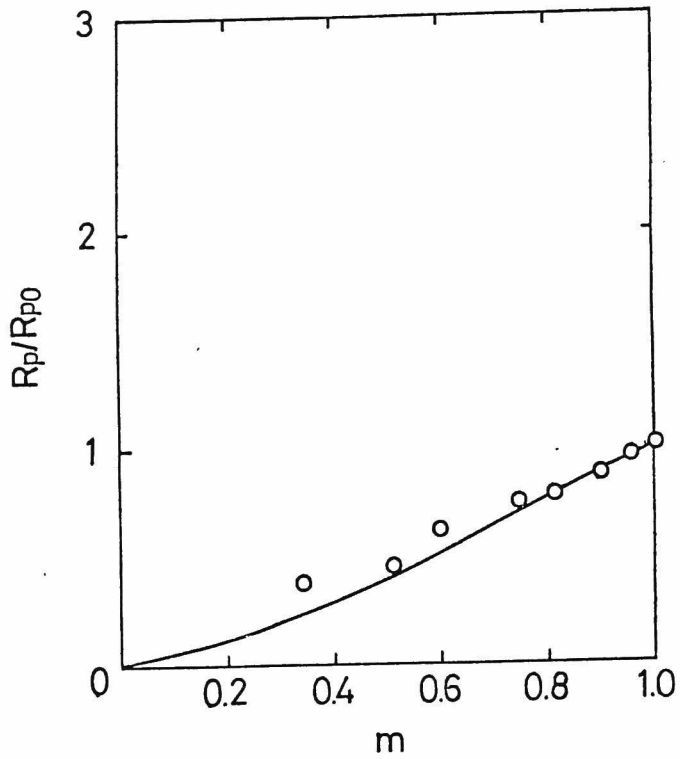

Figure 6 Relative rates of polymerization R_p/R_{p0} of vinyl acetate in the presence of CCl_4 as a function of the mole fraction of monomer m (dose rate=7.8 rad·sec^{-1}, temp=0°C). o observed, —— theoretical according to eqs.(A3) and (A11) with $k_{re}/k_{t3}^{1/2}=2.2\times10^{-2}$ $l^{1/2}\cdot mol^{-1/2}\cdot sec^{-1/2}$, $G_{VAc}=6.2$, and $G_{CCl_4}=15.4$.

merizations. This implies that the energy transfer may be not operative in the VAc-CCl_4 polymerization, in other words, P_{rel} is approximately unity. The similar speculation has been also given by Chapiro and his coworkers[7].

DISCUSSION

The modes of initiation, termination, and chain transfer in the vinyl polymerization have generally decisive effect on the nature and content of end-groups of vinyl polymers formed. Though the termination would be exclusively governed by the nature of monomer and the temperature of polymerization, both the initiation and the chain transfer can be much more widely varied. For instance, if we add to monomer such a solvent that has a high tendency to be decomposed by radiation into radicals capable of initiating the polymerization of monomer, the polymer may be produced which carries the fragment of solvent molecule on the chain-end.

A typical example for this is the radiation polymerization of styrene containing AC. As demonstrated above, AC does not cause any appreciable chain transfer, similar to the styrene monomer and the high α_s value strongly indicates that the active species responsible for the initiation may not be the radicals from styrene, but predominantly radicals from AC. Provided that the COCl group is stable against radiation, the solvent radicals may be $\cdot CH_2\dot{C}OCl$. Since the termination is known to proceed through recombination in the polymerization of styrene[8,9], the radiation polymerization may produce polymer with two COCl end-groups and hence the number of COCl end-groups in one PS molecule is expected to be two on the average. This is fairly higher than the findings

given in Table II, but seems not to be unreasonable if one recalls that the COCl end-group is very apt to be hydrolyzed by moisture in air .

It should be emphasized that any conventional, catalytic polymerization of styrene in the presence of AC would not result in producing the PS having COCl end-groups because of insignificant chain transfer to AC. However, this interesting characteristics of radiation polymerization becomes less noticeable, if the actual chain length is governed by the chain transfer to the solvent or the monomer. This case is the polymerizations of styrene-TCAC and VAc-CCl_4, where the additives behave as a very strong chain transfer agent, leading to formation of polymers, most of which carry one COCl end-group for PS and one CCl_3 for PVAc, even though the mode of termination is recombination. This polymerization scheme gives a satisfactory explanation for the result in Table II that the number of COCl end-groups in one PS polymer chain formed in the presence of TCAC is slightly smaller than unity, if hydrolysis of COCl is assumed to take place, similar to PS formed in the presence of AC.

Even in these cases, the radiation polymerization has some advantages. One of them is independency of the initiation reaction on the temperature. Accordingly the polymerization can be effected even at low temperatures without serious reduction in the polymerization rate, leading to

a high kinetic chain length, especially in the case of VAc polymerization. As made clear in chapter 1, the fraction of polymer molecules missing the desired end-group decreases with increase in the kinetic chain length. Other advantages of the radiation telomerization are the ease for raising the rate of initiation to a much higher level than in the catalytic polymerization and no inclusion of undesired fragments from the initiators. In the telomerization using a conventional initiator, a large amount of initiator may be required if the strong degradative chain transfer takes place. This contaminates inevitably the telomer to a significant extent, while a purer telomer can be produced in a high yield by the radiation polymerization even at a low temperature.

In summary one may state that the radiation polymerization is a good method for synthesizing polymers with terminal functional groups. In addition this method is simple compared, for instance, with the radical polymerization with 4:4'-azobis-4-cyanopentanoic acid[10,11] and the anionic living polymerization which is often applied in obtaining polymers with functional end-groups[12].

APPENDIX

Calculation of Rates of Polymerization

When the radiation polymerization in a binary mixture is not accompanied by degradative chain tranfer reaction, the rate of polymerization, R_p, can be calculated simply by[13]

$$\frac{R_p}{R_{p0}} = \frac{1}{[m+(1-m)v_s/v_M]^{3/2}}\left[\frac{1+\phi_{rel}P_{rel}(1-m)/m}{1+P_{rel}(1-m)/m}\right]^{1/2} m \qquad (A1)$$

where v_M and v_s are the molar volumes of monomer and solvent. ϕ_{rel} is ϕ_s/ϕ_M, where ϕ_M and ϕ_s are the probabilities of free radical production from the monomer and the solvent molecule, resp., expressed per unit dose. P_{rel} is defined as the ratio of the probability of energy transfer from the excited monomer molecule M^* to the solvent molecule S, to the probability of the energy transfer from the excited solvent molecule S^* to M. ϕ_{rel} and P_{rel} are generally determined by comparing the observed R_p/R_{p0} with those calculated assuming various ϕ_{rel} and P_{rel} values. The styrene-AC polymerization seems to belong to this case.

However, the expression for R_p becomes more complicated, when an appreciable degradative chain transfer takes place, as in the polymerizations of styrene-TCAC and VAc-CCl_4. In such cases we should use the following expression for R_p, irrespective of the initiation mode :

$$R_p = k_p[P\cdot][M] + k_{re}[S\cdot][M] \tag{A2}$$

$$= \frac{k_p}{k_{t1}^{1/2}}[M]R_i^{1/2}\left\{\frac{(R_i k_{t1})^{1/2} + \frac{k_{re}k_{t1}^{1/2}}{k_{t3}^{1/2}}([M]+C_s[S])}{(R_i k_{t1})^{1/2} + k_{tr}[S] + \frac{k_{re}k_{t1}^{1/2}}{k_{t3}^{1/2}}[M]}\right\} \tag{A3}$$

The elementary reactions assumed for derivation of this kinetic equation and the definition of rate constants in the equation are as follows:

Initiation	$M, S \xrightarrow{\text{radiation}} A\cdot$	R_i	(A4)
	$A\cdot + M \longrightarrow P\cdot$		
Propagation	$P\cdot + M \longrightarrow P\cdot$	$k_p[P\cdot][M]$	(A5)
Chain transfer	$P\cdot + S \longrightarrow P + S\cdot$	$k_{tr}[P\cdot][S]$	(A6)
Reinitiation	$S\cdot + M \longrightarrow P\cdot$	$k_{re}[S\cdot][M]$	(A7)
Termination	$P\cdot + P\cdot \longrightarrow P$	$k_{t1}[P\cdot]^2$	(A8)
	$P\cdot + S\cdot \longrightarrow P$	$k_{t2}[P\cdot][S\cdot]$	(A9)
	$S\cdot + S\cdot \longrightarrow S\text{-}S$	$K_{t3}[S\cdot]^2$	(A10)

In this scheme the symbols have the conventional meaning and other reactions which are not involved in the above are assumed to be negligible. In addition k_{t2} is approximated as the geometrical mean of k_{t1} and k_{t3}[14]. As for the rate of initiation, which is here assumed to proceed independently of other elementary reactions such as termination, the following expression has been proposed by

Nikitina and Bagdasaryan[15] for the radiation polymerization:

$$R_i = I([M]+[S])\left(\frac{\phi_M+\phi_s P_{rel}[S]/[M]}{1+P_{rel}[S]/[M]}\right) \qquad (A11)$$

where I is the dose rate.

Comparison of the observed R_p with that calculated from eqs.(A3) and (A11) taking ϕ_{rel} and P_{rel} as variable parameters allows us to determine the most fitting ϕ_{rel} and P_{rel} values. To do this, however, the kinetic rate constants in eq.(A3) should be available.

Styrene-TCAC Polymerization

k_p and k_{t1} are available from literatures; k_p is 117 $l\cdot mol^{-1}\cdot sec^{-1}$ and k_{t1} is 6.87×10^7 $l\cdot mol^{-1}\cdot sec^{-1}$ [16]. As for k_{re} and k_{t3} the previous study on the catalytic polymerization of styrene in the presence of TCAC at 60°C presents an indication that $k_{re}/k_{t3}^{1/2}$ would be in the present case about 2.6×10^{-4} $l^{1/2}\cdot mol^{-1/2}\cdot sec^{-1/2}$. ϕ_{rel} and P_{rel} were adjusted to obtain the best fit between the observed and calculated values of R_p/R_{p0}. As can be seen from Fig. 2, comparison of both values give a good agreement for ϕ_{rel}=20 and P_{rel}=30.

VAc-CCl_4 Polymerization

In this case it is assumed that P_{rel} is unity and, in addition, that $(R_i k_{t1})^{1/2}$ is negligibly small compared to $(k_{re}k_{t1}^{1/2}/k_{t3}^{1/2})[M]$. The latter assumption can be easily proven to be reasonable in telomerization. ϕ_M and ϕ_s were

estimated with the help of G-values of radical formation from VAc(G_{VAc}) and CCl_4(G_{CCl_4}). The values employed here are 6.2 for G_{VAc} and 15.4 for G_{CCl_4}[15]. The $k_{re}/k_{t3}^{1/2}$ parameter was adjusted to fit in with the experimental result. Apparently, a good agreement is seen in Fig. 6 between the observed and calculated R_p/R_{p0}, when $k_{re}/k_{t3}^{1/2}$ is assumed to be 2.2×10^{-2} $l^{1/2} \cdot mol^{-1/2} \cdot sec^{-1/2}$.

REFERENCES

1. S. Matumoto and M. Maeda, Kobunshi Kagaku, 12, 428 (1955).
2. T. Asahara and T. Makishima, Kogyo Kagaku Zasshi, 69, 2173 (1966).
3. L. J. Lohr, Anal. Chem., 32, 1166 (1960).
4. E. Sawicki, T. R. Hauser, T. W. Stanley, and W. Elbert, Anal. Chem., 33, 93 (1961).
5. D. C. Pepper, J. Polymer Sci., 7, 347 (1951).
6. K. Noma and O. Nishiura, Kobunshikagaku, 7, 269 (1950).
7. A. Chapiro, E. Goethals, and S. Munk, J. Chim. Phys., 57, 47 (1960).
8. C. H. Bamford, R. W. Dyson, and G. C. Eastmond, Polymer, 10, 885 (1969).
9. J.c. Bevington, Radical Polymerization, Academic Press, London and New York, 1961
10. H. W. Melville et al., J. Polymer Sci., 30, 29 (1958); Makromol. Chem., 28, 140 (1958).
11. C. H. Bamford, A. D. Jenkins and R. P. Wayne, Trans. Faraday Soc., 56, 932 (1960).
12. Y. Avny and R. F. Schwenken, Textile Res. J., 37, 817 (1967). M. N. Berger, J. J. K. Boulton, and B. W. Brooks, J. Polymer Sci., A-1, 7, 1339 (1969).

13. A. Chapiro, Radiation Chemistry of Polymeric Systems, John Wiley & Sons, Inc., New York.London (1962).

14. P. W. Allen, F. M. M. Merrett, and J. Scanlan, Trans. Faraday Soc., 51, 95 (1955).

15. T. S. Nikitina and Kh. S. Bagdasaryan, Sbornik Rabot po Radiatsionnoi Khimii, Academy of Science of the USSR, Moscow (1955).

16. M. S. Matheson, E. E. Auer, E. B. Bevilacqua, and E. J. Hart, J. Am. Chem. Soc., 73, 1700 (1951).

CHAPTER 3.

Synthesis of Poly(vinyl Alcohol) Having Terminal Functional Groups by Oxidation

INTRODUCTION

Mino and coworkers[1,2] reported that ceric ion Ce(IV) may be used as an oxidant for the graft or block copolymerization onto PVA and the rate of disappearance of Ce(IV) ion in aqueous solution of PVA without 1,2-glycol unit is smaller than PVA with 1,2-glycol unit. In addition the oxidation of glycols such as pinacol[3] and 2,3-butandiol[4] by Ce(IV) is found to proceed through cleavage of the carbon-carbon bond.

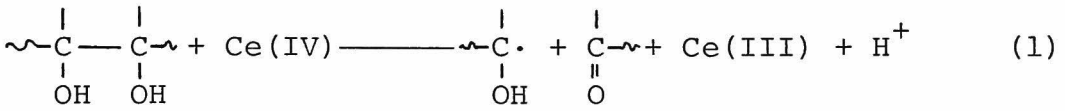

(1)

Therefore, it seems highly possible that the cleavage of the -C-C- bond takes place during the oxidation of polyalcohols such PVA and cellulose which contain 1,2-glycol unit by some amounts in polymers.

This chapter is devoted to shed more insight into the mechanism of the reaction between Ce(IV) and the PVA and to prepare the reactive polymer possessing terminal functional groups.

EXPERIMENTAL

Reaction of PVA with Ce(IV)

Commercial PVA was purified by re-saponification and subsequent Soxhlet extraction with methanol. The number-average degree of polymerization is 1,340 and the content of the 1,2-glycol unit is 1.8 mole%. For comparison, we used also PVA's containing 1.20 and 0.65 mole% 1,2-glycol unit, which were synthesized by radiation-induced polymerization of vinyl acetate at 0 and -78°C[5], respectively. Unless specially mentioned, the PVA containing 1,2-glycol by 1.8 mole% was used in the present work. The ceric salt used is ceric ammonium nitrate, and the stock solution was prepared by dissolving the ceric salt in aqueous HNO_3 solution. The concentration of Ce(IV) was determined volumetrically with ferrous ammonium sulfate using o-phenanthroline as an indicator[2] just prior to the reaction with PVA. The concentration of HNO_3 in the mixture was always adjusted to 0.02N. The reaction was initiated by adding requisite quantity of Ce(IV) solution to PVA solution. The reaction period was recorded from the time when the flask containing the reaction mixture was put in a thermostat kept at a given temperature. In all cases, no attempt was made to exclude air from the reaction mixture. Mino and his co-workers reported the rate of the oxidation of pinacol by ceric sulfate to be the same in nitrogen and in air[3].

Measurement of Absorption Spectra, Solution Viscosity and Gel point

The visible spectra were measured at 20 °C with the use of ESP-3T Hitachi spectrophotometer. The viscosity was measured in an Ostwald viscometer. The gel point of the mixture was determined by visual observation.

Determination of Aldehyde and Carboxyl Groups

After the reaction was allowed to proceed for a given time, the mixture was dialyzed against deionized water to remove ions such as NO_3^- and H^+, since they might interfere with functional group analysis and might cause further reactions. Dialysis was continued for 5 hrs at 0 °C and then for 3 days at room temperature. The amount of aldehyde and carboxyl groups were determined directly with the dialyzed solution by the $NaHSO_3$ method[6] and by the conductivity measurement,[7] respectively.

RESULTS

Visible Spectra Change

The visible spectra exhibit a new peak around 415 nm as shown in Figure 1, indicating the formation of the complex between Ce(IV) and PVA

As is obvious from the lower curve in Figure 2, this absorption increased rapidly with time, reached a maximum and then gradually disappeared.

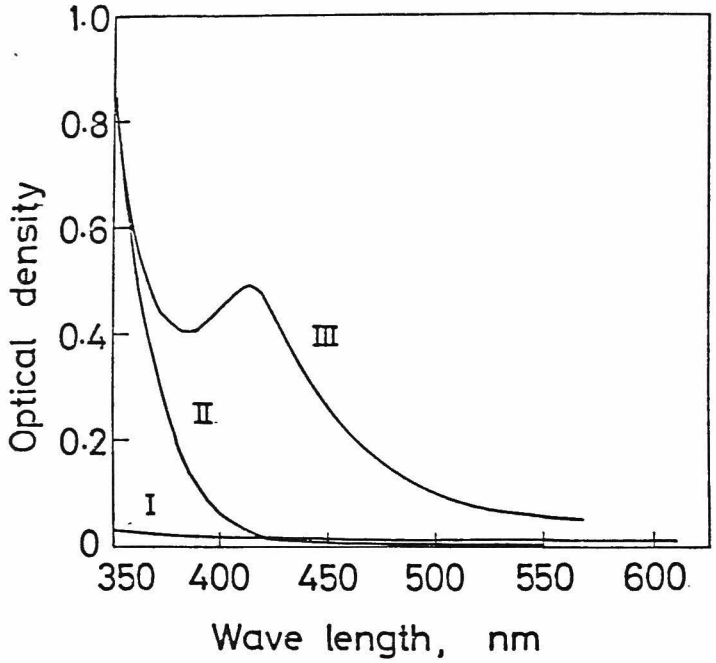

Fig. 1. Visible spectra of aqueous solutions of PVAL, Ce(IV), and the mixture (20 °C): (I) 0.5 wt% PVA solution; (II) 7.2×10^{-4} M Ce(IV); (III) the mixture ([PVA] = 0.5 wt%, [Ce(IV)] = 7.2×10^{-4} M, and [HNO_3] = 0.02 N).

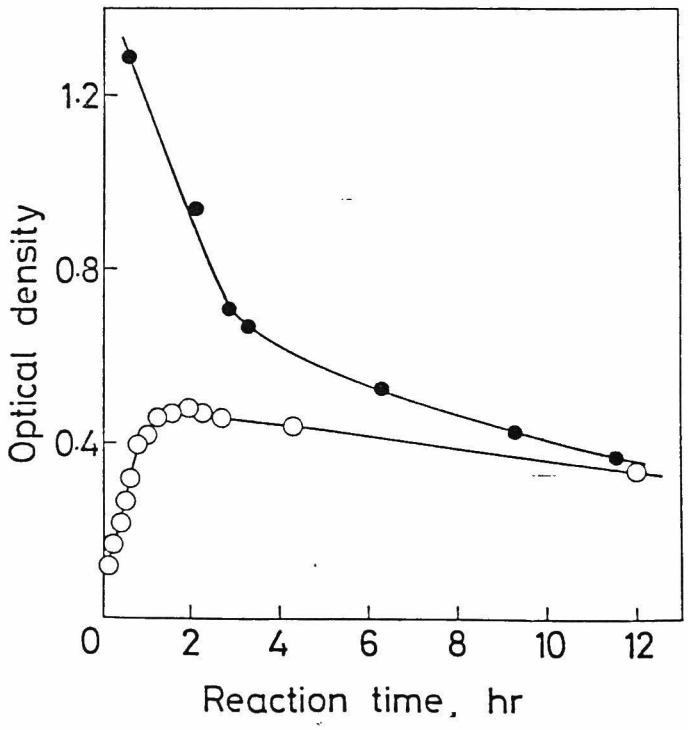

Fig. 2. Change of optical density at 415 nm with time ([PVA] = 0.5 wt% and temp. = 20 °C): (o) 7.2×10^{-4} M Ce(IV); (•) 8.9×10^{-3} M Ce(IV).

This change occurred so markedly at high concentrations of PVA and Ce(IV), and at high temperatures, that the initial steep increase in absorption could not be detected in the upper curve.

Viscosity Change

Figure 3 shows the viscosity change of the reaction mixture at 50 °C and a PVA concentration of 7.0 wt%.

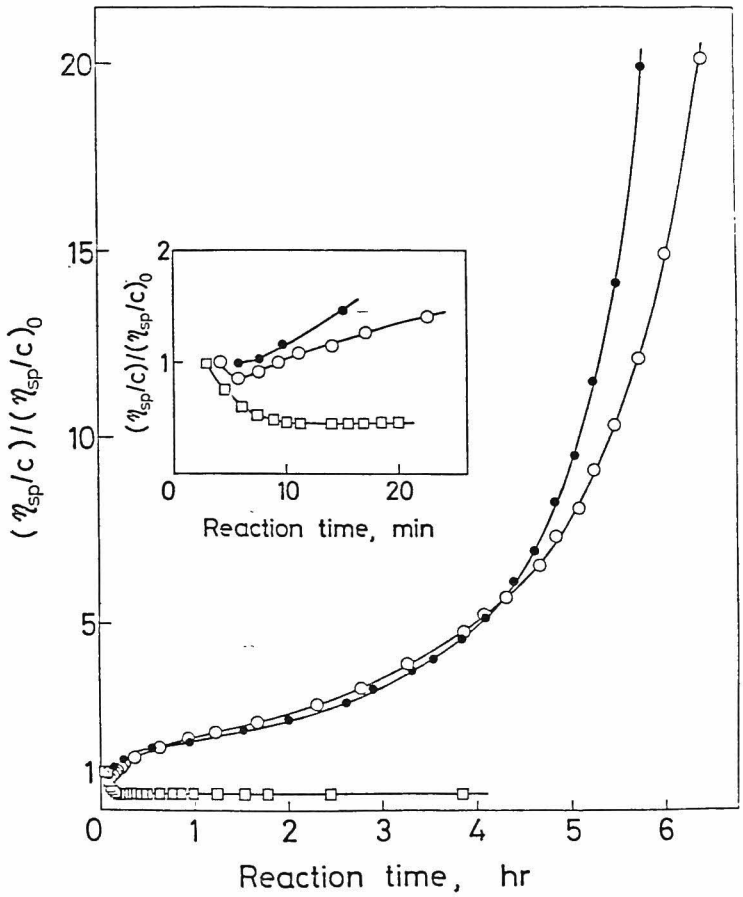

Fig. 3. Change of solution viscosity at different Ce(IV) concentrations ([PVA] = 7.0 wt% and temp. = 50 °C): (o) 0.033 M Ce(IV); (•) 0.075 M Ce(IV); (□) 0.383 M Ce(IV).

It is observed that the viscosity exhibited merely a decrease, wh the Ce(IV) concentration was increased to as high as 0.383 M. On the contrary, gelation of the solution took place at lower Ce(IV) concentrations (0.033 and 0.075 M), though the viscosity decrease in the initial stage of the reaction. The red color of the soluti remained till the viscosity decreased to the minimum.

The dependence of viscosity change on the reaction temperature is given in Figure 4.

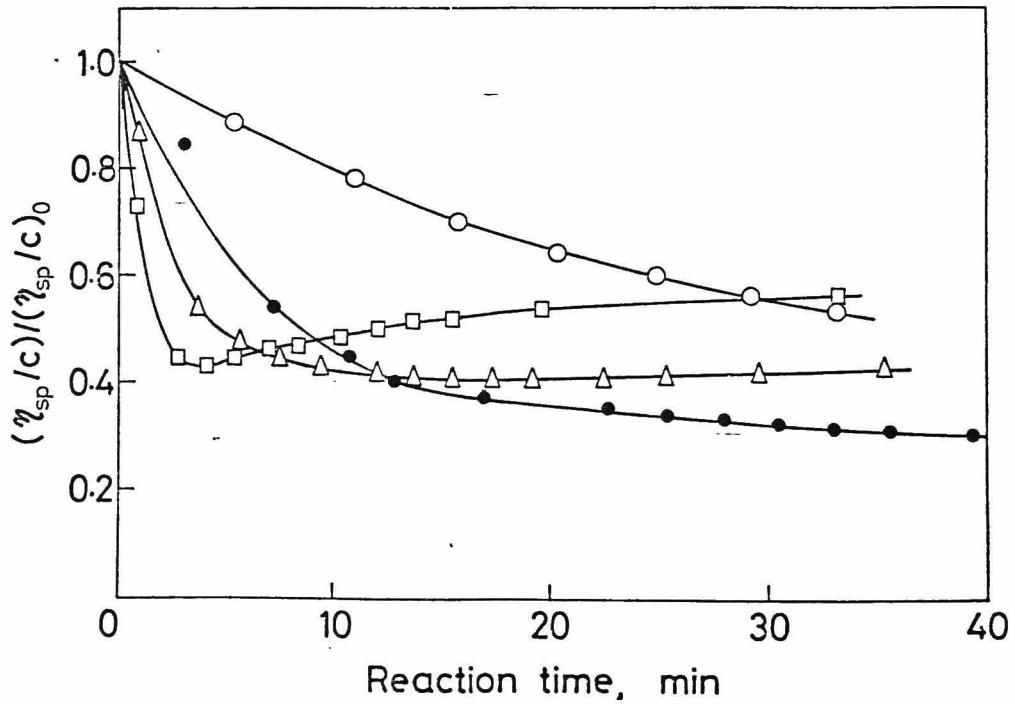

Fig. 4. Change of solution viscosity at different temperatures ([PVA] = 6.0 wt% and [Ce(IV)] = 0.060 M): (o) 0 °C; (•) 20 °C; (Δ) 30 °C; (□) 50 °C.

Clearly, the viscosity decreased sharply in all cases in the initial stage, while it increased again at temperatures higher than 30 °C, finally resulting in gelation. When the temperature was as low as 0 °C, the viscosity did not show a further increase. However, as given in Figure 5, if the temperature was raised, the viscosity increased again and the solution set to a gel. The red color of the solution remained for 50 hrs at 0 °C, but disappeared instantly upon heating to 50 °C.

As is obvious from Figure 3, the change of solution viscosity depends on the Ce(IV) concentration. This influence of Ce(IV) concentration is seen more clearly in Figure 6, which demonstrates the effect of the Ce(IV) and PVA concentrations on the gel point of solution at 50 °C.

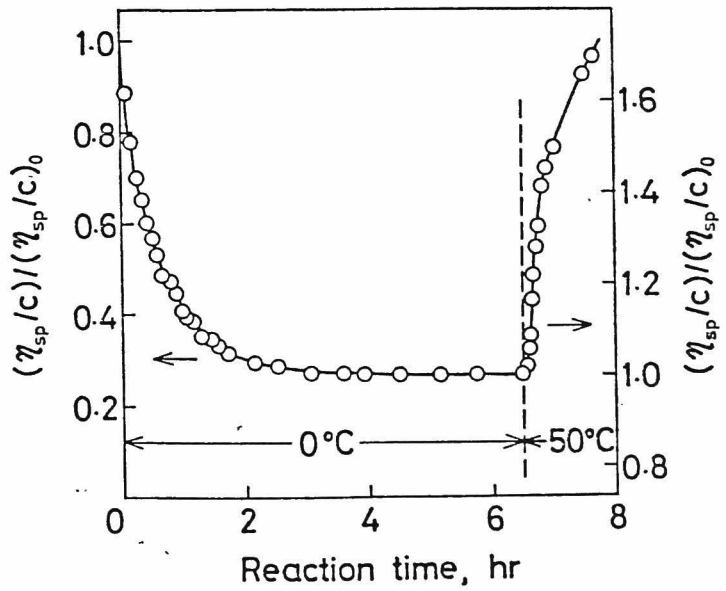

Fig. 5. Change of solution viscosity by temperature rise ([PVA] = 6.0 wt% and [Ce(IV)] = 0.060 M).

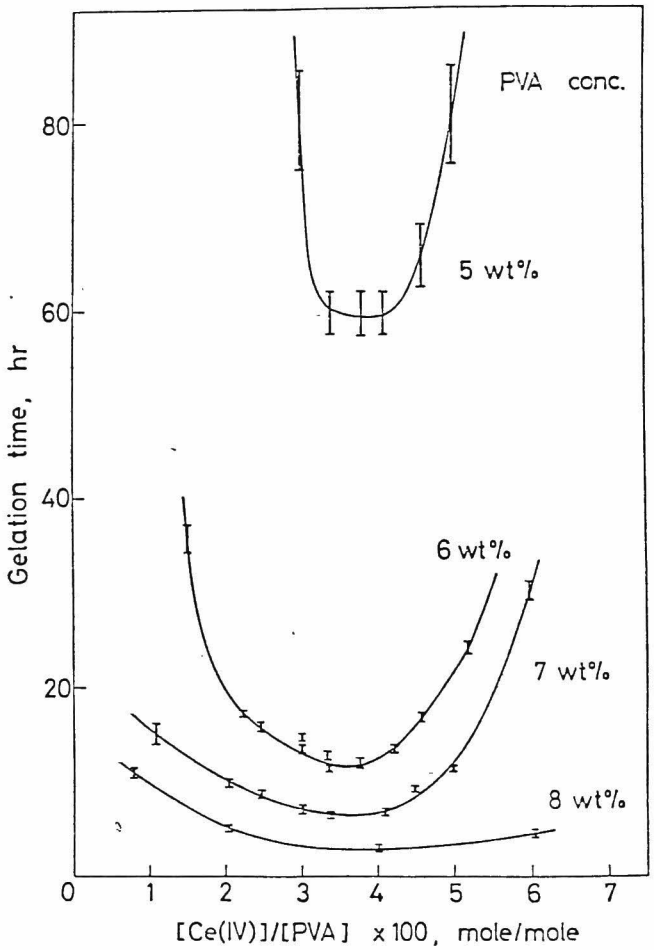

Fig. 6. Gelation of aqueous PVA solution in the presence of Ce(IV) at 50 °C.

Evidently, the gelation of the solution depends strongly on the concentration of PVA as well as that of Ce(IV). The PVA solution of 4 wt% concentration did not set to a gel at 50 °C at least within a week. This trend differs apparently from those observed at the radiation-induced gelation [8] and the gelation by persulfate [9] and vanadium ion [10]. In such cases, gelation occurred in much shorter time, practically independent of the initial polymer concentration, so far as it was higher than 0.1 - 1 wt%, below which formation of micro-gels was observed.

Formation of Aldehyde and Carboxyl Groups

Alcohols of low molecular weight are known to be oxidized by Ce(IV) quantitatively to aldehyde or ketone and, if Ce(IV) is present in excess, further to carboxylic acids [4,11]. Table I describes the amount of aldehyde and carboxyl groups formed on PVA by the oxidation of PVA in 6.0 wt% solution with Ce(IV) at various concentrations.

The reaction was conducted at 0 °C to avoid as much as possible the further oxidation of aldehyde group with Ce(IV). The amount of the aldehyde group formed was determined after the reaction proceeded for 72 hrs, because the red color of solution remained for about 50 hrs. The result given in Table I indicates the formation of aldehyde group, but no carboxyl group. However, the aldehyde group was further oxidized to carboxylic acid, when the temperature of the reaction mixture was raised from 0 to 50 °C. The result is described in Table II.

TABLE I

Determination of Aldehyde and Carboxyl Groups Formed on the PVA [a]

([PVA] 6.0 wt% and Temp. = 0 °C)

$\frac{[Ce(IV)]}{[PVA]}$ [b] x 100, mole/mole	1.00	2.78	3.60	4.59	5.98	6.98	10.0	11.0
$\frac{[-CHO]}{[PVA]}$ [b] x 100, mole/mole	0.89	1.64	2.22	1.96	2.45	2.18	2.16	2.34
$\frac{[-COOH]}{[PVA]}$ [b] x 100, mole/mole		0			0			0

a) The 1,2-glycol content is 1.8 mole%.

b) Based on the monomer unit of PVA .

TABLE II

Change of Amounts of Aldehyde and Carboxyl Groups by Temperature Rise ([PVAL] = 6.0 wt% and [Ce(IV)]/[PVA] [a,b] = 0.15 mole/mole)

	Reacted for 72 hrs at 0 °C	Reacted for 24 hrs after temp. rise to 50 °C
$\frac{[\text{-CHO}]}{[\text{PVA}]^{b)}} \times 100$, mole/mole	1.75	0
$\frac{[\text{-COOH}]}{[\text{PVA}]^{b)}} \times 100$, mole/mole	0	2.19

a) The 1,2-glycol content is 1.8 mole%.

b) Based on the monomer unit of PVA .

DISCUSSION

One of the features found in the present investigation is the peculiar dependence of gelation on the Ce(IV) concentration (Figure 6); there is an optimum Ce(IV) concentration for gel-formation, independent of the PVA concentration. It is of interest to point out that this optimum concentration is 0.036 mole of Ce(IV) to one basic mole of PVA and just twice as large as the content of 1,2-glycol unit present in the PVA molecule (1.8 mole%). To make sure of this relation, a similar experiment was carried out using the PVA samples containing 1,2-glycol unit by 1.20 and 0.65 mole%. The result presented in Figure 7 shows that the PVA containing 1.20 mole% glycol unit exhibits a lowest gelation time at the Ce(IV) concentration corresponding to twice as large as the content of 1,2-glycol unit.

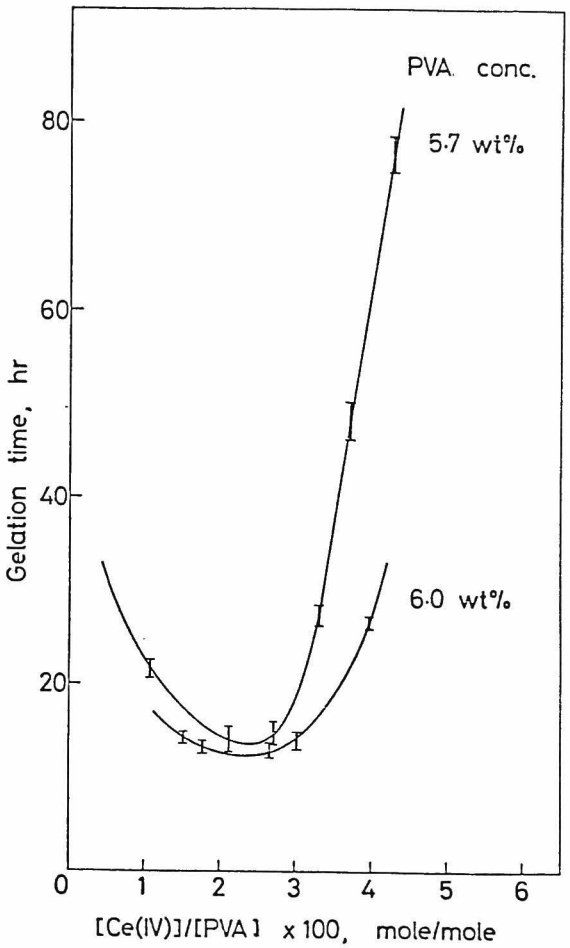

Fig. 7. Gelation of aqueous solutions of the PVA with 1.20 mole% 1,2-glycol unit in the presence of Ce(IV) at 50 °C.

The PVA containing only 0.65 mole% glycol unit did not set to a gel irrespective of Ce(IV) concentration. The other noticeable finding is that aldehyde groups were formed during the reaction at low temperatures, concurrently accompanying a decrease in solution viscosity, as seen in Figure 4 and Table I.

These results suggest strongly that the peculiar viscosity change and the gel-formation occur as a consequence of the oxidative cleavage of 1,2-glycol unit followed by acetalization of aldehyde end groups with hydroxyl groups of PVA . The plausible reaction mechanism is given below.

The 1,2-glycol unit in the PVA seems to be much faster oxidized by Ce(IV) than the 1,3-glycol unit, as also Mino and his co-workers have pointed out[2]. As a result, main-chain scission would occur to give PVA molecules with aldehyde groups at the both chain ends except those produced by the cleavage of the 1,2-glycol unit nearest from the end of PVA chain.

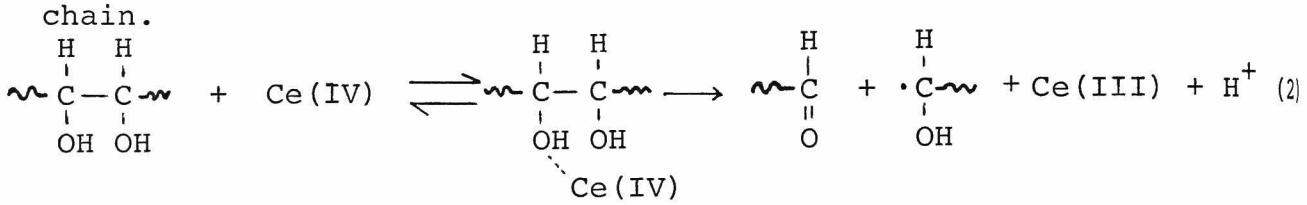

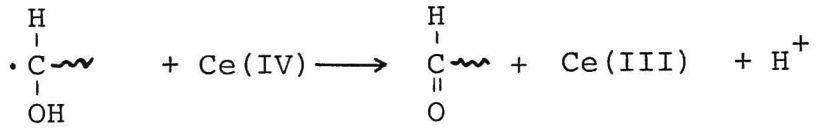

The formation of the complex is evident, since a new absorption band is observed at 415 nm (Figure 1). Trahanovsky and his coworkers have concluded the intermediate to be a monodentate complex[12]. According to the above reaction scheme, two moles of Ce(IV) are needed for the oxidation of one mole of 1,2-glycol unit and two moles of aldehyde are produced from one mole of 1,2-glycol unit[12]. However, the data of Table I demonstrate that the observed aldehyde amount is less than the expected. This may be ascribed to consumption of aldehyde by further reactions. The possibility of the oxidation to carboxyl groups seems very low at 0°C, since the table shows that the materials contain no carboxyl groups.

The degree of polymerization of PVA should decrease as a result of oxidative cleavage of the 1, 2-glycol units present in the main-chain of PVA. On the other hand, the aldehydes formed on the PVA chain end are capable of reacting with hydroxyl groups of PVA to yield acetals, if a sufficient activation energy is given and the medium is acidic.

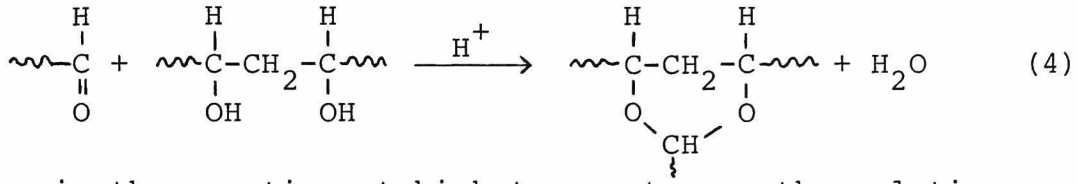

(4)

Hence, in the reaction at high temperatures, the solution viscosity increases again and a gel is finally formed, since the oxidized PVA carrying aldehydes at both chain ends acts as acetalization crosslinker. More detailed studies above the acetalization of the PVA having aldehyde groups at the chain ends are discribed in later chapters.

Another evidence for the occurrence of acetalization is that the gel transforms to sol in plenty of water on heating to 100°C under acidic condition. As is known, the rate of deacetalization is considerably high under suitable conditions. In the present case, the reversible transition between gel and sol took place readily by a slight change in temperature. In Figure 8 the sol-gel transition temperature is plotted as a function of concentration of the PVA solution which contains Ce(IV) by the amount of twice as large as the 1,2-glycol content.

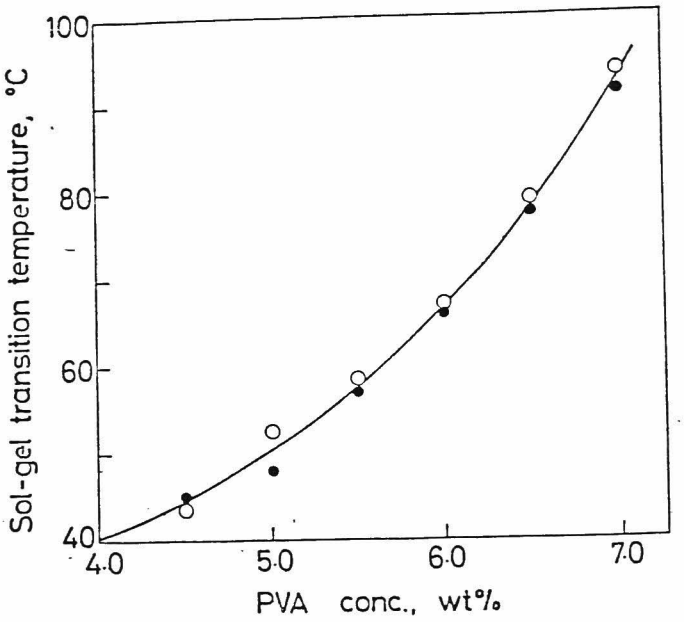

Fig. 8. Comparison of the sol-gel transition temperature - the polymer concentration relationship for solutions of PVA containing Ce(IV) and solutions of periodate-oxidized PVAL: (o) solution of PVAL containing Ce(IV); (•) solution of periodate-oxidized PVA .

The sol-gel transition temperature of solution of the PVA originally possessing aldehyde groups at both chain ends was also given in Figure 8 for comparison. This PVA was obtained by oxidation of the PVA with 1.8 mole% glycol unit by sodium periodate. The good agreement between the both temperatures strongly supports the formation of aldehyde by the oxidation reaction of PVA by Ce(IV).

The retardation in gelation at high Ce(IV) concentrations seen in Figures 3, 6, and 7 is undoubtedly attributed to disappearance of aldehydes owing to the oxidation to carboxyl groups by Ce(IV), a strong oxidizing agent, existing in excess.

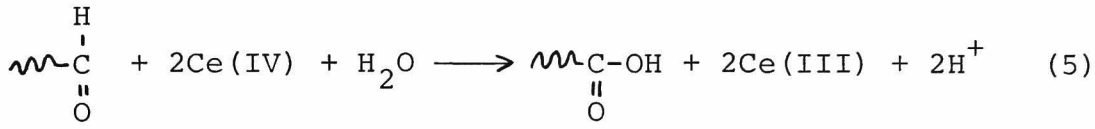

(5)

Table II illustrates that the carboxyl groups are indeed formed at high temperatures. In summary we can introduce aldehyde or carboxyl groups at the both chain ends of PVA under suitable Ce(IV) concentration and temperature as shown in Tables I and II.

REFERENCES

1. G. Mino and S. Kaizerman, J. Polym. Sci., 31, 242 (1958).
2. G. Mino, S. Kaizerman, and E. Rasmussen, J. Polym. Sci., 39, 523 (1959).
3. G. Mino, S. Kaizerman, and E. Rasmussen, J. Amer. Chem. Soc., 81, 1494 (1959).
4. F. R. Duke and R. F. Bremer, J. Amer. Chem. Soc., 73, 5179 (1951).
5. I. Sakurada, Y. Ikada, and Y. Nishizaki, Bull. Inst. Chem. Res., Kyoto Univ., 48, 1 (1970).
6. I. Sakurada and G. Takahashi, Nippon Kagaku Sen'i Kenkyusho Koenshu, 14, 37 (1957).
7. I. Sakurada and O. Yoshizaki, Kobunshi Kagaku, 14, 284 (1957).
8. I. Sakurada and Y. Ikada, Bull. Inst. Chem. Res., Kyoto Univ., 42, 22 (1964).
9. Y. Ikada, Y. Nishizaki, and I. Sakurada, J. Polym. Sci. Polym. Chem. Ed., 12, 1829 (1974).
10. Y. Ikada, Y. Nishizaki, Y. Uyama, T. Kawahara, and I Sakurada,,,,,,,,, J. Polym Sci. Polym. Chem. Ed., 14, 2251 (1976).
11. W. H. Richardson, Oxidation in Organic Chemistry , K. B. Wiberg, Ed., Academic Press, New York & London, Part A, p.244, 1965.
12. W. S. Trahanovsky, J. R. Gilmore, and P. C. Heaton, J. Org. Chem., 38, 760 (1973).

CHAPTER 4.

Interpretation of Rates of Polymer-Polymer Reactions in Terms of Statistical Thermodynamics of Dilute Polymer Solutions

INTRODUCTION

The polymer-polymer reaction may be defined as the reaction where all the reactive groups are attached to the same or different polymeric chains. In this category can be also included the catalytic reaction between polymers carrying reactive and catalytic sites. The reaction of the reactants attached to the same chain is an intramolecular reaction, while the reaction taking place between the different chains is intermolecular. One of the most outstanding features discriminating such reactions of polymeric reactants from the ordinary polymer reactions where either of the interacting groups is a corresponding low-molecular-weight analog, may be contribution of long-range interactions among the segments composing the polymer coils, which would result in resistance to free chain interpenetration, at least in good solvent media.

Such long-range intra- and intermolecular interactions are known to lead to the excluded volume effects in the

statistical thermodynamics of polymer solutions. The intramolecular excluded volume effect has been formulated in terms of expansion coefficient α and the intermolecular excluded volume effect in terms of second virial coefficient A_2. Similar to these coefficients, rate constants of the polymer-polymer reactions in dilute solution have been observed to depend more or less on the molecular weight of polymer reactants, concentrations and the solvating power of the solvent[1,2,3]. It follows that the rate constant may be characterized as a function of physical parameters familiar in theories of dilute polymer solutions. Moreover, one may state that the kinetic study on polymer-polymer reactions may provide good alternative methods to characterize the long-range interactions of polymer coils.

The purpose of this work is to relate the kinetic parameter in the polymer-polymer reactions to the physical parameters in modern theories on dilute polymer solutions. In addition the intramolecular reaction rate constant will be briefly discussed in terms of statistics of polymer chains. In both cases the theories will be developed on the basis of the configurational partition functions of polymeric reactants and their transition state complex. Such rigorous formalization by using recent statistical mechanics on polymer solutions may provide deeper insight concerning the excluded volume effect on the polymer-polymer reactions and allow us to disclose the relationship of the rate constant

with, for instance, the cluster integral β, the penetration function or A_2, in contrast to that by other workers.

Further, we will study in somewhat detail the dependence of the location of the interacting groups along the length of the macromolecule on the reaction rate. The dependence was also studied by Morawetz and his coworkers[4] using a Monte Carlo calculation, but they could not take into account the solvent-polymer interaction and confined themselves to two extreme cases where each reactive (and catalytic) group was attached either to the central segment or to the end of flexible chains.

RESULTS

Reaction Forming a Bonding between two Polymer Chains

To evaluate the contribution of the long-range interaction of polymer segments on the rate of a bimolecular reaction in which the rate-determining step is not the diffusion-controlled but chemical processes, let us consider two flexible polymer chains which are identical except for the incorporation of a small number of reactive groups A to polymer 1 and a small number of reactive groups B, which interact with the groups A, to polymer 2. Under the following assumptions

we derive the rate constant for the reaction by which a bonding is formed between polymers 1 and 2.

a) The solution of the reacting polymers is so dilute that only binary interactions need to be considered.

b) The energy of activation of the reaction under consideration is sufficiently high so that the rate of diffusion of reactants is not a limiting factor for the reaction rate.

Based on the theory of absolute reaction rates[4,5,6], the second-order rate constant k_2 is written as

$$k_2 = \kappa \frac{kT}{h} \frac{Q_{12}^*}{Q_1 Q_2} e^{-\frac{\Delta E_0}{kT}} \qquad (2)$$

where κ is the transmission coefficient, h is the Planck constant, k is the Boltzmann constant, T is the absolute temperature, Q_1, Q_2 and Q_{12}^* are partition functions of the polymeric reactants(1 and 2) and their transition state complex, and ΔE_0 is the difference between the zero-point energy of the polymeric reactants and their transition state complex. A partition function can be approximately expressed as a product of partition functions for each kind of translation, rotation, etc.:

$$\begin{aligned} Q_\nu &= q_\nu \Omega_\nu \qquad (\nu = 1 \text{ or } 2) \\ Q_{12}^* &= q_{12}^* \Omega_{12}^* \end{aligned} \qquad (3)$$

where Ω_ν, Ω_{12}^* are the configurational partition functions of polymeric reactants and their transition state complex, and q_ν, q_{12}^* are the configurational partition functions of polymeric reactants and their transition state complex, and q_ν, q_{12}^* are the products of residual partition functions.

Thus, inserting eq.(3) into eq.(2) we obtain

$$k_2 = \kappa \frac{kT}{h} \frac{q_{12}^*}{q_1 q_2} \frac{\Omega_{12}^*}{\Omega_1 \Omega_2} e^{-\frac{\Delta E_0}{kT}} \tag{4}$$

To derive the configurational partition functions, polymers 1 and 2 are assumed to be linear chains consisting of n+1 segments with complete flexibility connected by n links and the distribution of the link vector $\underset{\sim}{r}$ to be Gaussian:

$$\tau(\underset{\sim}{r}) = \left(\frac{3}{2\pi a^2}\right)^{3/2} \exp\left(-\frac{3\underset{\sim}{r}^2}{2\,a^2}\right) \tag{5}$$

where a is the root-mean-square length of the link. Further, the mean-force potential of segment interaction is assumed to be additive over segment pairs. For the sake of convenience, we assign for a while the notation with different subscripts $w_1(\underset{\sim}{R}_{ij})$ or $w_2(\underset{\sim}{R}_{ij})$, for the pair potential of mean force as a function of the separation $\underset{\sim}{R}_{ij}$ between segments i and j, depending on whether two segments belong to the same chain or to different chains. These are identical

in nature and in magnitude with each other. For the pair potential, it is further assumed that they approach zero so rapidly as $\underset{\sim}{R}_{ij}$ increases that we may approximate as

$$\exp\left(-\frac{W_\sigma(\underset{\sim}{R}_{ij})}{kT}\right)=1-\beta_\sigma\delta(\underset{\sim}{R}_{ij}) = \exp[-\beta_\sigma\delta(\underset{\sim}{R}_{ij})] \qquad (\sigma=1 \text{ or } 2) \tag{6}$$

where β_σ is the familiar cluster integral, $\delta(\underset{\sim}{R}_{ij})$ is the three-dimensional Dirac delta function. The distribution function $f_0(\nu)$ (ν=1 or 2) is represented as

$$f_0(\nu)=\prod_{i_\nu=1}^{n}\tau(\underset{\sim}{r}_{i_\nu}) \qquad (\nu=1 \text{ or } 2) \tag{7}$$

Using eqs.(6) and (7) we can express Ω_ν as

$$\Omega_\nu=\int f_0(\nu)\exp\left[-\beta_1\sum_{i_1=0}^{n}\sum_{j_1=i_1+1}^{n}\delta(\underset{\sim}{R}_{i_1 j_1})\right]d(\nu) \qquad (\nu=1 \text{ or } 2) \tag{8}$$

The Ω_{12}^* value depends on the location of the reactive groups along the length of the chain molecule.

First, we deal with the case that the reacting group A is incorporated to the ℓ_1th segment of polymer 1 and the other group B to the m_2th segment of polymer 2. Then the transition state complex will be a random flight cruciform molecule joined at the segments ℓ_1 and m_2, as illustrated in Fig. 1(a).

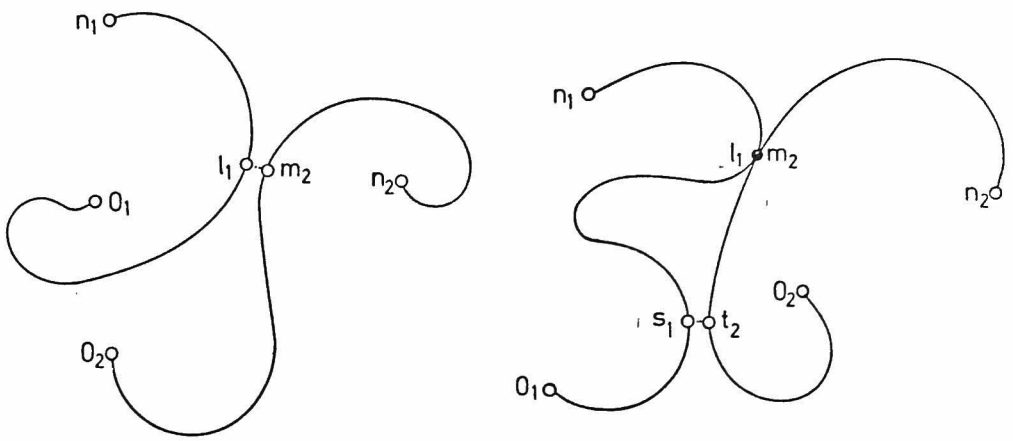

Fig. 1 Schematic representation of intermolecular(a) and intramolecular(b) reactions.

This leads to

$$\Omega_{12}^{*} = \int \delta(\underset{\sim}{R}_{l_1 m_2}) \exp[-\beta_1 \sum_{i_1=0}^{n} \sum_{j_1=i_1+1}^{n} \delta(\underset{\sim}{R}_{i_1 j_1}) - \beta_1 \sum_{i_2=0}^{n} \sum_{j_2=i_2+1}^{n} \delta(\underset{\sim}{R}_{i_2 j_2})$$

$$- \beta_2 \sum_{j_1=0}^{n} \sum_{j_2=0}^{n} \delta(\underset{\sim}{R}_{j_1 j_2})] \, f_0(1) f_0(2) d(1,2) \qquad (9)$$

where (ν) and $(1, 2)$ represent the total coordinates of n+1 segments of polymer ν and those of 2n+2 segments of cruciform molecule, respectively.

Inserting eqs.(7), (8) and (9) into (4) we obtain

$$k_2=\kappa\frac{kT}{h}\frac{q_{12}^*}{q_1q_2}e^{-\frac{\Delta E_0}{kT}}\int\delta(\underset{\sim}{R}_{\ell_1m_2})\exp[-\beta_2\sum_{j_1=0}^{n}\sum_{j_2=0}^{n}\delta(\underset{\sim}{R}_{j_1j_2})]f(1)f(2)d(1,2)$$

$$=\kappa\frac{kT}{h}\frac{q_{12}^*}{q_1q_2}e^{-\frac{\Delta E_0}{kT}}I_{\ell_1m_2}(\beta_2) \qquad (10)$$

with

$$f(\nu)=\frac{f_0(\nu)\exp[-\beta_1\sum_{i_\nu=0}^{n}\sum_{j_\nu=i_\nu+1}^{n}\delta(\underset{\sim}{R}_{i_\nu j_\nu})]}{\int f_0(\nu)\exp[-\beta_1\sum_{i_\nu=0}^{n}\sum_{j_\nu=i_\nu+1}^{n}\delta(\underset{\sim}{R}_{i_\nu j_\nu})]d(\nu)} \qquad (\nu=1 \text{ or } 2) \qquad (11)$$

$$I_{\ell_1m_2}(\beta_2)=\int\delta(\underset{\sim}{R}_{\ell_1m_2})\exp[-\beta_2\sum_{j_1=0}^{n}\sum_{j_2=0}^{n}\delta(\underset{\sim}{R}_{j_1j_2})]f(1)f(2)d(1,2) \qquad (12)$$

The rate constant k_2^0 of reaction where the long-range interference does not exist, is simply given by

$$k_2^0=\kappa\frac{kT}{h}\frac{q_{12}^*}{q_1q_2}e^{-\frac{\Delta E_0}{kT}}I_{\ell_1m_2}(0)=\kappa\frac{kT}{h}\frac{q_{12}^*}{q_1q_2}e^{-\frac{\Delta E_0}{kT}} \qquad (13)$$

Then

$$\frac{k_2}{k_2^0}=I_{\ell_1m_2}(\beta_2) \qquad (14)$$

Thus the excluded volume effect on k_2 is reduced to estimation of $I_{\ell_1m_2}(\beta_2)$ which can be derived by the following methods.

a. Smoothed-density model[7,8] We assume for the flexible chain the uniform expansion which consists of replacing the original chain by an effective Gaussian chain with a conventional link length, $\bar{a}=\alpha a$, where α is the expansion coefficient of one polymer molecule.

The distribution function $f(\nu)$ (ν=1 or 2) may then be written as

$$f(\nu) = \bar{f}_0(\nu) = \prod_{i_\nu=0}^{n} \bar{\tau}(\underset{\sim}{r}_{i_\nu}) \qquad (\nu=1 \text{ or } 2) \tag{15}$$

with

$$\bar{\tau}(\underset{\sim}{r}_{i_\nu}) = \left(\frac{3}{2\pi\bar{a}^2}\right)^{3/2} \exp\left(-\frac{3\underset{\sim}{r}_{i_\nu}^2}{2\bar{a}^2}\right) \qquad (\nu=1 \text{ or } 2) \tag{16}$$

By using eqs.(12) and (15), $I_{\ell_1 m_2}(\beta_2)$ can be expressed as

$$I_{\ell_1 m_2}(\beta_2) = \int \delta(\underset{\sim}{R}_{\ell_1 m_2}) \left[\prod_{j_1=0}^{n} \prod_{j_2=0}^{n} (1-\beta_2 \delta(\underset{\sim}{R}_{j_1 j_2})) \right] \bar{f}_0(1) \bar{f}_0(2) d(1,2)$$

$$= \int \left[\delta(\underset{\sim}{R}_{\ell_1 m_2}) - \beta_2 \sum_{j_1=0}^{n} \sum_{j_2=0}^{n} \delta(\underset{\sim}{R}_{\ell_1 m_2}) \delta(\underset{\sim}{R}_{j_1 j_2}) + \cdots \right] \bar{f}_0(1) \bar{f}_0(2) d(1,2) \tag{17}$$

Let us introduce the distribution function $\bar{P}_0(\underset{\sim}{S}_{i_\nu}, \underset{\sim}{S}_{j_\nu}, \cdots \underset{\sim}{S}_{t_\nu})$ (ν=1 or 2):

$$\bar{P}_0(\underset{\sim}{S}_{i_\nu}, \underset{\sim}{S}_{i_\nu}, \cdots, \underset{\sim}{S}_{t_\nu}) = \frac{\bar{f}_0(\nu) d(\nu)_{int}}{d\underset{\sim}{S}_{i_\nu} d\underset{\sim}{S}_{j_\nu} \cdots d\underset{\sim}{S}_{t_\nu}} \qquad (\nu=1 \text{ or } 2) \tag{18}$$

where the symbol $(\nu)_{int}$ represents the total internal coordinates of polymer ν and $\underset{\sim}{S}_{i_\nu}$ the distance between the center of mass and the i_νth segment of polymer ν (ν=1 or 2). In this model the following factorization approximation is employed:

$$\bar{P}_0(\underset{\sim}{S}_{i_\nu}, \underset{\sim}{S}_{j_\nu}, \cdots, \underset{\sim}{S}_{t_\nu}) = \bar{P}_{0,i_\nu}(\underset{\sim}{S}_{i_\nu}) \cdots \bar{P}_{0,t_\nu}(\underset{\sim}{S}_{t_\nu}) \qquad (19)$$

where $\bar{P}_{0,i_\nu}(\underset{\sim}{S}_{i_\nu})$ may be written as

$$\bar{P}_{0,i_\nu}(\underset{\sim}{S}_{i_\nu}) = \left(\frac{3}{2\pi\langle S^2_{i_\nu}\rangle}\right)^{3/2} \exp\left(-\frac{3\underset{\sim}{S}^2_{i_\nu}}{2\langle S^2_{i_\nu}\rangle}\right) \quad (\nu=1 \text{ or } 2) \qquad (20)$$

with

$$\langle S^2_{i_\nu}\rangle = \frac{1}{3} n\bar{a}^2\left[1-\frac{3i_\nu(n-i_\nu)}{n^2}\right] \qquad (21)$$

Then $I_{\ell_1 m_2}(\beta_2)$ can be obtained as

$$I_{\ell_1 m_2}(\beta_2) = \iint [\bar{P}_{0,\ell_1}(\underset{\sim}{S}_{\ell_1})\bar{P}_{0,m_2}(\underset{\sim}{S}_{\ell_1}-\underset{\sim}{S}_{12}) \exp\left(-\beta_2 \sum_{j_1=0}^{n}\sum_{j_2=0}^{n}\int P_{0,j_1}(\underset{\sim}{S}_{j_1})\bar{P}_{0,j_2}(\underset{\sim}{S}_{j_1}-\underset{\sim}{S}_{12})d\underset{\sim}{S}_{j_1}\right)] d\underset{\sim}{S}_{l_1} d\underset{\sim}{S}_{12} \qquad (22)$$

where $\underset{\sim}{S}_{12}$ is the distance between the center of mass of polymer 1 and that of polymer 2. Here let us use the Flory-Krigbaum potential:

$$-\beta_2 \sum_{j_1=0}^{n}\sum_{j_2=0}^{n}\int \bar{P}_{0,j_1}(\underset{\sim}{S}_{j_1})\bar{P}_{0,j_2}(\underset{\sim}{S}_{j_1}-\underset{\sim}{S}_{12})d\underset{\sim}{S}_{j_1} = n^2\beta_2\left(\frac{3}{4\pi\langle S^2\rangle}\right)\exp\left(-\frac{3\underset{\sim}{S}^2_{12}}{4\langle S^2\rangle}\right) \qquad (23)$$

with

$$\langle S^2 \rangle = \frac{1}{6} n \bar{a}^2 \tag{24}$$

Then, using eqs.(20) and (23), we obtain

$$I_{\ell_1 m_2}(\beta_2) = \left(\frac{1}{2-3\frac{\ell_1}{n}(1-\frac{\ell_1}{n})-3\frac{m_2}{n}(1-\frac{m_2}{n})}\right)^{3/2} \sum_{k=0}^{n} \frac{(-3^{3/2}\bar{z})^k}{k![k+\frac{1}{2-3\frac{\ell_1}{n}(1-\frac{\ell_1}{n})-3\frac{m_2}{n}(1-\frac{m_2}{n})}]^{3/2}} \tag{25}$$

with

$$\bar{z} = \left(\frac{3}{2\pi a^2}\right)^{3/2} \beta n^{1/2} \frac{1}{\alpha^3} \qquad (\because \beta_2 = \beta_1 = \beta) \tag{26}$$

b. Differential-equation approach According to Kurata et al.[9], $I^{-1}_{\ell_1 m_2}(\beta_2) \frac{\partial I_{\ell_1 m_2}(\beta_2)}{\partial \beta_2}$ can be written as

$$I^{-1}_{\ell_1 m_2}(\beta_2) \frac{\partial I_{\ell_1 m_2}(\beta_2)}{\partial \beta_2} = - \sum_{j_1=0}^{n} \sum_{j_2=0}^{n} P^*(0_{j_1 j_2})_{\ell_1 m_2} \tag{27}$$

where $P^*(0_{j_1 j_2})_{\ell_1 m_2}$ is the conditional probability that segments j_1 and j_2 are in contact given the initial contact between ℓ_1 and m_2. This is written in the form:

$$P^{*}(0_{j_1 j_2})_{\ell_1 m_2} = \left(\frac{3}{2\pi a^{*2}(\ell_1 m_2)}\right)^{3/2} C_1^{-\frac{3}{2}} = \left(\frac{3}{2\pi \bar{a}^{2}}\right)^{3/2} C_1^{-3/2} \frac{1}{\alpha^{*3}(\ell_1 m_2)} \tag{28}$$

with

$$C_1 = |j_1 - \ell_1| + |j_2 - m_2| \tag{29}$$

When we assume $\alpha^{*3}(\ell_1, m_2)$ as

$$\alpha^{*3}(\ell_1, m_2) = 1 + \kappa(\ell_1, m_2) Z \tag{30}$$

where α^{*} is the additional expansion factor of the cruciform molecule due to the interaction between polymers 1 and 2, then, we obtain

$$I_{\ell_1 m_2}(\beta_2) = \{1 + \kappa(\ell_1, m_2)\bar{Z}\}^{-\frac{A}{\kappa(\ell_1, m_2)}} \tag{31}$$

with

$$A = 4\times\{2\left(\frac{\ell_1}{n}\right)^{1/2} + 2\left(\frac{m_2}{n}\right)^{1/2} + 2\left(1-\frac{\ell_1}{n}\right)^{1/2} + 2\left(1-\frac{m_2}{n}\right)^{1/2}$$

$$- \left(\frac{\ell_1}{n}+\frac{m_2}{n}\right)^{1/2} - \left(1-\frac{\ell_1}{n}+\frac{m_2}{n}\right)^{1/2} - \left(1+\frac{\ell_1}{n}-\frac{m_2}{n}\right)^{1/2} - \left(2-\frac{\ell_1}{n}-\frac{m_2}{n}\right)^{1/2}\} \tag{32}$$

Second, we estimate the average rate constant of the reaction which takes place between the reactive group A linked to any segment of polymer 1 with equal probability and the reactive group B linked to any segment of polymer 2 with equal probability. Clearly, this rate constant $\bar{k}_2$ can be given by averaging the rate constant derived above:

$$\bar{k}_2 = \frac{1}{n^2} \sum_{\ell_1=0}^{n} \sum_{m_2=0}^{n} \kappa \frac{kT}{h} \frac{q_{12}^*}{q_1 q_2} e^{-\frac{\Delta E_0}{kT}} I_{\ell_1 m_2}(\beta_2) \tag{33}$$

then

$$\frac{\bar{k}_2}{k_2^0} = \frac{1}{n^2} \sum_{\ell_1=0}^{n} \sum_{m_2=0}^{n} I_{\ell_1 m_2}(\beta_2) = I(\beta_2) \tag{34}$$

Here $\bar{k}_2^0$ denotes the rate constant of the reaction in which the excluded volume effect is absent. On the other hand, the second virial coefficient A_2 is expressed as

$$A_2 = \left(\frac{N_A n^2 \beta_2}{2M^2}\right) h_0(\bar{Z}) \tag{35}$$

where M is the molar mass of polymer, N_A is Avogadro's number, and $h_0(\bar{Z})$ is a function of $\bar{Z}$. Differentiation of A_2 with respect to β_2

$$\frac{\partial A_2}{\partial \beta_2} = \left(\frac{N_A n^2}{2M^2}\right) I(\beta_2) = \frac{N_A n^2}{2M^2} \frac{\partial}{\partial \bar{Z}} [\bar{Z} h_0(\bar{Z})] \tag{36}$$

Then we obtain

$$I(\beta_2) = \frac{\partial}{\partial \bar{Z}}[\bar{Z}h_0(\bar{Z})] \tag{37}$$

$\bar{Z}h_0(\bar{Z})$ is called the penetrating function which characterizes the mutual interpenetration of polymer coils. Thus eq.(34) can be written as

$$\frac{\bar{k}_2}{k_2^0} = I(\beta_2) = \frac{\partial}{\partial \bar{Z}}[\bar{Z}h_0(\bar{Z})] \tag{38}$$

In contrast with the case where the reacting groups A and B are attached to the respective, given segments, the average rate constant for the reaction of the reactive groups attached to any of segments, is simply equal to the first derivative of the penetrating function which has been computed by various workers.

Reaction Forming a Bonding within Two Chains Linked to Each Other

Finally we will assess the rate constant for the reaction after formation of the first bonding between polymer 1 carrying g_1 reactive groups A and polymer 2 carrying g_2 groups B. When the first bonding has been formed with the rate constant k_2 to link the two chains to each other, the remain-

ing group A of the chain 1 is assumed to react with the group B in the chain 2 linked to the chain 1, resulting in formation of the second bonding. This assumption seems to be reasonable, since the reactive groups B belonging to other, non-linked chains are existing more remotely in dilute solution than those in the linked chain. As schematically represented in Fig.1(b),we assume that the first bonding has been formed between the reactive group on the ℓ_1th segment of polymer 1 and the group on the m_2th segment of polymer 2. Then the pseudo first-order rate constant k_1 for the formation of the second bonding can be readily shown to be

$$k_1 = k_2^0 \frac{1}{n^2} \sum_{\ell_1=0}^{n} \sum_{m_2=0}^{n} \sum_{s_1=0}^{n} \sum_{t_2=0}^{n} g_{j_1} g_{j_2} \frac{\Omega_{\ell_1 \ell_2, s_1 t_2}}{\Omega_{\ell_1 \ell_2}} \qquad (39)$$

Here $\Omega_{\ell_1 m_2}$ and $\Omega^*_{\ell_1 m_2, s_1 t_2}$ are the configurational partition functions of the polymeric reactant and the transition state complex in which the reactive group on the s_1th segment of polymer chain 1 is to react with that on the t_2th segment of chain 2, respectively. k_2^0 is the rate constant corresponding to the low-molecular-weight analogs. g_{s_1} (or g_{t_2}) is taken to be unity if the s_1th(or t_2th) segment has the reactive group A (or B) and zero if it has no reactive group. Provided that any of the reactive groups can participate in the reaction, g_{s_1} and g_{t_2} should be equal to

$$\varsigma_{s1} = \frac{g_1}{n}, \qquad \varsigma_{t_2} = \frac{g_2}{n} \tag{40}$$

Since the polymeric reactant molecule is a cruciform, $\Omega_{\ell_1 m_2}$ in eq.(39) is identical to that given by eq.(9). Thus $\Omega^*_{\ell_1 m_2, s_1 t_2}$ can be expressed as

$$\Omega^*_{\ell_1 m_2, s_1 t_2} = \int \delta(\underset{\sim}{R}_{s_1 t_2})\delta(\underset{\sim}{R}_{\ell_1 m_2})\exp[-\beta_2 \sum_{\ell_1=0}^{n} \sum_{m_2=0}^{n} \delta(\underset{\sim}{R}_{\ell_1 m_2})]f(1)f(2)d(1,2) \tag{41}$$

Substitution of eqs.(9), (40), and (41) into eq.(39) leads to

$$k_1 = k_2^0 \frac{g_1 g_2}{n^2} \frac{1}{n^2} \sum_{\ell_1=0}^{n} \sum_{m_2=0}^{n} \sum_{s_1=0}^{n} \sum_{t_2=0}^{n} P^*(0_{s_1 t_2})_{\ell_1 m_2} \tag{42}$$

$P^*(0_{s_1 t_2})_{\ell_1 m_2}$ has the same definition as in eq.(27). Then, from eqs.(27) and (28) one can get

$$k_1 = k_2^0 \, g_1 g_2 \, \frac{5.73}{[1+\kappa\bar{z}]} \left(\frac{3}{2\pi a^2 n}\right)^{3/2} \frac{1}{\alpha^3} \tag{43}$$

In the above derivation $\kappa(\ell_1, m_2)$ in eq.(30) was assumed to be κ, independent of location of ℓ_1 and m_2.

DISCUSSION

In the foregoing theories we have developed the computation, starting with the polymer reactants carrying a so small number of reactive groups that may not interefere with the estimation of configurational partition functions of the polymeric reactants and their transition state complexes. It is noteworthy that the present theory is also applicable to catalytic reactions yielding no irreversible chemical bonds. In the derivation of the bimolecular rate constant k_2 it was implicitly assumed that two or more bondings would not be formed at the same time between the polymers 1 and 2. This may be a reasonable assumption because the possibility for two or more groups A belonging to the same chain to encounter other groups B at the same time, must be extremely low, as the number of reactive groups is small. However, after formation of the first bonding which links two polymer chains 1 and 2 to each other, the second reaction between the groups A and B would be readily followed by the successive reactions within the linked chains, till all the reactive groups are consumed or some steric hindrance, pointed out by Vollmert[10], becomes predominant. For simplicity, therefore, we will confine ourselves to discussion on reactions with the polymers carrying two respective reactive groups in a chain.

Eqs.(14) and (38) allow us to estimate the rate constants for the intermolecular reactions. As an example we will compute the rate constant of the reaction between the reactive group A attached to the end segment (the 0th or the nth) of polymer 1 and the reactive group B attached to the m_2th segment of polymer 2. The ratios of the rate constant to be observed for the reaction in dilute solutions of good solvent media to that in dilute solutions without the excluded volume effect were calculated according to eqs.(25) and (31) and plotted against m_2/n, which specifies the location of the reactive groups, in Figs. 2 and 3, respectively. As also

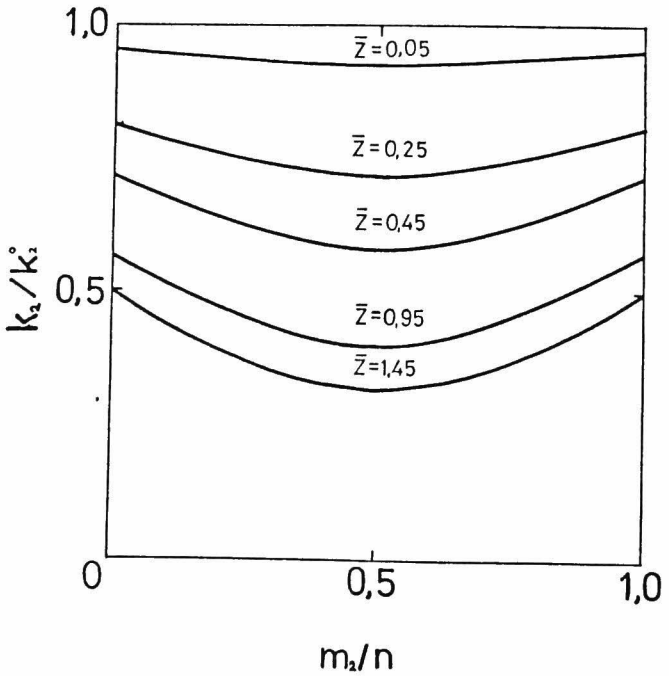

Fig. 2 Plots of k_2/k_2^0 against m_2/n for different $\bar{Z}$'s based on eqs.(14) and (25).

predicted by Morawetz and his coworkers[4], the results of theory clearly indicate that the reaction should be faster between the end segments (m_2/n=0 or 1). However, this dependence of reaction rate on the location of the reactive group is not large, so that it would not be surprising even if a reaction of polymers carrying more than one reactive groups randomly distributed follows strictly second-order kinetics over the whole reaction period, unless the veriation in rate with time is determined with extremely high precision.

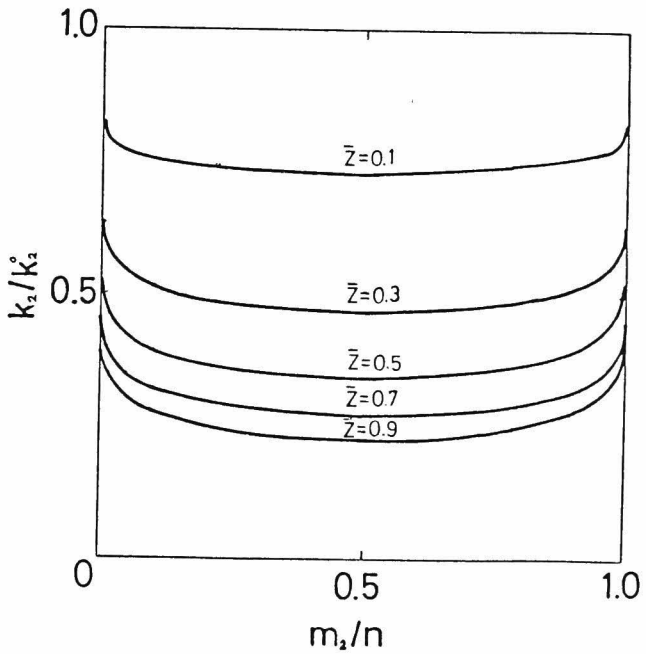

Fig. 3 Plots of k_2/k_2^0 against m_2/n for different $\bar{Z}$'s based on eqs.(14) and (31) with K=3.903[8].

The rate constant averaged with respect to the location of the reactive groups is shown in Fig. 4. In this calculation we used a set of $h_0(\bar{z})$-$\bar{z}$ relations derived by various workers. In any cases it is apparent that with the increasing $\bar{z}$ the rate constant decreases rapidly followed by a slow change. The most striking feature is that the excluded volume effect does not remarkably reduce the rate of polymer-polymer

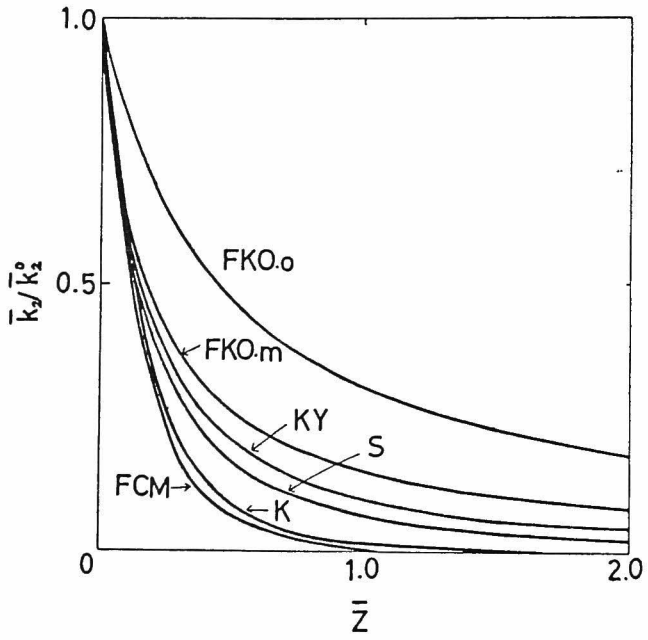

Fig. 4 Plots of $\bar{k}_2/\bar{k}_2^0$ against $\bar{z}$ based on eq.(38). Various theoretical values of $h_0(\bar{z})$ were employed for the estimation, Curve FKO, o: the original Flory-Krigbaum-Orofino theory[11], Curve FKO, m: the modified Flory-Krigbaum-Orofino theory[12], Curve KY: the Kurata-Yamakawa theory[8], Curve S: the Stockmayer equation[12], Curve K: the Kurata theory[9]. Curve FCM: the Fixman-Casassa-Markovitz theory[13].

reactions. Since among many theories in dilute polymer solutions those of Kurata-Yamakawa(KY) and modified Flory-Krigbaum-Orofino(FKO, m) are known to be the most compatible with the observed experimental data and $\bar{z}$ is generally not larger than 2, the k_2/k_2^0 ratio seems to range between 1 and 0.1 in the ordinary reactions. In an intermolecular acetalization of poly(vinyl alcohol) having an aldehyde we have found that the k_2/k_2^0 ratios are in this range when the reaction is carried out in dimethylsulfoxide, a good solvent for PVA ..

In view of the rather small excluded volume effect and the relatively poor accuracy in determining the rate constant for the polymer-polymer reaction in dilut solution, a satisfactory comparison of the theoretical with the experimental result will be not easy.

Following the above-stated first bond formation resulting in linking of the two polymer chains, the second reaction will take place within the domain involving the two chains linked, with the rate constant k_1 given by eq.(43). Fig. 5 gives the estimates of k_2'/k_2^0 plotted against the stoichiometric molar concentration of the reactive group A, C_A. k_2' represents the apparent second-order rate constant and related to k_1 by the equation

$$-d\, C_A/dt = k_1\, C_B = k_2'\, C_A\, C_B \qquad (44)$$

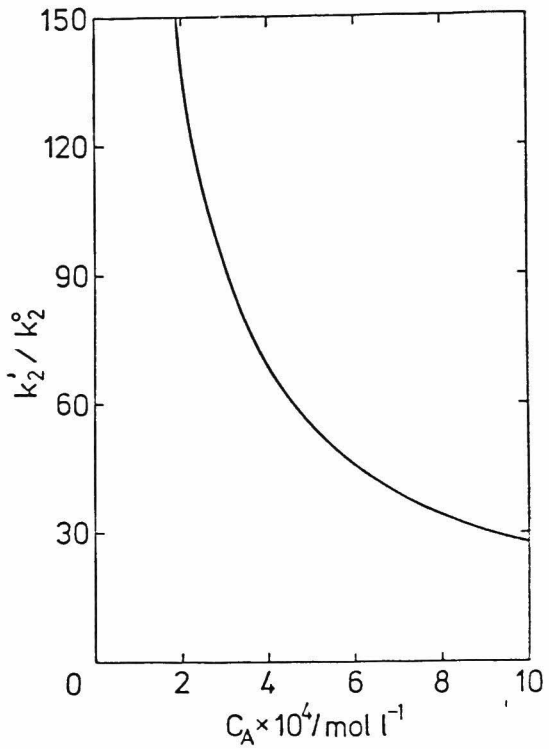

Fig. 5 Plots of k_2'/k_2^0 against C_A based on eq.(43) for $g_1=10$, $g_2=10$, $\bar{Z}=0$, $\alpha=1$, and $na^2=5.07\times10^{-12}$ (e.g., polystyrene with molecular weight of 10^5).

Here C_B is the concentration of the reactive group B in the solution. The subscripts A and B are interchangeable. For simplicity, the solution is assumed to be in a Ⓗ state. As can be seen, k_2'/k_2^0 becomes exceedingly higher than unity, as C_A is decreased. The high k_2'/k_2^0 observed by Morawetz and his coworkers[1] might be explained partly in terms of this intramolecular reaction. Very high k_2'/k_2^0 ratios seen in the range of low C_A is not unexpected, because it is readily shown that

$$\frac{k_2'}{k_2^0} = \frac{C_B^{eff}}{C_B} \qquad (45))))$$

where C_B^{eff} is the effective concentration of the group B in the neighborhood of the group A. This has the same definition as Morawetz and his coworkers[14] gave. We have also determined the effective concentration for the intramolecular acetalization of PVA with an aldehyde end-group and found that the agreement of the experimental result with the estimate was satistactory.

Finally it should be noted that much more kinetic experimental data must be accumulated, till the excluded volume effect on the polymer-polymer reactions is able to be understood in a more quantitative manner.

REFERENCES

1. J.-R. Cho and H. Morawetz, Macromolecules, 6, 628 (1973).
2. J. G. Wetmur and N. Davidson, J. Mol. Biol., 31, 349 (1968).
3. B. Vollmert and H. Stutz, Angew. Makromol. Chem., 3, 182 (1968); 20, 71 (1971). B. Vollmert, H. Stuty, and J. Stemper, Angew. Makromol. Chem., 25, 187 (1972).
4. H. Morawetz, J.-R. Cho, and P. J. Gans, Macromolecules, 6, 624 (1973).
5. A. A. Frost and R. G. Peason, "Kinetics and Mechanism" John Wiley and Sons. Inc. New York (1961).
6. S. Glasstone, K. J. Laidler, and H. Eyring, "The Theory of Rate Process", McGraw-Hill Book Company (1941).
7. P. J. Flory, "Principles of Polymer Chemistry", Cornell University Press, Ithaca, N.Y., 1953.
8. H. Yamakawa, "Modern Theory of Polymer Solution" Harper and Row, New York, N.Y., 1971.
9. M. Kurata, M. Fukatsu, H. Sotobayashi, and H. Yamakawa, J. Chem. Phys., 41, 139 (1964).
10. B. Vollmert, "Polymer Chemistry", Springer Verlag, New York, 1973.
11. T. A. Orofino and P. J. Flory, J. Chem. Phys., 26, 1067 (1957)
12. W. H. Stockmayer, Makromol. Chem., 35, 54 (1960).
13. E. F. Casassa and H. Markovitz, J. Chem. Phys., 29, 473 (1958)
14. N. Goodman and H. Morawetz, J. Polym. Sci., A2, 9, 1657 (1971); ibid., Part C, 31, 177 (1970).

CHAPTER 5.

Kinetic Study on the Inter- and Intramolecular Acetalization Reactions of Polymeric Reactants

INTRODUCTION

Chapter 3 has revealed that terminal aldehyde groups of poly(vinyl alcohol)(PVA) formed upon its oxidation with ceric ion can readily react with hydroxyl groups in the same or different PVA molecules to give acetal linkages. Since this acetalization reaction seems to provide an adequate model for studying the inter- and intramolecular reactions involving the chemically controlled step as the rate-determining, we have kinetically studied the acetalization reaction of PVA with terminal aldehyde groups. In the present work PVA having one or two terminal aldehyde groups were synthesized and the acetalization reaction was followed in water and in dimethylsulfoxide(DMSO) over a wide range of the polymer concentration. DMSO is known to be a good solvent[1] and water nearly a Ⓗ solvent for PVA [2]. The rate constants observed for the intermolecular reaction will be compared with those predicted from dilute solution theories on an excluded volume effect and further with those observed for the acetalization of PVA with low-molecular-weight aldehyde analogues.We will also present results on the intramolecular acetalization.

EXPERIMENTAL

Materials

PVA having only one terminal aldehyde group was synthesized according to the chapter 2 except that 2, 2'-azobisisobutyronitrile(AIBN) was used as an initiator. The procedure is reproduced here briefly. Vinyl acetate was polymerized at 60°C in the presence of CCl_4 as a chain transfer agent, the concentration of CCl_4 being 0.103 $mol \cdot l^{-1}$ and that of AIBN 5×10^{-5} $mol \cdot l^{-1}$. Hydrolysis of this poly(vinyl acetate)(PVAc) yielded PVA having one terminal aldehyde group, hereafter designated as PVA-1, because the end-group of the PVAc, $-CH_2-CH(OCOCH_3)Cl$, was converted to $-CH_2-CHO$ on hydrolysis, liberating CH_3COOH and HCl. The viscosity-average degree of polymerization of this PVA is 119 and the end-group determination described below shows that it has 0.81 aldehyde group per molecule. The other PVA carrying two aldehyde groups on both of the chain-end, designated as PVA-2, was obtained by oxidizing a conventional PVA with sodium periodate which cleaves selectively and quantitatively the 1, 2 glycol bonds present in PVA under formation of two aldehyde end-groups. The viscosity-average degree of polymerization of PVA-2 is 114 and it may contains 1.83 aldehyde groups per molecule, based on the amount of sodium periodate consumed for the oxidation. Both PVA-1 and PVA-2 were subjected to the acetalization without fractionation. Aldol selected as a low-molecular-weight model compound for the PVA with the terminal aldehyde group was distilled twice under reduced pressure.

Acetaldehyde was purified by distilling paraldehyde over sulfuric acid. Other low-molecular-weight aldehydes were distilled once at atmospheric pressure. These aldehydes were stored in water and in DMSO as 2% solution. DMSO was dried over calcium hydride and then distilled under reduced pressure.

Acetalization

The acetalization reaction was carried out in water or in DMSO throughout in the presence of 0.05 N HCl as a catalyst. In the acetalization in DMSO, water was always added to DMSO by 2.78 $mol \cdot l^{-1}$, so that we may not need to consider the water molecules liberated (or consumed) as a result of acetalization (or deacetalization) in the kinetic analysis. The amount of added water is much larger than that of the water to be liberated (or consumed), but small enough not to influence the solvency of DMSO to PVA. The polymer concentration was changed from about 0.5 to 25 $g \cdot dl^{-1}$. Erlenmeyer flasks containing the reaction mixtures were stoppered and kept in a water bath at the given temperatures. In the acetalization of PVA with low-molecular-weight aldehydes, the aldehyde concentration was kept to 5.45×10^{-3} $mol \cdot l^{-1}$ and that of PVA-0 1.88 $g \cdot dl^{-1}$. PVA-0 means that it does not have any terminal aldehyde group; we used for this purpose a conventional PVA with the degree of polymerization of 1340.

The reaction rate of acetalization, that is, the rate of aldehyde consumption was determined as follows. At regular time intervals, the aliquot of reaction mixture was pipetted out and then neutralized with NaOH aqueous solution to stop

the reaction. Instead of determining acetal formation the concentration of aldehyde remaining unreacted was determined with 3-methyl-2-benzothiazolone hydrazone hydrochloride [3]. The calibration curve required for determining the aldehyde end-group attached to PVA was constructed with the use of the conventional PVA oxidized to various extents with known amounts of sodium periodate.

RESULTS

The acetalization is a reversible reaction and proceeds as expressed by eq.(1) in the case of PVA with a terminal aldehyde group:

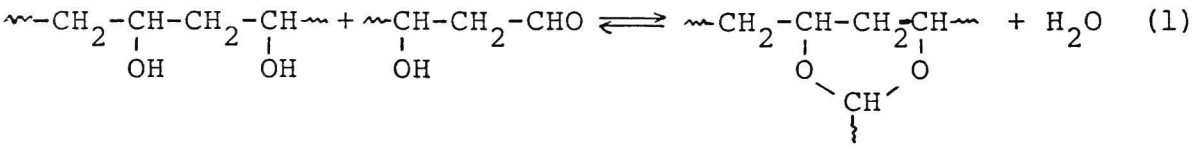

(1)

The aldehyde group of PVA may undergo either intermolecular or intramolecular acetalization coupling reactions. This is illustrated schematically in Fig. 1. Then the rate of acetalization is given by

$$-\frac{d[CHO]}{dt} = k_1[CHO] + k_2[OH][CHO] - k_{-2}[acetal][H_2O] \qquad (2)$$

where k_1 is the first-order rate constant of intramolecular acetalization, k_2 the second-order rate constant of intermolecular acetalization, and k_{-2} the second-order rate

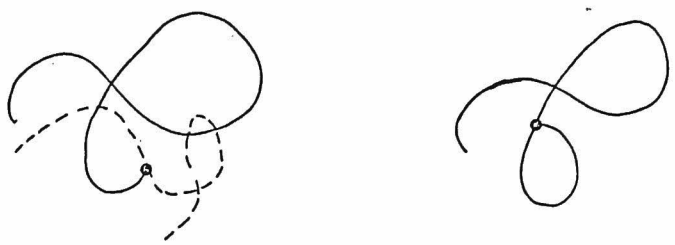

Fig. 1 Schematic representation of inter- and intramolecular reactions.

constant of deacetalization. In our experiment the concentrations [OH] and $[H_2O]$ are by far higher than [CHO] and [acetal]. Thus eq.(2) may be written as

$$-\frac{d[CHO]}{dt} = (k_1+k_2[OH]_0)[CHO] - k_{-2}[H_2O]_0[acetal] \qquad (3)$$

where $[OH]_0$ and $[H_2O]_0$ are the initial concentrations of the hydroxyl group and H_2O, respectively. At the equilibrium

$$-\frac{d[CHO]}{dt} = 0 = (k_1+k_2[OH]_0)[CHO]_e - k_{-2}[H_2O]_0[acetal]_e \qquad (4)$$

Here the subscript e refers to the equilibrium concentration. Eq.(3) can be integrated to give

$$\ln\left(\frac{[CHO]_0-[CHO]_e}{[CHO]-[CHO]_e}\right) = (k_2+k_1[OH]_0+k_{-2}[H_2O]_0)t \qquad (5)$$

An example of the plot of $\ln\left(\frac{[CHO]_0-[CHO]_e}{[CHO]-[CHO]_e}\right)$ versus

the reaction time t is given in Fig. 2. It is seen that eq.(5) holds satisfactorily over the whole time range, though the reactant molecules become much branched in structure with increasing degree of polymerization as the reaction proceeds. The good linearity seen in Fig. 2 was also observed for the acetalization in H_2O. This finding suggests that the degree of polymerization of polymeric reactants might not have a marked effect on the reaction. Since the slope gives $(k_1+k_2[OH]_0+k_{-2}[H_2O]_0)$ and the ratio $(k_1+k_2[OH]_0)/k_{-2}[H_2O]_0$

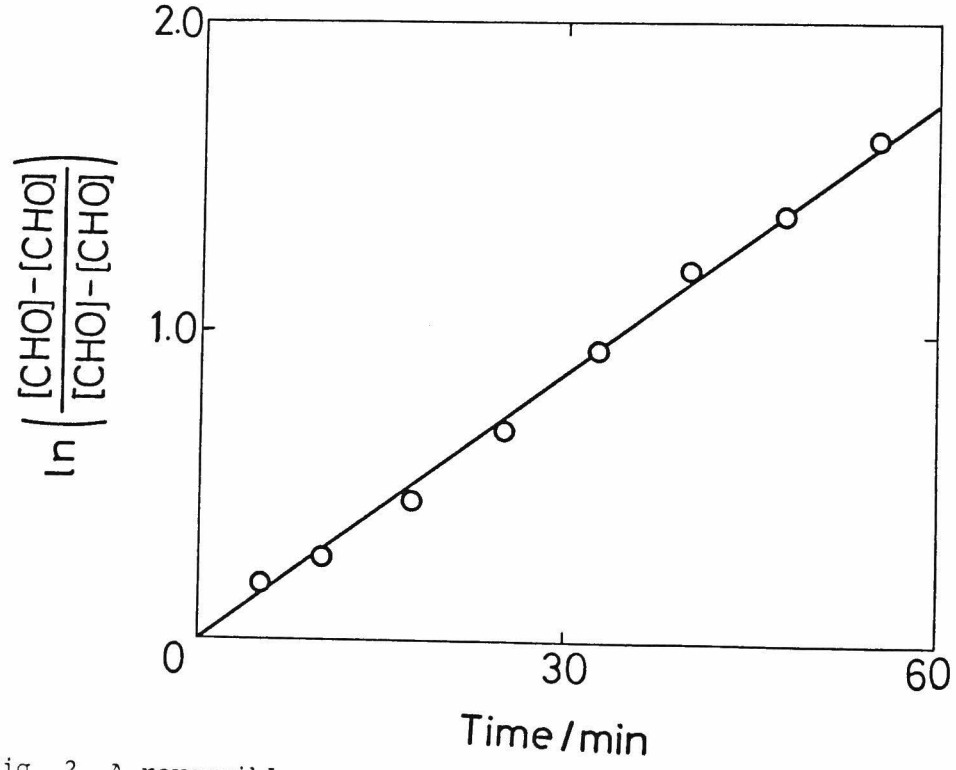

Fig. 2 A reversible pseudo first-order plot for acetalization of PVA-1 in DMSO solution at 50°C. $[OH]_0$=1.39 mol·l^{-1}, $[H^+]$=0.05N, $[H_2O]_0$=2.78 mol·l^{-1}.

is obtained from eq.(4), $k_2[OH]_0+k_1$ and $k_{-2}[OH]_0$ can be calculated. The dependence of the determined $(k_1+k_2[OH]_0)$ values on the PVA concentration expressed by $[OH]_0$ is plotted in Figs. 3 and 4 for the reactions carried out at various temperatures in H_2O and in DMSO, respectively. The PVA samples used are PVA-2 for the acetalization in H_2O and PVA-1 for the acetalization in DMSO. For comparison the acetalization of PVA-1 was conducted also in H_2O and the result is given in Fig. 3. Clearly, there is no notice-

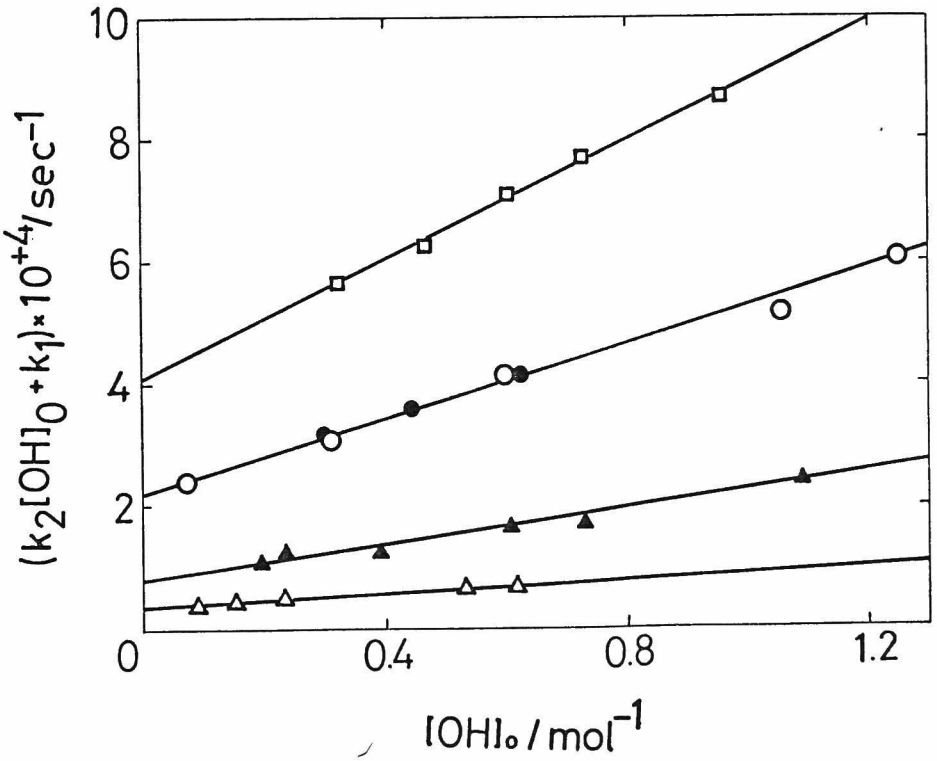

Fig. 3 Dependence of $(k_2[OH]_0+k_1)$ on the initial polymer concentration for acetalization of PVA-2 in aqueous solution. $[H^+]$=0.05N, (△) 30°C; (▲) 40°C; (o) 50°C; (□) 60°C; (●) 50°C(PVA-1).

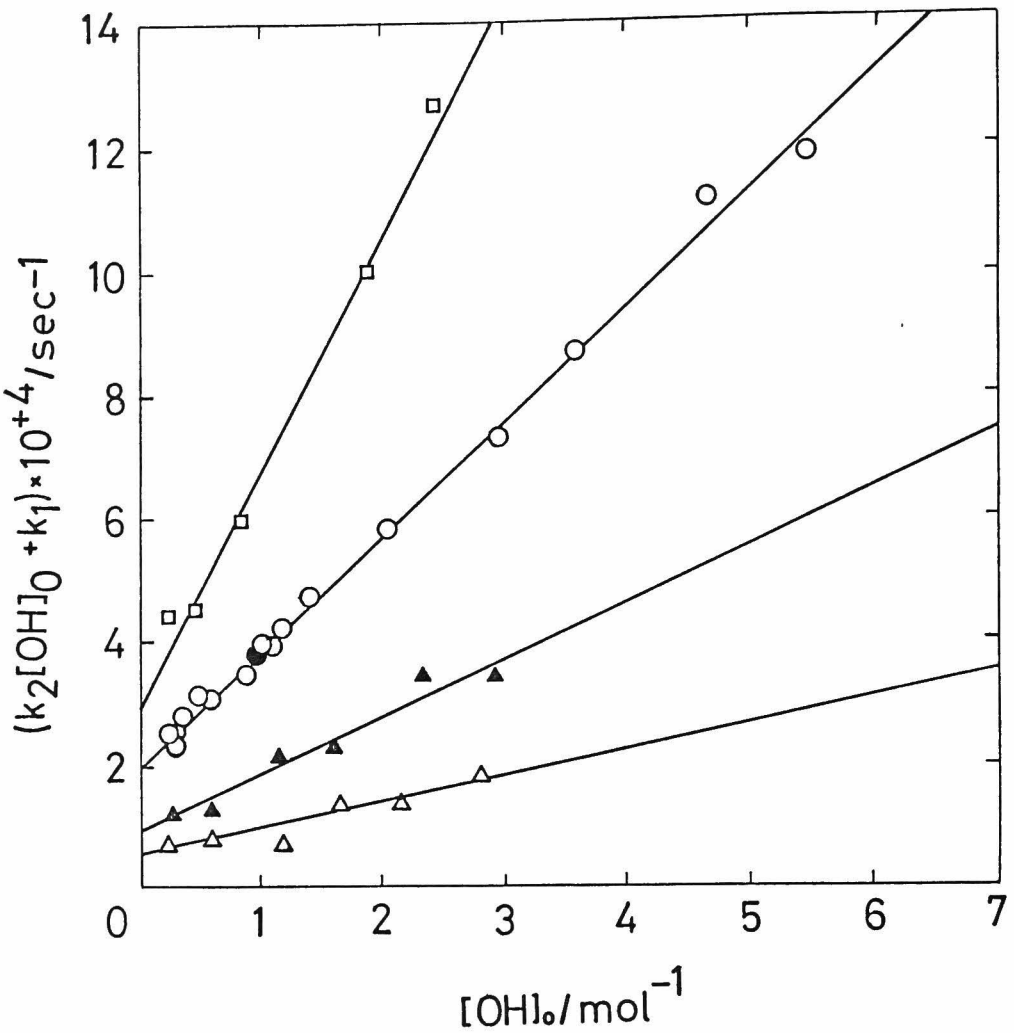

Fig. 4 Dependence of $(k_2[OH]_0+k_1)$ on the initial polymer concentration for acetalization of PVA-1 in DMSO solution. $[H^+]$=0.05N; $[H_2O]_0$=2.78 mol·l^{-1}, (△) 30°C; (▲) 40°C; (○) 50°C; (□) 60°C; (●) 50°C(PVA-1+PVA-0)

able difference between PVA-1 and PVA-2, indicating that the branching formed during the acetalization has virtually no influence on the reaction rate. The branching must take place much stronger for the acetalization of PVA-2 than PVA-1, because the former has about two functional aldehyde groups in one starting molecule. Indeed, the acetalization of PVA-2 gave rise to gelation, when conducted at polymer concentra-

tions higher than those in the present experiment. Further we have studied the effect of an addition of PVA-0 which has no aldehyde group but a high degree of polymerization. As is seen in Fig. 4, PVA-0 does not exhibit any effect even when added to the reaction mixture in an amount twice that of PVA-1, again supporting the finding that the degree of polymerization does not practically influence the reaction.

The rate constants k_2 and k_1 can be calculated from the slope and the intercept of the plots in Figs. 3 and 4. Arrhenius plots of k_2 are shown in Fig. 5 for the reactions in H_2O and Fig. 6 for those in DMSO together with the Arrhenius plots for the acetalization of PVA-0 with low-molecular-weight aldehydes. Figs. 7 and 8 give similar Arrhenius plots for k_{-2}. The activation enthalpy $\Delta H^{\ddagger}$ and the activation entropy $\Delta S^{\ddagger}$ were calculated from these figures and tabulated in Table I, together with the rate constants k_2 and k_{-2} found at 50°C.

If the intramolecular reaction is regarded to be a bimolecular reaction and its rate constant is assumed to be identical to that of the intermolecular reaction k_2, the rate of intramolecular acetalization $k_1[CHO]$ can be written as

$$k_1[CHO] = k_2[OH]_{intra}[CHO] \qquad (6)$$

Here $[OH]_{intra}$ is the apparent concentration of the hydroxyl group which is effective in the intramolecular reaction and

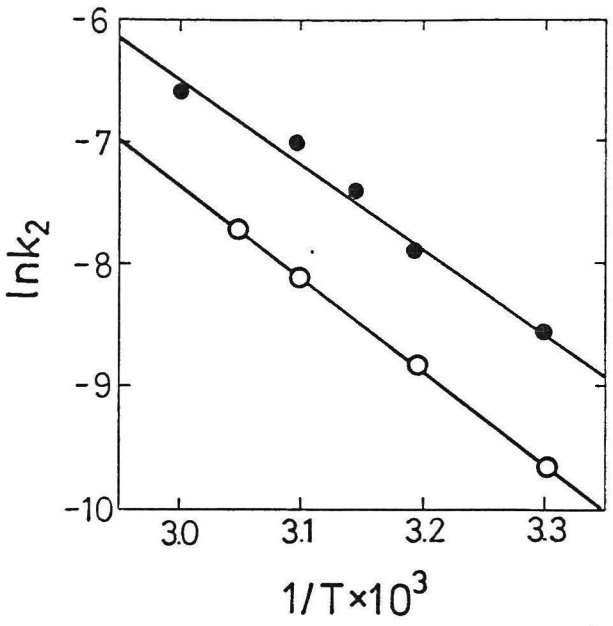

Fig. 5 Arrhenius plots of second-order rate constant k_2 of acetalization in aqueous solution. $[H^+]$=0.05N; (o) PVA-2; (•) aldol.

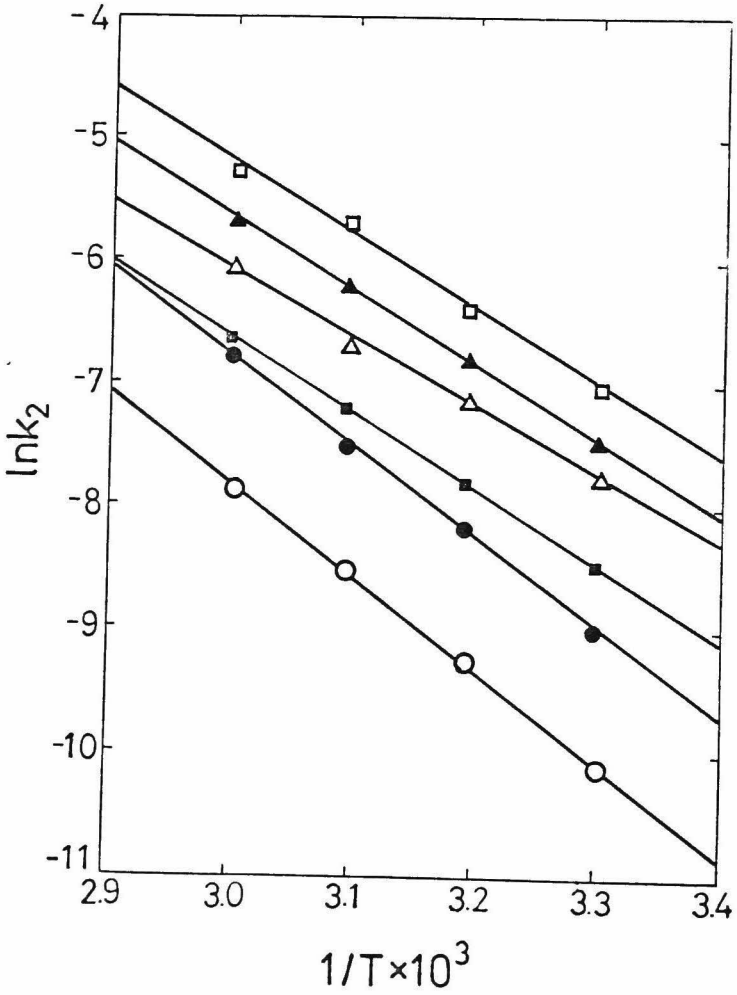

Fig. 6 Arrhenius plots of second-ord rate constant k_2 of acetalization in DMSO solution. $[H^+]$=0.05N; $[H_2O]_0$= 2.78 $mol.l^{-1}$; (o) PVA-1; (•) aldol; (□) acetaldehyde; (■) propionaldehyde; (△) n-butyraldehyde; (▲) i-butyraldehy

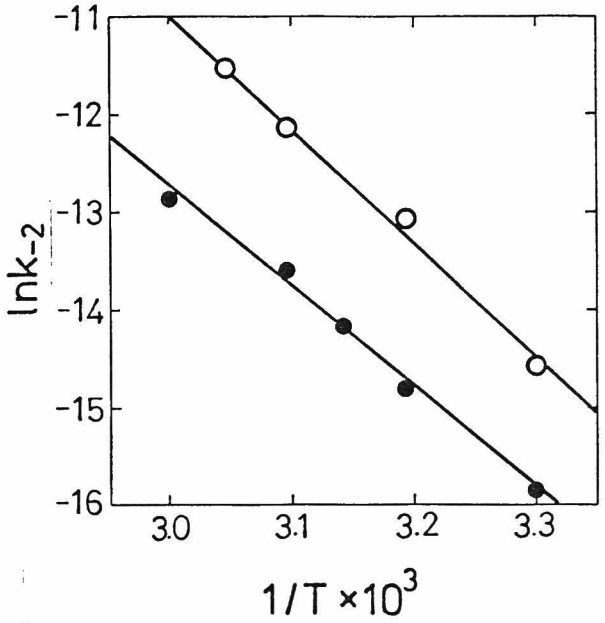

Fig.7 Arrhenius plots of second-order rate costant k_{-2} of deacetalization in aqueous solution. $[H^+]$=0.05N; (o) PVA-2; (•) aldol.

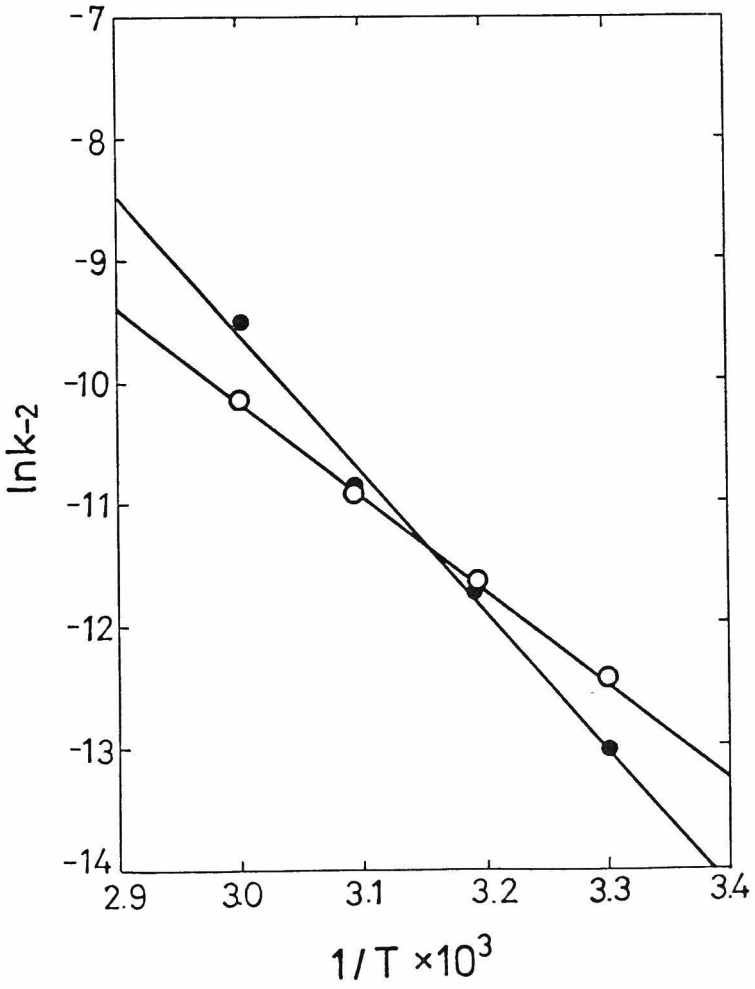

Fig. 8 Arrhenius plots of second-order rate constants k_{-2} of deacetalization in DMSO solution. $[H^+]$=0.05N; $[H_2O]_0$= 2.78 mol.l^{-1} (o) PVA-1; (•) aldol.

Table I

Kinetic Parameters for Acetalization and Deacetalization in DMSO Solution at 50°C

Aldehyde	k_2	$\Delta H_2^{\neq}$	$\Delta S_2^{\neq}$	k_{-2}	$\Delta H_{-2}^{\neq}$	$\Delta S_{-2}^{\neq}$
	$l \cdot mol^{-1} \cdot sec^{-1}$	$kcal \cdot mol^{-1}$	e.u.	$l \cdot mol^{-1} \cdot sec^{-1}$	$kcal \cdot mol^{-1}$	e.u.
PVA-1	2.00×10^{-4}	14.3	-31.5	1.75×10^{-5}	14.7	-34.9
Aldol	5.37×10^{-4}	14.1	-30.0	1.86×10^{-5}	22.1	-12.1
Acetaldehyde	3.30×10^{-3}	11.1	-35.7			
Propionaldehyde	1.98×10^{-3}	11.4	-35.8			
n-Butyraldehyde	1.20×10^{-3}	10.9	-38.3			
i-Butyraldehyde	7.35×10^{-4}	11.5	-37.5			
PVA-2(in water)	3.04×10^{-4}	14.7	-29.4	5.56×10^{-6}	21.8	-15.4
Aldol(in water)	8.91×10^{-4}	12.9	-32.7	1.26×10^{-6}	20.8	-21.3

hence belongs to the same polymer chain as the aldehyde group. The concentrations $[OH]_{intra}$ estimated from eq.(6) are tabulated in Table II together with the rate constants k_1. For the low-molecular-weight aldehyde analogs such as aldol and acetaldehyde, the intramolecular reaction is not possible to occur, so that the constant k_1 in the above equations should be omitted.

Table II
Rate Constants k_1 of Intramolecular Acetalization and Intramolecular OH Concentrations $[OH]_{intra}$

	Water			DMSO		
T °C	$k_1 \times 10^{-4}$ sec^{-1}	$[OH]_{intra}$ $mol \cdot l^{-1}$	$[OH]_{intra}$ $g \cdot dl^{-1}$	$k_1 \times 10^{-4}$ sec^{-1}	$[OH]_{intra}$ $mol \cdot l^{-1}$	$[OH]_{intra}$ $g \cdot dl^{-1}$
30	0.310	0.484	2.13	0.513	1.28	5.63
40	0.741	0.508	2.24	0.823	0.864	3.80
50	2.24	0.736	3.46	1.74	0.869	3.82
55	4.04	0.890	3.92	—	—	—
60	—	—	—	2.92	0.763	3.36

DISCUSSION

Dependence of the Intermolecular Reaction Rate Constant k_2 on the Polymer Concentration $[OH]_0$

It is expected that the degree of interpenetration of random coils in a polymer solution may affect the rate of intermolecular polymer-polymer reaction. In order to discuss the interpenetration effect it is convenient to

classify the polymer solution into two groups based on the concentration range, that is, the concentrated solution and the dilute solution, since the degree of mutual interpenetration of polymer coils must depend largely on the polymer concentration.

Two extremely different models on the structure of polymer coils are schematically shown for the case of concentrated solution in Fig. 9. According to thermodynamic consideration the polymer molecules seem to interpenetrate each other in sufficiently concentrated solutions, regardless of the solvency as shown in Fig. 9a[4]. Vollmert and his coworkers have, however, concluded from their experiments on the polymer reactions that there is resistance to chain interpenetration even in concentrated systems where the excluded volume effect should disappear and presented the individual cell structure model as shown in Fig. 9b[5]. If the polymer

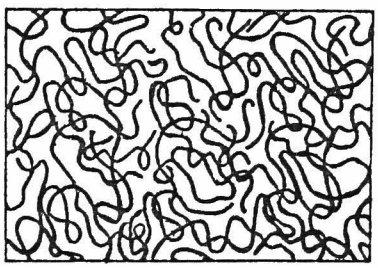

(a)

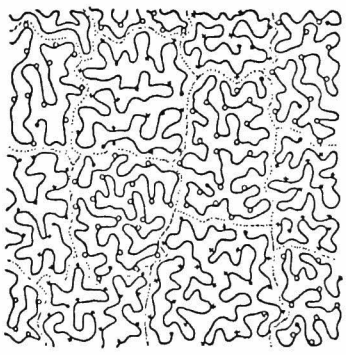

(b)

Fig. 9a Schematic representation of the freely interpenetrating random coil model.

Fig. 9b Schematic representation of the individual cell structure model.

coils would behave as in the individual cell structure model, the rate of intermolecular reaction would be greatly reduced in comparison with that of the analogous small molecule reactions and in addition depend on the polymer concentration. In this connection the plot of $(k_2[OH]_0+k_1)$ versus the PVA concentration $[OH]_0$ in Figs. 3 and 4 can give helpful information. Evidently, all the data satisfy the straight lines, even though $[OH]_0$ is raised up to 5.5 $mol \cdot l^{-1}$, i.e., 24 $g \cdot dl^{-1}$ in the acetalization in DMSO at 50°C. This fact strongly indicates that the rate constant k_2 as well as k_1 remain unchanged in this polymer concentration range. Thus it follows that there is no strong restriction for the polymer coils to interpenetrate each other, as illustrated in Fig. 9a. If this is true, the rate constants k_2 for the PVA with the aldehyde group should be comparable with those found for the low-molecular-weight model compound, aldol. Indeed, the result in Table I seems to confirm this expectation. The small difference in k_2 may not be attributed to resistance to mutual free interpenetration. It should be explained rather in terms of other causes such as the induced effect of substituent groups which often appears in the usual organic reactions, because such difference in k_2 is also observed among low-molecular-weight aldehydes (see Table I). In addition, the values of $\Delta H^{\ddagger}$ and $\Delta S^{\ddagger}$ for PVA-1 and PVA-2 do not exhibit any significant departure

from those of low-molecular-weight analogs. Therefore it may be concluded that the polymer coils are present in the concentrated solution in a homogeneous state, interpenetrating freely, at least in our experimental condition.

For the case of dilute solutions, it has been recognized that the polymer coils can freely interpenetrate each other in Ⓗ solvents, whereas there is some difficulty for mutual interpenetration in good solvents. All the theories[6] concerned with the excluded volume effect on the rate of reaction involving two randomly coiled polymers predict that the reaction rate is low in good solvent media compared with the case where the excluded volume effect is not operative as in Ⓗ solvent. In practice we do not find any deviation from the straight line in Fig. 3, where the result of acetalization in water is given, which is approximately a Ⓗ solvent for PVA. This implies that k_2 is really held constant, irrespective of the polymer concentration. On the other hand, it is expected that k_2 in DMSO, a good solvent for PVA, must be smaller in dilute solution than in concentrated solution, resulting in the smaller slope of curves at the lower concentration. Contrary to the expectation, no deviation from the straight line can be observed in Fig. 4. However, this is not understandable, if the excluded volume effect may not be large enough to be detectable under the experimental conditions of this study. Indeed, the rate constant estimated on the basis of the excluded volume effect is in

agreement with the observed rate constant, as will be shown below.

In chapter 4 we have demonstrated that the ratio of the rate constant in a good solvent, k_2, to that for the ideal low-molecular-weight analogs, k_2^0 is given by

$$\frac{k_2}{k_2^0} = (3.903\ \bar{z} + 1)^{-\frac{4(2-\sqrt{2})}{3.903}} \tag{7}$$

$$\bar{z} = \left(\frac{3}{2\pi a^2}\right)^{3/2} \beta_2 n^{3/2} \frac{1}{\alpha_s^3} = \frac{z}{\alpha_s^3} \tag{8}$$

where a is the effective bond length, n+1 is the number of segments in a polymer chain, β_2 is the binary cluster integral for a pair of segments, and α_s is the expansion factor. To obtain k_2/k_2^0 we have to estimate the $\bar{z}$ value. To this end we have applied intrinsic viscosity data of PVA in DMSO solutions[1] to the familiar Stockmayer-Fixman relation [7,8] and found z to be 0.34 when the degree of polymerization is 119. $\bar{z}$ is then calculated to be 0.29 from this z value and the equation for α_s [9]. Thus inserting this $\bar{z}$ value into eq.(7) we obtain k_2/k_2^0=0.56. This ratio, which is not far smaller than unity, implies that the excluded volume effect on k_2 is not large enough to be detectable in such dilute solutions. It may be also taken into consideration that the polymer concentrations studied might not be sufficiently low, allowing the mutual interpenetration to occur to some extent.

OH Concentration $[OH]_{intra}$ Effective for Intramolecular Acetalization

In the analogy of derivation of k_2 for the intermolecular reaction , the rate constant $k_{1,i}$ for the intramolecular reaction of OH groups belonging to the ith segments with the terminal aldehyde attached to the 0th segment can be written

$$k_{1,i} = k_2^0 \frac{g\Omega_i^*}{\Omega_0} \tag{9}$$

Here k_2^0 is the rate constant which would be obtained if the aldehyde end-group was separated from the mother polymer chain. Ω_0 and Ω^* are the configurational partition functions of the PVA reactant and the transition state complex, respectively. The weight factor g is introduced, because one segment possesses more than one reactive group. We assume this number to be g.

Since the segments other than the ith one can also participate in the intramolecular reaction, we must sum up $k_{1,i}$ regarding to i to find the overall rate constant.

$$k_1 = \sum_{i=j}^{n} k_{1,i} \tag{10}$$

The lower limit j for summation comes from the fact that the OH groups neighboring too closely to the terminal aldehyde

cannot take part in the intramolecular reaction because of bulkiness of the resulting acetal linkage:

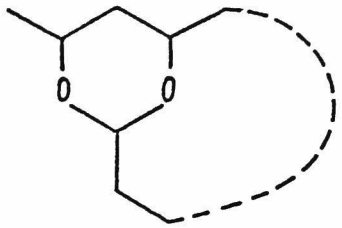

With the use of the probability distribution function of the end-to-end distance of freely jointed chains, Morawetz and his coworkers [10] have shown k_1 to be given by

$$k_1 = k_2^0 \left(\frac{3}{2\pi}\right)^{3/2} \frac{\Phi_0}{K} \sum_{i=j}^{n} g(iM_s)^{-3/2} \qquad (11)$$

where M_s is the molar mass of the segment, K is the parameter in the empirical formula for the intrinsic viscosity in Ⓗ solvent ($[\eta]=KM^{0.5}$) and Φ_0 is the universal constant ($=2.5\times10^{23}$). Comparison of eq.(6) with (11) yields

$$[OH]_{intra} = \frac{1000}{N_A} \left(\frac{3}{2\pi}\right)^{3/2} \frac{\Phi_0}{K} \sum_{i=j}^{n} g(iM_s)^{-3/2} \qquad (12)$$

$$= \frac{1000}{N_A} \left(\frac{3}{2\pi}\right)^{3/2} \frac{\Phi_0}{K} \sum_{i'=gj}^{p} (i'M_0)^{-3/2} \qquad (13)$$

where N_A is Avogadro's number, M_0 is the molar mass of repeating unit, and p is the degree of polymerization of the polymer chain. In this derivation $1000/N_A$ was introduced to express the concentration unit by $mol\cdot l^{-1}$ and k_2^0 was assumed to be identical to k_2, since this calculation was confined to the

solution in Ⓗ state. $[OH]_{intra}$ is identical to C°_{eff} defined by Morawetz and his coworkers[10]. As shown in chapter 4, eq.(11) can be also derived from the partition functions of the polymer reactant and their transition state complex.

We can compare the $[OH]_{intra}$ estimated from eq.(13) with that observed for the acetalization in the aqueous solutions, because H_2O is almost a Ⓗ solvent, at least in a range of high temperatures. The observed concentrations $[OH]_{intra}$ given in Table II agree with the theoretical estimation, if the gj value is assumed to be round 15. This result suggests that the intramolecular acetalization does not lead to appreciable formation of small rings consisting of the segment number less than j. It is interesting to point out that with increasing temperature $[OH]_{intra}$ decreases in water, but increases in DMSO. This is in accordance with the well-known fact that solution of PVA is endothermic in water and exothermic in DMSO.

Finally, it should be stressed that the intramolecular reaction contributes rather markedly to the whole polymer reaction even in concentrated solutions, although the intramolecular reaction is often regarded to be negligible compared with the intermolecular reaction.

REFERENCES

1. R. Naito, Kobunshi Kagaku, 15, 597 (1958).
2. A. Nakajima and K. Furutachi, Kobunshi Kagaku, 6, 460 (1949).
3. E. Sawichi, T. R. Hauser, T. W. Stanley and W. Elbert, Anal. Chem., 33, 93 (1961).
4. G. S. Y. Yeh, J. Macromol. Sci.- Phys., B6, 451, 463 (1972).
5. B. Vollmert and H. Stutz, Angew, Makromol. Chem., 3, 182 (1968); 20 71 (1971). B. Vollmert, H. Stutz, and J. Stemper Angew. Makromol. Chem., 25, 187 (1972).
6. H. Morawetz, J.-R. Cho and P. J. Gans, Macromolecules, 6, 624 (1973).
7. W. H. Stochmayer and M. Fixman, J. Polymer Sci., Part C, 1, 137 (1963).
8. H. Yamakawa, "Modern Theory of Polymer Solutions" in Harper's Chemistry Series, Ed. S. H. Rice, Harper and Row, New York (1971).
9. H. Yamakawa and G. Tanaka, J. Chem. Phys., 47, 3991 (1967).
10. N. Goodman and H. Morawetz, J. Polym. Sci., A2, 9, 1657 (1971); J. Polym. Sci., Part C, 31, 177 (1970) and references therein.

CHAPTER 6.

Gelation of Poly(vinyl alcohol) Having Terminal Aldehyde Groups by Acetalization

INTRODUCTION

Since Flory's pioneering work[1], several authors have presented theories on gelation which results from polymerizations in the presence of multifunctional monomers as well as crosslinking of prepolymers[2-4]. However, only few works[5] have been devoted to compare the gelation theories with experiments because of difficulty in determining the extent of the reaction, in particular near the so-called gel point at which macromolecules with an infinite weight-average molecular weight are to be formed.

We have undertaken to study gelation of poly(vinyl alcohol) (PVA) having aldehyde groups at both chain-ends in acidic aqueous solution. As acetalization proceeds between hydroxyl and aldehyde groups in different PVA molecules, the solution becomes increasingly viscous, finally setting to a gel In chapter 3 we have revealed that aldehyde groups are generated at ends of PVA molecules upon oxidation with ceric ions in aqueous HNO_3 medium at low temperatures . Indeed, the terminal aldehyde groups underwent acetalization with hydroxyl groups of PVA, leading to gelation. In chapter 5 , kinetic studies were carried out on the inter- and

intramolecular acetalization of PVA carrying terminal aldehyde groups in an attempt to assess the effect of long-range interaction on the polymer-polymer reaction rate . A theory on the excluded volume effect on polymer-polymer reactions has been described in chapter 4.

The present study is aimed to determine the extent of reaction at the gel point and to compare the result with a theoretical prediction in order to estimate the crosslinks ineffective for gelation.

EXPERIMENTAL

Preparation of PVA Carrying Terminal Aldehyde Groups

Vinyl acetate(VAc) was subjected to simple distillation and then fractionally distilled after polymerization up to a ca. 15% conversion by addition of 2, 2'-azobisisobutyronitrile. A middle fraction of the distillate giving a boiling point of 72-73°C was used for the subsequent radiation polymerization. It was conducted with gamma rays from a Co-60 source after degassing with a freeze-thaw method, followed by sealing. The temperature and the dose rate employed for the polymerization are tabulated in Table I, together with $\bar{P}_n$ and the content of 1, 2-glycol units in PVA obtained on complete hydrolysis of the PVAc formed. The PVA materials were subjected to oxidation with sodium periodate to cleave

Table I Characteristics of PVA_c Obtained by Radiation Polymerization

	Polym.Tem. °C	Dose rate rad.sec^{-1}	$\bar{P}_n$	1,2-glycol unit mol %
PVAc-1	0	4.94	4750	1.20
PVAc-2	-78	13.9	811	0.65

Table II Characteristics of Periodate-Oxidized PVA

Starting PVAc	Oxidized PVA	$\bar{P}_n$	Number of aldehyde groups per molecule	λ	μ	α_g
PVA-C[a)]	PVA-0	53	1.92	0.08	0.92	0.260
PVAc-1	PVA-1	513	1.80	0.20	0.80	0.279
PVAc-2	PVA-2	176	1.57	0.43	0.57	0.325

a) a commercial PVA with $\bar{P}_n$ of 1340 and a 1,2-glycol content of 1.8 mole%.

selectively the 1, 2-glycol units present in PVA under formation of aldehyde groups at both chain-ends of the degraded PVA. The oxidation was carried out in aqueous PVA solution of 5 $g \cdot dl^{-1}$ at room temperature for 1 hr. Determination of the concentration of periodate consumed by the oxidation permits us to calculate the number of terminal aldehydes per oxidized PVA molecule, which is given in Table II, together with $\bar{P}_n$ of the oxidized PVA. The table also includes the result of oxidation for a commercial PVA with $\bar{P}_n$ of 1340 and a 1, 2-glycol content of 1.8 mol%. Values of λ, μ, and α_g given in Table II will be discussed later.

Acetalization

As the gel point we determined the critical temperature at which reversible sol-gel transition of reaction mixtures took place. For this purpose, acetalization in aqueous solutions of different polymer concentrations was allowed to proceed at room temperature in the presence of 0.5 N HCl as a catalyst till formation of a gel. Then temperature was raised to the point at which the gel was transformed into a sol as a result of shift of equilibrium between acetalization and deacetalization. The sol-gel transition temperature could be readily determined with visual inspection. In the case of determination of variation in the extent of acetalization with time, the reaction was performed at 50°C in the presence of

0.05 N HCl at a polymer concentration of 4.88 $g \cdot dl^{-1}$. At regular time intervals, the aliquot of reaction mixture was pipetted out and neutralized with aqueous NaOH solution to prevent the further reaction. The concentration of aldehyde groups remaining unreacted was determined with 3-methyl-2-benzothiazolone hydrazone hydrochloride(MBH)[6].

RESULTS

Acetalization is a reversible reaction in which the rates of forward and backward reaction become considerably high under a suitable condition. In the case of PVA with terminal aldehydes acetalization may proceed as follows:

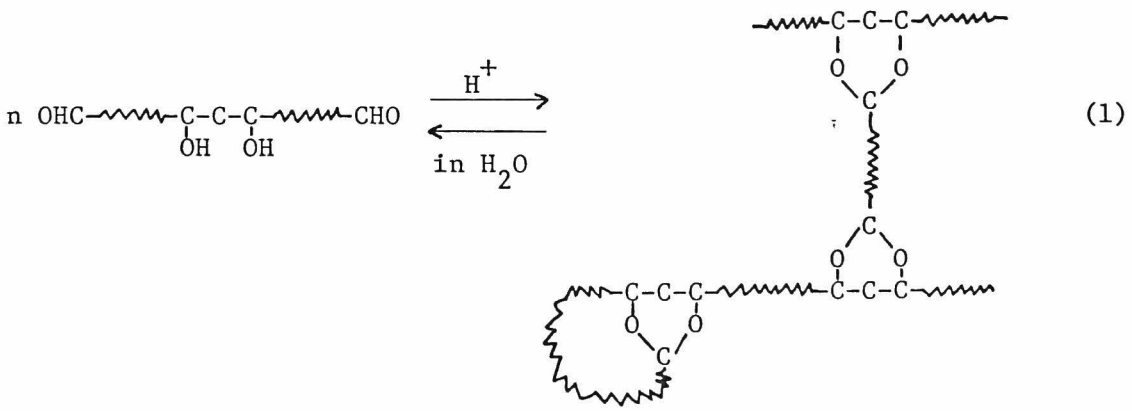

(1)

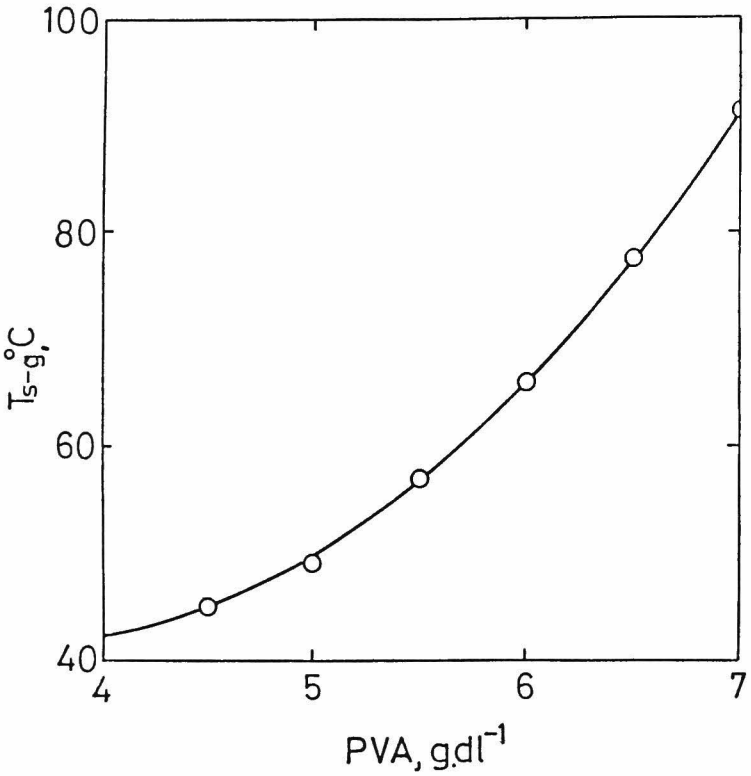

Fig. 1 Dependence of sol-gel transition temperature, T_{s-g}, on polymer concentration (PVA-0, 0.5 N HCl).

A clear transition between sol and gel takes place promptly in a reversible manner on a slight change in temperature. Fig. 1 illustrates an example of a plot of the sol-gel transition temperature as a function of concentration of PVA solutions. The polymer employed is PVA-0.

The critical extent of reaction of terminal aldehydes at the gel point can be estimated on the basis of theory derived by Saito[7], if it is assumed that only intermolecular crosslinking occurs. When the reaction mixture contains three kinds of polymers, i.e., a polymer without terminal

functional group, a polymer with one terminal functional group, and a polymer with two terminal functional groups, the theory predicts that the distribution function $m_i(p, \tau)$ of degree of polymerization p is to satisfy the following differential equation.

$$\frac{\partial m_i(p, \tau)}{\partial \tau} = -\{pf_{01}(\tau) + if_{10}(\tau)\}m_i(p, \tau) + \sum_{j=0}^{i}(i-j+1)\int_0^p \ell m_j(\ell, \tau)m_{i-j+1}(p-\ell, \tau)d\ell \quad (2)$$

Here, i, j, and i-j+1 mean the numbers of reactive groups in starting and resultant macromolecules.

τ is related to the extent of reaction α by the equation

$$\alpha = 1 - e^{-\tau} \quad (3)$$

$f_{01}(\tau)$ and $f_{10}(\tau)$ are defined as

$$f_{st}(\tau) = \sum_{i=0}^{\infty} i^t \int_0^{\infty} p^s m_i(p,\tau)dp \quad (4)$$

Provided that our prepolymers have a random molecular weight distribution, irrespective of the number of aldehydes attached, the solution of eq.(2) leads that $\bar{P}_n$ and $\bar{P}_w$ to be observed at α are equal to

$$\bar{P}_n(\alpha) = \frac{\bar{P}_n(0)}{1-\alpha\mu(1+\lambda)} \quad (5)$$

$$\bar{P}_w(\alpha) = \frac{C_1 C_2}{C_2^2\{\sqrt{C_1}+C_3(1-\alpha)\}^2-(1-\alpha)^2} \tag{6}$$

with

$$C_1 = \frac{\bar{P}_n(0)}{\mu}, \qquad C_2 = \frac{(\lambda+2\mu-1)^2}{2\bar{P}_n(0)} - \frac{2\mu}{\bar{P}_n(0)}$$

$$C_3 = -\frac{1}{C_2}\sqrt{1+\frac{C_2\bar{P}_n(0)}{2\mu}} - \sqrt{C_1} \tag{7}$$

where λ and μ are the fractions of prepolymer molecules having one and two terminal aldehyde groups, respectively. These values are given in Table II. Fig. 2 shows $\bar{P}_n(\alpha)$ and $\bar{P}_w(\alpha)$ calculated with the use of eqs.(5) and (6) for PVA-1.

Since $\bar{P}_w$ should become infinite at the gel point, inserting $1/\bar{P}_w=0$ into eq.(6) leads to

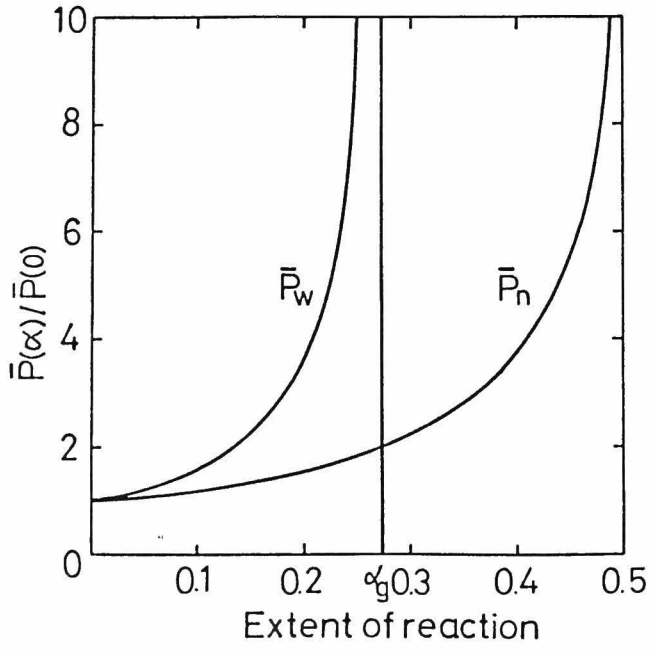

Fig. 2 Variation of $\bar{P}_w(\alpha)/\bar{P}_w(0)$ and $\bar{P}_n(\alpha)/\bar{P}_n(0)$ as a function of extent of reaction α, when the crosslinking is exclusively due to intermolecular reaction (PVA-1).

$$\alpha_g = 1 + \frac{C_2\sqrt{C_1}}{1 + C_2C_3} \qquad (8)$$

where α_g is the extent of reaction at the gel point and was given in the last column of Table II.

On the other hand, the extent of reaction can be directly determined from reduction in the aldehyde concentration during reaction. Fig. 3 demonstrates the result of acetalization carried out at 50°C for a polymer concentration of 4.88 $g \cdot dl^{-1}$. Contrary to the theoretical prediction, gelation did not occur even when the reaction proceeded to extents significantly higher than 0.261, i.e., α_g of this PVA.

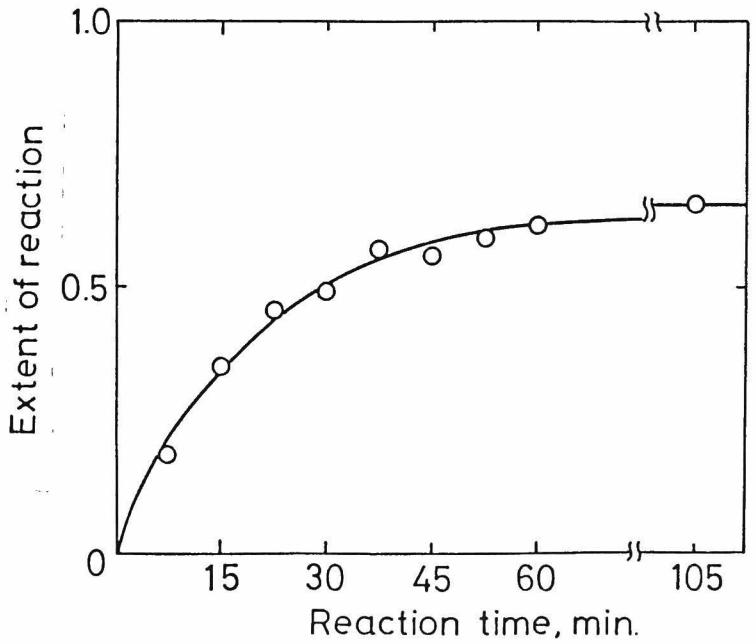

Fig. 3 A plot of extent of acetalization against time (PVA-0, $[OH]_0$=1.11 $mol \cdot l^{-1}$, 50°C, 0.05 N HCl).

Under this reaction condition, the mixture reached an equilibrium without setting to a gel. Lowering temperature brought about gelation expectedly, but in this case it was very difficult to follow the change of the aldehyde concentration with the MBH method. Thus an alternative method was required to measure the true extent of reaction at the gel point, α_t. The method we applied will be described in the following.

The rate of acetalization is in our case given by

$$-\frac{d[CHO]}{dt} = k_1[CHO]+k_2[OH]_0[CHO]-k_{-2}[acetal][H_2O]_0 \qquad (9)$$

Here the concentrations of hydroxyl groups and water are assumed to be equal to the initial concentrations, $[OH]_0$ and $[H_2O]_0$, resp., because the concentrations of aldehyde, [CHO], and acetal formed, [acetal], are extremely low compared with $[OH]_0$ and $[H_2O]_0$. k_2 and k_{-2} are the rate constants of acetalization and deacetalization, resp., while k_1 is the first-order rate constant for intramolecular acetalization in the same prepolymer. As an equilibrium is reached at the sol-gel transition temperature with

$$-\frac{d[CHO]}{dt} = 0 \qquad (10)$$

the α_t value can be obtained from eqs.(9) and (10).

$$\frac{1}{\alpha_t} = \frac{[acetal]+[CHO]}{[acetal]} = 1 + \frac{[H_2O]_0}{(k_1/k_{-2})+(k_2/k_{-2})[OH]_0} \qquad (11)$$

The dependence of k_1/k_{-2} and k_2/k_{-2} on temperature has been determined in chapter 5 as

$$\frac{k_2}{k_{-2}} = \exp(-7.05 + \frac{3,570}{T}) \quad (12)$$

$$\frac{k_1}{k_{-2}} = \exp(2.29 + \frac{450}{T}) \quad (13)$$

By inserting eqs.(12) and (13) into eq.(11), we obtain α_t as a function of the sol-gel transition temperature that is identical to the gel point. The calculated α_t are given in Fig. 4. It is clearly seen that discrepancy between the theoretically estimated α_g and the α_t is very large.

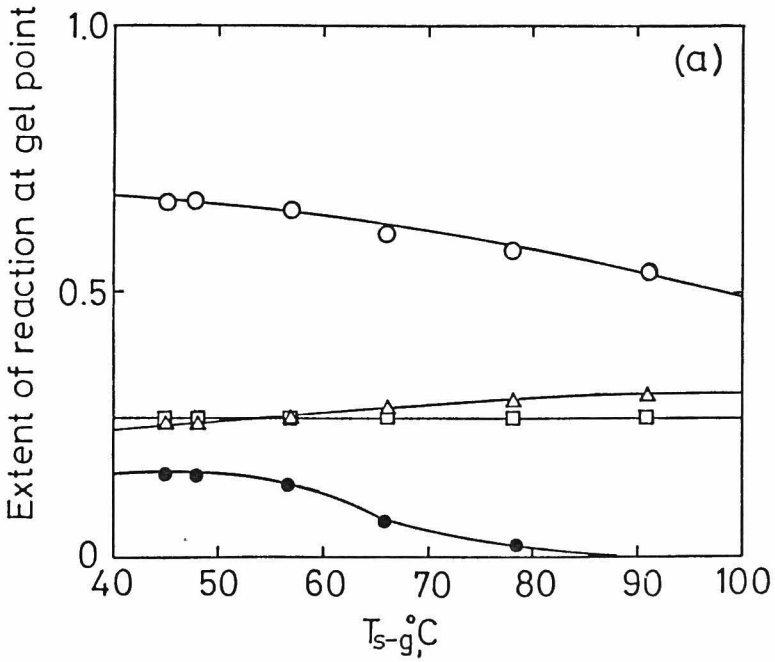

Fig. 4 Extents of each reaction at gel point for different PVA materials ((a) PVA-0).
o α_t (total); □ α_g (INTER); △ $\alpha_{INTRA-I}$ (INTRA-I);
● $\alpha_{INTRA-II}$ (INTRA-II)

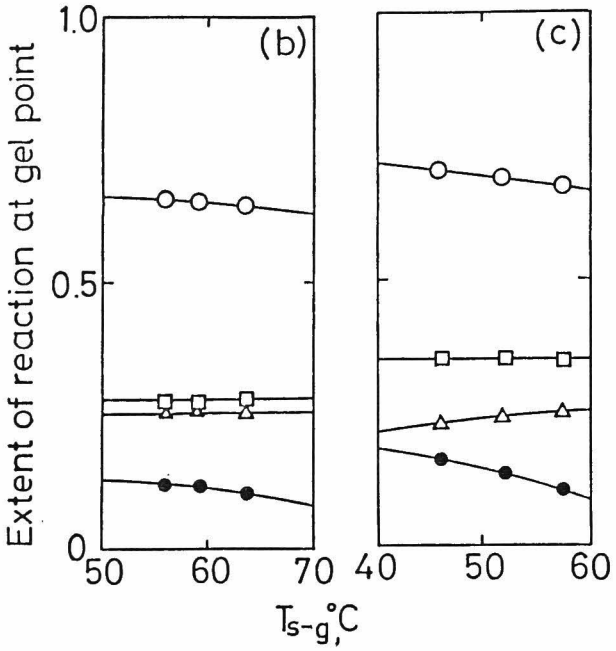

Fig. 4 Continued ((b) PVA-1; (c) PVA-2).

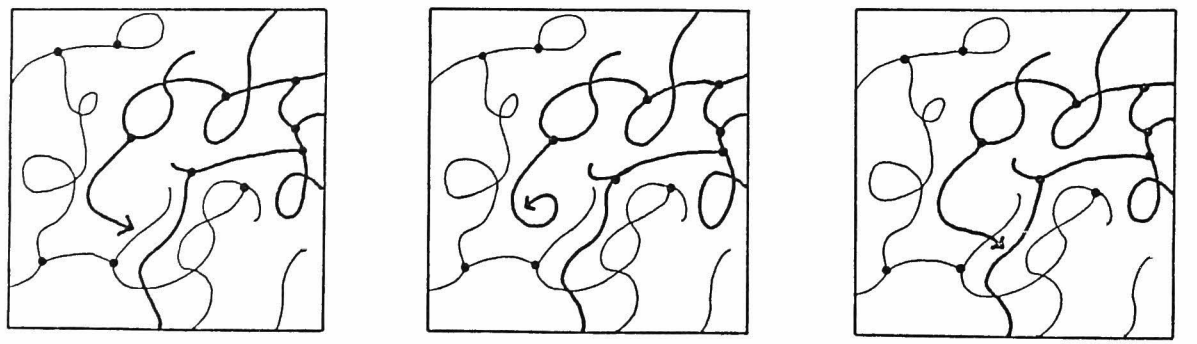

Fig. 5 Schematic representation of inter- and intramolecular reactions.

DISCUSSION

The terminal aldehyde groups of PVA may undergo either intermolecular or intramolecular acetalization reaction. This is schematically illustrated in Fig. 5. It is likely that the intramolecular acetalization of aldehyde involves two types of reaction; the one is with the hydroxyl groups belonging to the same prepolymer as the aldehyde, while the other reaction takes place with the hydroxyl groups of other prepolymers that are linked directly or indirectly to its own prepolymer. Both the intramolecular reactions lead to ineffective crosslinks, in contrast to the intermolecular acetalization. Let us designate the former ineffective acetalization INTRA-I, the latter INTRA-II and the effective intermolecular acetalization INTER. In the following we will formulate the contribution of these reactions.

In eq.(9) the first term represents the rate of acetalization in infinitely dilute solution, that is, acetalization between the terminal aldehyde and the hydroxyl groups belonging to the same prepolymer. Thus the first term can be rewritten as

$$k_1[\mathrm{CHO}]=k_2[\mathrm{OH}]_{\mathrm{INTRA\text{-}I}}[\mathrm{CHO}] \tag{14}$$

or

$$\frac{k_1}{k_2} = [\mathrm{OH}]_{\mathrm{INTRA\text{-}I}} \tag{15}$$

where $[OH]_{INTRA-I}$ is the concentration of hydroxyl groups effective for the intramolecular reaction, INTRA-I.

As is evident from eqs.(9), (14), and (15), the contribution of INTRA-I to the overall extent of acetalization at gel point is given by

$$\alpha_{INTRA-I} = \alpha_t \times \frac{[OH]_{INTRA-I}}{[OH]_0 + [OH]_{INTRA-I}} \qquad (16)$$

From this equation $\alpha_{INTRA-I}$ can be evaluated with use of the following kinetic relation found in chapter 5

$$[OH]_{INTRA-I} = \frac{k_1}{k_2} = \exp(9.34 - \frac{3120}{T}) \quad (\text{unit:mol}\cdot l^{-1}) \qquad (17)$$

and is plotted in Fig. 4 against temperature for PVA-0, PVA-1, and PVA-2, As is clearly seen, $\alpha_{INTRA-I}$ is as large as α_g, that is, the extent of intermolecular acetalization. The main reason for the large $\alpha_{INTRA-I}$ is because the reaction is occurring in dilute solutions. It should be further emphasized that the sum of α_g and $\alpha_{INTRA-I}$ is significantly lower than α_t, at least in the temperature range below about 70°C. This strongly suggests that INTRA-II acetalization cannot be ignored.

In contrast to the INTRA-I acetalization, whose rate is not dependent of $[OH]_0$, the INTRA-II acetalization is not so simple. Near the gel point, any of the aldehyde groups

remaining unreacted in the resultant branched polymer will undergo acetalization with the hydroxyl groups of its own prepolymer ($[OH]_{INTRA-I}$), with those of the other prepolymers constituting the branched polymer ($[OH]_{INTRA-II}$), or with those of any other polymers ($[OH]_0-[OH]_{INTRA-II}$). Therefore the hydroxyl concentration in the vicinity of this aldehyde group may be equal to

$$[OH]_{INTRA-I} + [OH]_{INTRA-II} + ([OH]_0-[OH]_{INTRA-II})$$

The last term refers to the hydroxyl groups which lead to intermolecular crosslinking, INTER. Acetalization with other hydroxyl groups than this $[OH]_{INTER}$ results in formation of ineffective crosslinks.

The $[OH]_{INTRA-II}$ cannot be determined experimentally, on the contrary to $[OH]_{INTRA-I}$. Its theoretical evaluation is also very difficult. Thus the $\alpha_{INTRA-II}$ given in Fig. 4 was obtained by substracting $\alpha_g+\alpha_{INTRA-I}$ from α_t.

The reason for the predominant temperature dependence of $\alpha_{INTRA-II}$ is not clear to us, but it seems likely that this may be partly originated from poor accuracy of k_1/k_2 ratios at high temperatures, because they were determined by extrapolating the k_1/k_2 ratios found in the narrow temperature range from 30°C to 55°C under the assumption of linearity of Arrhenius plots.

On the other hand, Saito concluded from his statistical theory that intramolecular reaction would be ignored. In his treatment the intramolecular reactive groups are assumed to be distributed homogeneously all over the reaction system. However, it is impossible for the reactive groups responsible to INTRA-I to exist far away from this terminal group because of attaching to the same prepolymer as the terminal group. In addition, the reactive groups of INTRA-II seem not to be diffusable throughout in the reaction system in a short time, especially near the gel point where the viscosity of the reaction system is very high. The discrepancy between our experimental results and his theoretical prediction may be attributed to inapplicability of his assumption to our experimental condition.

In conclusion, we may state that the disagreement of the true extent of reaction α_t with the theoretically estimated extent α_g at the gel point will be attributed to occurrence of two types of intramolecular reactions. One of them is the reaction INTRA-I producing small rings in the vicinity of the end of polymer chain. The other is the reaction INTRA-II producing large rings in the polymer network. In any of gelation theories attempting to assess the extent of reaction at the gel point, both of these intramolecular reactions should be taken into account, in particular for the reaction in solution, although they do not participate in the net-work formation.

REFERENCES

1. P. J. Flory, J. Amer. Chem. Soc., 63, 3083, 3091, 3096 (1941).
2. W. H. Stockmayer, J. Chem. Phys., 11, 45 (1943); 12, 125 (1944).
3. A. Charlesby, :Atomic Radiation and Polymers", 1960, Pergamon Press, New York.
4. O. Saito, in "The Radiation Chemistry of Macromolecules", Vol. I, M. Dole Ed., 1972, Academic Press, New York.
5. P. J. Flory, "Principles of Polymer Chemistry, 1953, Cornell Univ. Press, Ithaca, New York.
6. E. Sawicki, T. R. Hanser, T. W. Stanley, and W. Elbert, Anal. Chem., 33, 93 (1961).
7. O. Saito, Polymer Engineering and Science, 19, 234 (1979).

CHAPTER 7.

The Synthesis of Graft Copolymer by Coupling Condensation through Acetalization

INTRODUCTION

This chapter will describe grafting through acetalization of hydroxyl groups in PVA with an aldehyde group attached to an end of PVAc chain produced by chain transfer polymerizations of VAc with monochloroacetaldehyde(MCA) or monochloroacetaldehyde diethylacetal(MCADA). The reaction scheme is represented in Figure 1. As is seen in reactions (3) and (4), acetylation of the backbone PVA of graft copolymer may give a comb-type PVAc, whereas hydrolysis of the

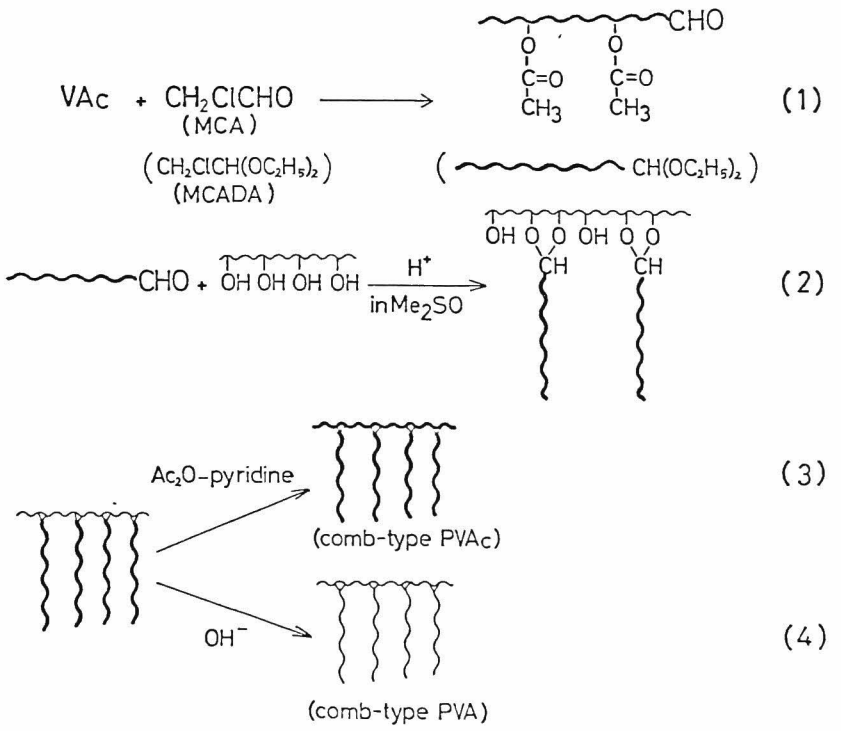

Fig. 1 Reaction scheme

PVAc branches in the graft copolymer under an alkaline condition may yield a comb-type PVA. The latter is possible because the acetal linkage is quite stable in alkaline media. In this paper we will study not only homogeneous grafting, but also heterogeneous grafting onto crosslinked PVA gels in dimethyl sulfoxide(Me_2SO) which is a common solvent for both PVA and PVAc. Use of such insoluble polymers as the substrate of grafting, makes it easy to isolate the unreacted homopolymer from a reaction product. Transformation of the resulting PVA-VAc graft copolymer into the comb-type PVAc or the comb-type PVA will be investigated in the future, together with their properties.

EXPERIMENTAL

Polymerization of VAc VAc was distilled after partial polymerization up to a 15 % conversion and other chemicals were purified by conventional distillation. Polymerization of VAc was initiated in vacuo with azobisisobutyronitrile (AIBN) at 60°C or irradiation with γ rays of 3.2×10^4 rad·hr^{-1} at 20°C. The reason for polymerization at the relatively low temperature was to reduce the radical transfer reaction to monomer to a low level. Concentrations of the chain transfer agents added to monomer are given in Tables I and II, together with other polymerization conditions. After allowing the polymerization to proceed for a given time, we recovered the

Table I

Catalytic Polymerization of VAc in the Presence of Monochloroacetaldehyde Diethylacetal (MCADA) or Monochloroacetaldehyde (MCA) (AIBN, 60°C)

Code number	A-0	A-1	B-1	B-2	B-3
Chain transfer agent(S)	—	MCADA	MCA	MCA	MCA
[AIBN]x10^4, mol·l^{-1}	2.85	2.85	3.11	3.11	3.11
[S]/[VAc], by mole	0	0.325	0.085	0.133	0.180
Polym. time, hr	6.6	12.8	22.0	29.7	36.7
Conversion, %	50	9.4	4.9	3.7	4.7
$\bar{P}_v$	3030	75(126[a])	151	65	60

a) Fractionated, code number A-2.

Table II

Radiation Polymerization of VAc in the Presence of Monochloroacetaldehyde Diethylacetal (MCADA) or Monochloroacetaldehyde (MCA) (3.2x10^4 Rad·hr^{-1},20°C)

Code number	A-3	A-4	A-5	A-6	B-4	B-5	B-6
Chain transfer agent(S)	MCADA	MCADA	MCADA	MCADA	MCA	MCA	MCA
[S]/[VAc], by mole	0	0.10	0.15	0.70	0.10	0.16	0.19
Polym. time, hr	1.36	1.36	1.36	5.37	7.49	23.1	24.6
Conversion, %	32.0	27.3	18.0	19.4	13.6	39.9	58.7
$\bar{P}_v$	8100	635	490	73[a]	201	124	103

a) $\bar{P}_n$=53 (by vapor pressure osmometry).

VAc polymer in the polymerization mixture by precipitating it with n-hexane and purified by repeating solution in acetone and precipitation in water. After extracting with boiling water the chain transfer agents occluded in the polymer, it was dried at 80°C under reduced pressure.

The result of polymerizations is summarized in Tables I and II for the AIBN and radiation polymerizations, respectively. Viscosity-average degrees of polymerization, $\bar{P}_v$, were calculated from $[\eta] = 7.94 \times 10^{-3} \bar{P}^{0.62}$ in acetone at 30°C[1]. Vapor pressure osmometry on A-6 ($\bar{P}_v$=73) revealed that the number-average degree of polymerization, $\bar{P}_n$, was 53. Chain transfer constants calculated from dependence of $\bar{P}_v$ on the chain transfer agent concentration of the monomer mixtures are 5.0×10^{-2} for MCA and 1.3×10^{-2} for MCADA at 20°C. The constant at 60°C for MCA is 9.8×10^{-2}. As given in TableII, $\bar{P}_v$ of PVAc obtained by polymerization at 20°C without the chain transfer agents was as high as 8100. The PVAc materials were subjected to grafting without fractionation except A-2 which was obtained by fractionation of A-1.

The VAc polymer having aldehyde groups at both chain-ends is a product of acetylation of PVA oxidized with sodium periodate to cleave selectively 1,2-glycol bonds in PVA. $\bar{P}_v$ of this PVAc is 92.

Grafting The PVA substrates employed for grafting are a noncrosslinked, soluble PVA with $\bar{P}_n$ of 1340, crosslinked porous beads, and a crosslinked membrane. The beads were prepared by electron-beam irradiation with a dose of 20 Mrads on water-swollen PVA powders that are commercially available, followed by rigorous extraction of the soluble part with boiling water. The crosslinked PVA membrane was also prepared by electron-beam irradiation. The details were described by Ikada etal[2].

Grafting through acetalization of the PVA substrates with PVAc carrying a terminal aldehyde group was carried out at 40-60°C in a Me_2SO medium with the use of HCl or H_2SO_4 as catalyst. The concentration of HCl was adjusted to 0.1 N by adding a 35% concentrated aqueous solution of HCl to the reaction mixture, while that of H_2SO_4, 0.4 N, was made with 98% H_2SO_4. Grafting of PVAc obtained by polymerization with the use of MCADA was always carried out in the presence of 0.1 N HCl. In this case the reaction mixture contained water enough for hydrolysis of the acetal end-group of the PVAc to the aldehyde. The sulfate ester eventually formed on the PVA beads in the grafting with 0.4 N H_2SO_4, was hydrolyzed by treating the grafted gel with plenty of water.

Grafting onto the linear PVA proceeded throughout in homogeneous solution, while the crosslinked beads as well as the membrane remained in a swollen gel state during grafting. In all cases the reaction was allowed to proceed under agita-

tion. Change of solution viscosity accompanying the homogeneous grafting was followed at 50°C in an Ostwald-type viscosimeter.

Separation of Homopolymers In the case of grafting in homogeneous solution, the reaction product was poured into 25 % NaCl aqueous solution to recover the whole polymer. After washing out the acid and NaCl from the precipitates with cold water, the unreacted PVAc was extracted with ethanol and toluene. The remaining polymer was then subjected to extraction with boiling water for removal of the unreacted PVA. When the crosslinked gels were grafted, the unreacted PVAc included inside the grafted gel was extracted with Me_2SO and acetone.

RESULTS

Change of solution viscosity accompanying grafting

Figure 2 shows the change of reduced viscosity of reaction mixtures with time. The concentration of PVA was in all cases kept to 1.0 $g \cdot dl^{-1}$ and weights of added PVAc were four or eight times that of PVA. The $\bar{P}_v$ of PVAc is 73(A-6), 124(B-5), and 490(A-5). It can be seen that no viscosity change occurs when only PVA or PVAc is present in the acidic solution. This fact indicates that reactions such as hydrolysis and degrada-

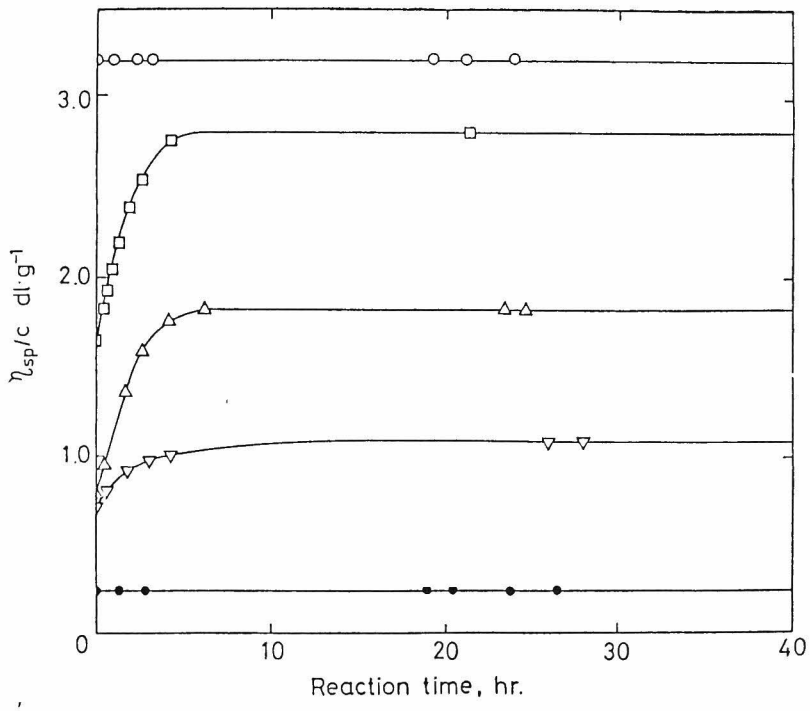

Fig. 2 Variation of solution viscosity with time ([PVA]=1.0 g·dl^{-1}, 0.1 N HCl, 50°C). o PVA; ● PVAc(B-5, [PVAc]=4.0 g·dl^{-1}); □ PVAc/PVA=4(A-5); △ PVAc/PVA=4 (A-6); ▽ PVAc/PVA=8(B-5)

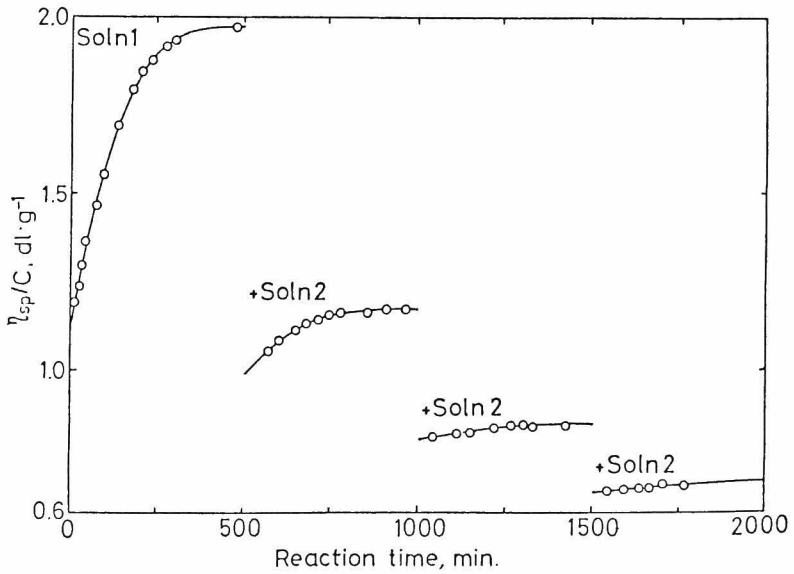

Fig. 3 Variation of solution viscosity accompanying successive addition of PVAc solution(A-2, 0.1 N HCl, 50°C).
Soln 1:PVAc 0.119 g, PVA 0.040 g, Me_2SO 4 ml
Soln 2:PVAc 0.093 g, Me_2SO 3ml

tion does not take place to a significant extent on both PVA and PVAc under this reaction condition(0.1 N HCl and 50°C). It follows that the remarkable increase in solution viscosity recognized for PVA-PVAc mixtures is an indication of occurrence of grafting.

To examine whether levelling off of viscosity changes observed after about 6 hrs is due to attainment of an acetalization equilibrium or to other reasons such as inhibitory effect of the grafted PVAc chains against further reactions, small amounts of PVAc prepolymer were newly added to the solution when its viscosity ceased to increase. The result is given in Figure 3. The first solution, Soln 1, contains 0.119 g of PVAc(A-2) and 0.040 g of PVA in 4 ml of Me_2SO, while the added solutions, Soln 2, have 0.093 g of A-2 dissolved in 3 ml of Me_2SO without PVA. As is seen in Figure 3, addition of Soln 2 to Soln 1 brings about instantly a large decrease in viscosity due to the dilution of solutions, followed by a gradual viscosity increase, indicating that the coupling reaction further takes place between PVA and the added PVAc. However, the extent of viscosity increase becomes very small on the third addition of Soln 2. Thus one may state that 0.040 g of this PVA is capable of being grafted, at most, with (0.119 g + 3x0.093 g) of this PVAc.

Grafting onto PVA gels Evidently, determination of the solution viscosity change with time gives a qualitative evidence for grafting as well as a measure of the rate of coupling reaction, but no information about the fraction of PVAc having the terminal aldehyde in the PVAc material used for the reaction. In this connection grafting onto insoluble gels may provide a useful means, since the PVAc molecules without terminal aldehyde, being not able to participate in grafting, can be separated from the reaction product with simple extraction.

To test the availability of this method, a coupling grafting onto crosslinked porous beads of PVA was undertaken with PVAc carrying aldehyde groups at both chain ends, which was obtained by oxidation of a conventional PVA with sodium periodate, followed by acetylation. Employing porous beads as the substrate for grafting is also advantageous in that these have a large specific surface area available for grafting, compared with a film, so far as grafting will be restricted to the surface region. The weight fraction of PVAc coupled to the PVA beads is given as a function of reaction time in Figure 4. The weight ratio of PVAc to PVA employed in the reaction is 0.5. As is seen, the weight of PVAc coupled increases rapidly with time and then reaches a plateau level. In this experiment the maximum fraction of PVAc coupled is smaller than unity, presumably because the

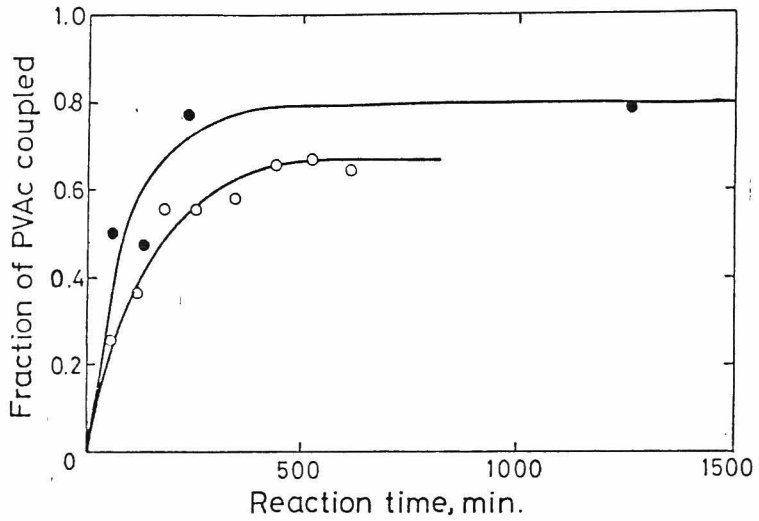

Fig. 4 Reaction of PVAc obtained from IO_4^--oxidized PVA with PVA beads (PVAc/PVA=0.5). o [PVAc]=0.461 g·dl^{-1}, 0.1 N HCl, 60°C; • [PVAc]=0.487 g·dl^{-1}, 0.4 N H_2SO_4, 40°C

amount of PVA gels used was not large enough to be reacted with all the reactive molecules present in the added PVAc. The slight difference in the weight fraction observed between the catalysts HCl and H_2SO_4 may be explained in terms of deacetalization; the reaction mixture where HCl is the catalyst contains a small amount of water (≈0.3 mol·l^{-1}) in contrast to the mixture with H_2SO_4 and hence deacetalization seems to have taken place to some extent.

Figure 5 shows the influence of weight ratio of PVAc to PVA on coupling of PVAc produced by the chain transfer polymerizations. It is seen that the weight of PVAc coupled increases first with increasing PVAc/PVA ratio and then reach-

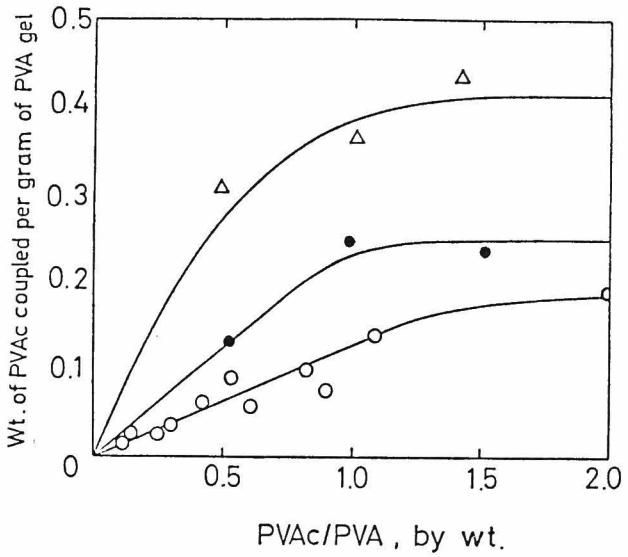

Fig. 5 Influence of PVAc/PVA ratio on grafting of PVAc onto PVA beads. o A-1, 0.1 N HCl, 60°C; • B-1, 0.4 N H_2SO_4, 40°C; △ B-2, 0.4 N H_2SO_4, 40°C

es a plateau, although large amounts of hydroxyl groups must still remain unreacted in the beads. This suggests that grafting is rather confined to the surface region of the beads. Obviously, initial slopes of the curves in Figure 5 should give the weight fraction of PVAc actually having the aldehyde end-group. The fractions estimated from the initial slopes are summarized in Table III. It is noteworthy that PVAc produced by the periodate oxidation has a high fraction close to unity as expected, whereas the fraction of PVAc with a terminal aldehyde (or acetal) is somewhat low for PVAc obtained by the polymerization in the presence of chain transfer agents.

Grafting was further conducted onto a crosslinked PVA

Table III

Fraction of PVAc Having Aldehyde End-group

PVAc	A-1	B-1	B-2	IO_4^--oxidized PVAc
$\bar{P}_v$	126	151	65	92
Fraction	0.13	0.25	0.54	0.96

Table IV

Grafting onto gel membrane of PVA (0.1 N HCl, 30°C, 16 hr)

PVAc	B-5			A-4		
Grafted branch	none	PVAc	PVA	none	PVAc	PVA
Weight increase, %	——	0.5	0.1	——	0.5	0.3
Water fraction of water-swollen membrane	0.678	0.663	0.686	0.678	0.663	0.674
Contact angle, deg.	41.3	68.7	40.8	41.3	77.5	40.3

Table V

Turbidity appearing at pouring the reaction mixture into different solvents at 25°C (reaction: A-5, 0.1 N HCl, 50°C, 19 hr)

	Solubility		PVAc/PVA		
	PVA	PVAc	0.5	1.0	2.0
Water	PS	NS	HT	HT	HT
Ethanol	NS	VPS	HT	HT	MT
Methanol	NS	PS	HT	MT	ST
Toluene	NS	GS	HT	MT	ST
MEK	NS	GS	MT	ST	C
Acetone	NS	GS	MT	ST	C

PS: good solvent; VPS: very poor solvent;
PS: poor solvent; NS : non-solvent
HT: highly turbid; MT: moderately turbid;
ST: slightly turbid; C: clear

membrane in Me_2SO at 30°C for 16 hrs. As is seen in Table IV, where the result is given, the weight increase of the membrane accompanying the reaction is insignificant. Yet, occurrence of grafting is evident, since the contact angle against water increases as a result of grafting of PVAc which is much more hydrophobic than PVA and again decreases to the value of ungrafted membrane upon hydrolysis of the grafted PVAc.

Homogeneous Grafting onto Linear PVA Grafting in a large scale was carried out in homogeneous solutions to obtain soluble PVA-PVAc graft copolymers. In this case, removal of homopolymers from the graft copolymer was not so easy, especially in the grafting which resulted in formation of the graft copolymer with a relatively large number of PVAc branches. Since a selective precipitation method involves several disadvantages [3], we adopted the conventional extraction technique in order to fractionate the product into three component polymers.

Table V gives the precipitation behavior observed when the mixtures of reaction with A-5 were poured into various solvents after reacting for 19 hrs. Strong turbidity appeared on pouring the reaction products into water, irrespective of the weight ratio of PVAc to PVA, but ethanol did not cause such strong turbidity. On the other hand, the amount of

polymer precipitated was much smaller when the mixture with a PVAc/PVA of 2 was poured into methanol and toluene. Interestingly, pouring the product of reaction with the PVAc/PVA ratio of 1 into methyl ethyl ketone (MEK) or acetone led to a slightly turbid appearance. However, when the mixture with a PVAc/PVA ratio of 2 was poured into MEK or acetone, no turbidity was observed, presumably because micelles may be formed in these solvents as a result of prevention of PVA chains from association into a large particle by soluble PVAc chains[4].

Based on the above findings, we decided to accomplish extraction of unreacted PVAc with ethanol and toluene, although it might be plausible that some of the graft copolymer would be also extracted. However, loss of a large amount of graft copolymer is not likely, since the extraction was performed for the precipitate recovered from the whole reaction mixture. The reaction products, if once precipitated, were no more dispersed even into acetone.

From the weights of starting PVA ($W_{PVA,0}$), starting PVAc ($W_{PVAc,0}$), and PVAc unextracted (W_{PVAc}) we can calculate the percent graft, defined as ($W_{PVAc}/W_{PVA,0}$)x100 and the grafting efficiency of PVAc, defined as ($W_{PVAc}/W_{PVAc,0}$). These are plotted against duration of the reaction in Figures 6 and 7. The PVAc samples used are A-5 and B-5, the PVAc/PVA ratios being 4 and 8, respectively. The reaction conditions are

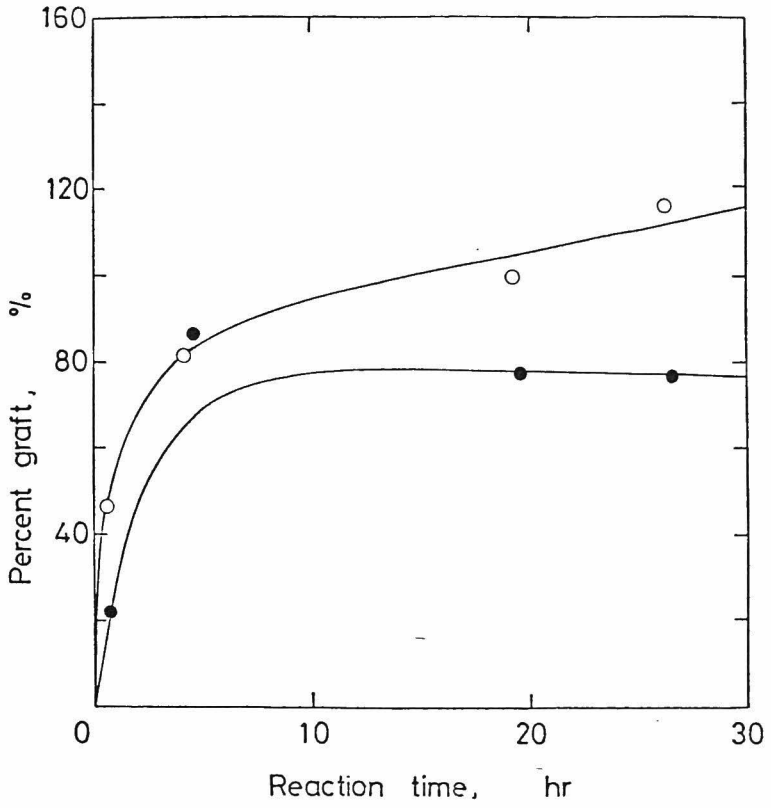

Fig. 6 Dependence of percent graft on reaction time for homogeneous reaction ([PVA]=1.0 g·dl^{-1}, 0.1 N HCl, 50°C). o PVAc/PVA=4(A-5); ● PVAc/PVA=8(B-5)

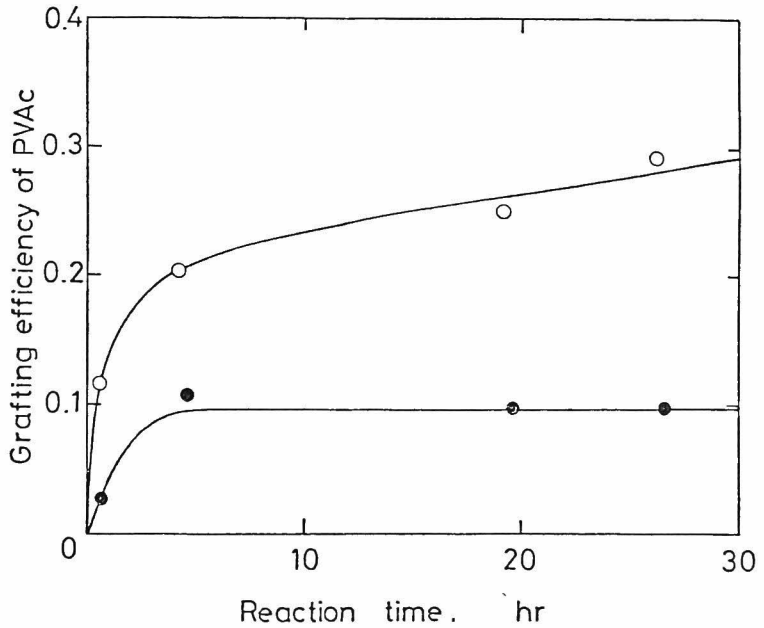

Fig. 7 Dependence of grafting efficiency of PVAc on reaction time for homogeneous reaction ([PVA]=1.0 g·dl^{-1}; 0.1 N HCl, 50°C). o PVAc/PVA=4(A-5); ● PVAc/PVA=8(B-5)

the same as in the grafting shown in Figure 2. It is seen that the time dependence of the percent graft as well as the grafting efficiency is in accordance with that of solution viscosity in Figure 2, except that in the grafting with A-5 the coupling reaction still takes place, though slowly, even after duration of 5 hr.

Figures 8 and 9 illustrate the dependence of the percent graft and the grafting efficiency of PVA on the PVAc/PVA ratio,,,,,, respectively. As is expected, the grafting efficiency of PVA approaches to unity with increasing PVAc/PVA ratio. In the PVAc/PVA range below 2, the percent graft appears to increase almost linearly as the PVAc/PVA becomes high, implying that the PVAc molecules having an aldehyde end-group may be effectively reacted with PVA .

DISCUSSION

Fraction of PVAc Having a Terminal Aldehyde Group

The synthesis of graft copolymers through condensation reactions between two different polymers requires the branch prepolymer possessing one functional end-group which is reactive with some specific groups on the backbone prepolymer. Such polymers with a functional end-group have often been produced by polymerizing a monomer in the presence of a chain

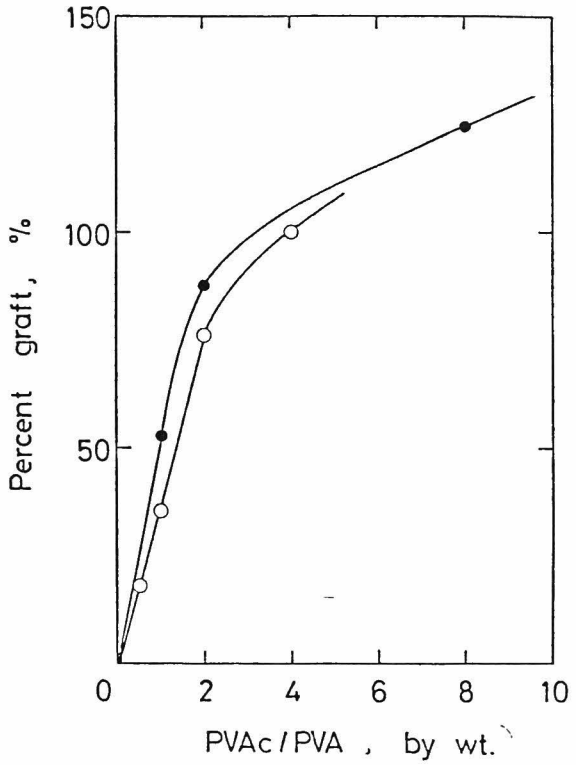

Fig. 8 Dependence of percent graft on PVAc/PVA ratio (total polymer conc.=5.0 g·dl^{-1}, 0.1 N HCl, 50°C).
o A-5, 19 hr, • A-6, 28 hr

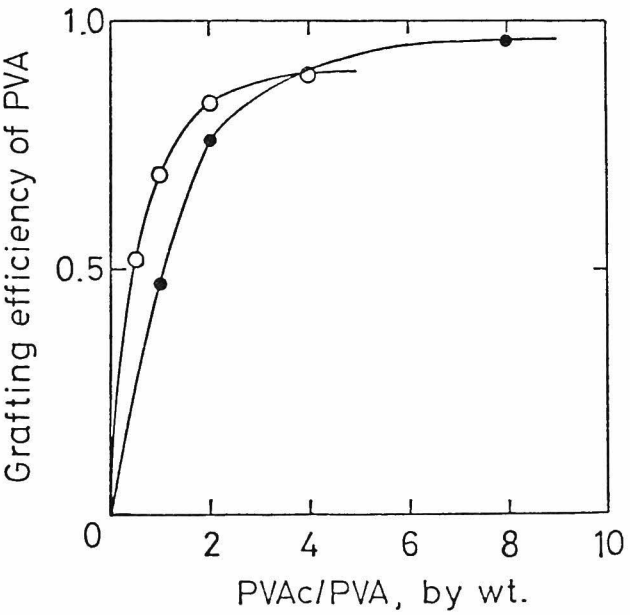

Fig. 9 Dependence of grafting efficiency of PVA on PVAc/PVA ratio (total polymer conc.=5.0 g·dl^{-1}, 0.1 N HCl, 50°C).
o A-5, 19 hr; • A-6, 28 hr

transfer agent carrying the functional group. This method is simple, but has difficulty in determining the fraction of the polymer that really carries the reactive fragment of the chain transfer agent at the chain end. Although this may be evaluated from the polymerization kinetics, the direct determination is not easy because of the extremely low content of end groups in the polymer. In chapter I, we have succeeded in determining the fraction by thin layer chromatography for polystyrene and poly(methyl methacrylate) polymerized using trichloroacetyl chloride and aminoethanethiol as chain transfer agent . However, this technique was not applicable for this PVAc, because attachment of only one aldehyde group to PVAc had virtually no effect on the chromatographic behavior of PVAc. A colorimetric titration has been reported to be promising for determination of low-molecular-weight aldehydes[5], but the molar absorption coefficient is dependent on the substituent neighboring to aldehyde group, which is not yet made clear for the PVAc used in the grafting.

In this work we attempted to utilize a grafting method with insoluble porous beads as a tool for determining the fraction of PVAc having aldehyde groups. As is demonstrated in Figure 5, this new method seems to be useful if the hydroxyl group that is accessible to the coupling reaction is available in excess and in addition the system contains

no water that will bring about deacetalization of grafted PVAc chains. It may be stated that this is a kind of affinity chromatography, in which some chemical bonds as in the coupling reactions are formed.

The observed fractions, given in Table III, are considerably smaller than unity, though addition of the chain transfer agents to monomer led to remarkable reduction in the chain length. Accordingly it seems likely that some of propagating radicals have abstracted hydrogen atoms directly from either aldehyde or acetal groups. For example, if the following radical is formed as a result of a radical transfer reaction to MCADA and

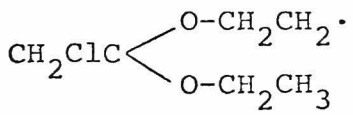

reinitiates the polymerization, the PVAc chain formed is not able to react with PVA, since the aldehyde resulting from hydrolysis of the acetal end-group must be liberated from the polymer chain. Therefore, it may be reasonable that PVAc obtained by polymerization with MCA or MCADA has a low content of the chain effective for acetalization with PVA.

Some Characteristics of Grafting through Acetalization

In principle, acetalization accompanies deacetalization

which has, however, exceedingly low rate constants in the reaction of PVA with low-molecular weight aldehydes. We have in chapter 5 determined the rate constants of acetalization and deacetalization between PVA reactants carrying terminal aldehydes in water as well as in Me_2SO. It has been found that the deacetalization normally proceeds with an appreciable rate owing to high concentration ratios of water to aldehyde.

Influence of a small amount of water on the reaction can be seen in Figure 4, where the fraction of PVAc coupled is compared for the reactions carried out with H_2SO_4 and HCl catalysts. As the HCl concentration of the reaction mixture was adjusted to 0.1 N by addition of 35 wt% aqueous solution of HCl, the reaction mixture contains water of 0.3 $mol \cdot l^{-1}$ which is much higher than the concentration of aldehyde group in the reaction mixtures($\simeq 10^{-3}$ $mol \cdot l^{-1}$). Although the extent of deacetalization may be not remarkable at low concentrations of water, elimination of water from the reaction mixture is desired for grafting to proceed in high yields. In this connection it should be noticed that the use of H_2SO_4 as catalyst will accompany sulfation of PVA unless water is sufficiently present in the mixture. The resultant sulfate ester is, however, readily hydrolyzed when it comes in contact with plenty of water.

In a condensation coupling between long polymric chains one might expect that some steric hindrance

would be operative. Slowing down of the coupling reaction observed at high extents of reaction (see Figures 6 and 8), might suggest that the condensation coupling would be indeed affected by resistance of chain interpenetration which would become more pronounced with increasing chain length[6].

Another interesting feature of this grafting is a surface-restricted reaction observed in the grafting onto the crosslinked PVA gels. The surface reaction here does not strictly mean the reaction occurring only at the surface, but includes that occurring close to the surface. An evidence of such surface grafting can be given by the results in Table IV, which clearly exhibits a negligibly small weight increase of membrane, but an appreciable increase in water contact angle brought about by grafting. Such a reaction seems to provide an novel method for surface modification without affecting the bulk properties of the substrate polymer. According to the result in Figure 5, it appears that the porous PVA beads also prevent the PVAc molecules from free penetration into the gel. A further investigation with PVA gels of different crosslinking densities as well as with PVAc of widely different molecular weights will give valuable information on diffusion of polymer molecules into a polymeric matrix.

Chemical Structure of Graft Copolymers

Provided that the grafted branches have the chain length identical to that of the PVAc prepolymer, the number of branches per 1000 repeating units of PVA can be calculated from the following equation with the use of the data on percent grafts and grafting efficiencies of PVA.

$$\text{Number of branches} = \frac{(\text{Percent graft}/100)}{\text{Grafting efficiency of PVA}} \frac{1000\ M_{VA}}{\bar{M}_{PVAc}}$$

where $\bar{M}_{PVAc}$ is the molecular weight of one PVAc branch and M_{VA} is the molar weight of repeating unit of PVA(44). The numbers of branches calculated from the results in Figures 8 and 9 are given in Table VI. In this calculation $\bar{M}_{PVAc}$ is assumed to be identical to the molecular weight of the PVAc prepolymers. It is seen that the graft copolymers prepared from PVAc with $\bar{P}_V$ of 490 possess very few branches even when the PVAc/PVA weight ratio in the reaction mixture is raised to 4. This agrees, however, well with the finding that a large portion of the PVAc has no terminal aldehyde and hence is ineffective for grafting. Since the plot of percent graft against PVAc/PVA in Figure 8 is, in nature, similar to that illustrated in Figure 5, the grafting effi-

Table VI

Number of Branches of Graft Copolymers ($\bar{P}_{n,0}$ of PVA=1340)

PVAc	A-5				A-6		
$\bar{P}_n$ of PVAc	490[a]				53		
PVAc/PVA	0.5	1.0	2.0	4.0	1.0	2.0	8.0
Percent graft, %	17.9	35.3	76.0	100.0	52.8	87.5	124.3
Grafting efficiency of PVA	0.52	0.69	0.84	0.90	0.47	0.76	0.97
Number of branches[b]	0.36	0.53	0.95	1.16	10.8	11.1	12.4

a) viscosity-average. b) per 1000 PVA monomer units.

ciency of PVAc which is obtained from the initial slope of curves in Figure 8 should correspond to the weight fraction of PVAc having the reactive end-group. The fraction estimated from Figure 8 is 0.4 for A-5 and 0.5 for A-6. If some errors arising from the tedious isolation step of graft copolymers are taken into consideration, it appears that the agreement of these calculated fractions with those given in Table III is satisfactory. The low fraction for A-1 may be, in part, due to the high temperature(60°C) during grafting, which would lead to significant deacetalization.

As is seen in Table VI, the graft copolymers synthesized from A-6 carry much more PVAc branches than those from A-5. Attachment of PVAc branches to the PVA backbone may make the solubilization behavior much complicated, as demonstrated in Table V. It is interesting to point out that PVA is known to exhibit a peculiar solubility behavior when partially acetylated; for instance, the PVA acetylated by about 10 mol% is readily soluble in water without heating.

REFERENCES

1. A. Nakajima, Kobunshi Kagaku, 6, 451 (1949).
2. Y. Ikada, T. Mita, F. Horii and I. Sakurada, Radiat. Phys. Chem., 9, 633 (1977).
3. Y. Ikada, Adv. Polym. Sci., 29 47 (1978).
4. F. Horii, Y. Ikada and I. Sakurada, J. Polym. Sci. Polym. Chem. Ed., 12 323 (1978).
5. E. Sawicki, T. R. Hauser, T. W. Stanley and W. Elbert, Anal. Chem., 33, 93 (1961).
6. H. Morawetz, J. Polym. Sci. Polym. Sym., 62, 271 (1978).

CHAPTER 8.

Coupling Reactions between Polystyrene Containing Acyl Chloride Endgroups and Poly(vinyl Acetate) Containing Amino Groups at the Chain End or along the Chain

INTRODUCTION

In this work we want to report preparation of block and graft copolymers by coupling reactions through condensation of amino and acyl chloride groups attached to prepolymers A and B. This condensation reaction does not require special experimental procedures such as living coupling reactions. In the polymer-polymer condensation coupling it is, however, desirable to select reactions with a high coupling rate constant k_2, since concentrations of the functional groups in the reaction mixture may be extremely low. The k_2 value of reactions between low-molecular-weight aliphatic compounds with amino and acyl chloride groups is known to be markedly high, ranging from 10^2 to 10^6 $l \cdot mol^{-1} \cdot sec^{-1}$ [1].

Recently Gupta and Nandi [2] have studied a similar synthesis of graft and block copolymers by means of amide linkages. The polymer-polymer coupling through acetalization which has a much lower k_2 than that of the above reaction was described in chapter 5.

EXPERIMENTAL

Materials

Styrene was purified by a conventional method. Vinyl acetate was washed, subjected to simple distillation and then fractionally distilled after polymerization up to ca. 15 % conversion by an addition of 2,2'-azobisisobutyronitrile; a middle fraction of the distillate giving a boiling point of 72-73°C was used for the subsequent polymerization.[3] Ethylene diamine (EDA), triethylamine (TEA), and chloroform were distilled after drying. Poly(vinyl alcohol) (PVA) of a commercial product was resaponified and then purified by Soxhlet extraction with methanol; it was used without fractionation.

Preparation of Polystyrene with One Terminal Acyl Chloride Group (PS-COCl)

PS-COCl was prepared by a radiation polymerization of styrene in the presence of trichloroacetyl chloride (TCAC) according to chapter 3 . After degassing styrene-TCAC mixtures by repeated freezing and thawing, they were sealed in ampoules, and irradiated at room temperature with gamma-rays from a Co-60 source under a dose rate of 1.0×10^4 rads/hr. The product was recovered by pouring the reaction mixture into n-hexane. To cut off

the low molecular weight fraction from this gross polymer, the polymer was roughly fractionated by addition of n-hexane to its chloroform solution. The fractionated polymer was dried under reduced pressure and desiccated over calcium chloride. The number of acyl chloride endgroups per unfractionated polymer chain was found to be 0.5-0.8 in chapter 2, but the present polymers seem to have smaller contents of acyl chloride endgroups, because some of them might have been deactivated during the subsequent fractionation process.

Preparation of Poly(vinyl Acetate) with One Terminal Amino Group ($PVAc-NH_2$)

In a similar manner as the styrene polymerization, vinyl acetate-TCAC mixtures were irradiated in vacuo with gamma-rays at a dose rate of 3.1×10^4 rads/hr. After opening the ampoules, the polymerization mixture was added to chloroform containing EDA in a large excess to convert acyl chloride endgroups into amino groups and then the resulting $PVAc-NH_2$ was precipitated with n-hexane. Repeated dissolution in acetone followed by precipitation with water was carried out to remove all traces of contaminants such as EDA and salts from the polymer. $PVAc-NH_2$ was stored in a desiccator after being dried under reduced pressure.

Preparation of PVAc with Amino Groups along the Chain ($PVAc/NH_2$)

Partial acetalization of PVA with aminoacetaldehyde diethyl acetal was carried out in the presence of 2.7 N hydrochloric acid at 60°C for 24 hr, the concentration of the aqueous PVA solution being 3.0 g/dl[4] . The reaction mixture was poured into acetone to precipitate the partially aminoacetalized PVA. The degree of acetalization was determined by a conductivity titration of the amino groups in the acetalized polymer[5] . The remaining hydroxyl groups in the polymer were acetylated in a mixture of acetic acid and concentrated hydrochloric acid (30 : 1) at 40°C for 30 hr[6] . The reaction mixture became a homogeneous solution during acetylation. The $PVAc/NH_2$ thus formed was recovered by pouring the whole reaction mixture into pure ice water or into ice water containing NaCl for salting-out. It was then purified by repeated dissolution in acetone followed by precipitation with water. Sodium chloride and other insoluble contaminants were removed from the polymer by centrifugation of its chloroform solution.

Condensation Coupling Reactions

Chloroform solutions of PS-COCl of various concentrations were mixed with chloroform solutions of $PVAc-NH_2$ or $PVAc/NH_2$. The equimolar mixing ratios with respect to

the functional endgroups, which give the highest yield of the block copolymer, were determined by viscosity measurements of reaction mixtures. The amino groups of the PVAc prepolymers are not free, but of ammonium chloride type. The coupling reactions to yield block copolymers (PS-COCl + PVAc-NH_2) and graft copolymers (PS-COCl + PVAc/NH_2) were allowed to proceed at 30°C. TEA was added to the solutions, as an acceptor of hydrogen chloride. After stirring, the whole polymers were recovered by pouring the reaction mixtures into n-hexane. The hydroxyl and unreacted amino groups in the polymer recovered from the graft coupling reaction mixture were thoroughly acetylated in a pyridine-acetic anhydride (2 : 1) mixture at 100°C.

Isolation and Characterization of the Copolymers

Pure block and graft copolymers were isolated from the reaction products by extraction of the PVAc homopolymer with methanol at room temperature and the PS homopolymer with cyclohexane at 40°C. The removal of the PS homopolymer from the product of the block coupling reaction involved a somewhat complicated procedure compared to the conventional extraction; the product was dispersed in cyclohexane at 50°C, cooled to 0°C to precipitate not only the block copolymer but also PS and then heated to 30°C to give a clear supernatant cyclohexane solution of the PS homo-

polymer. The block copolymer remained in a precipitated state throughout the procedure. The methanol extract was confirmed by infrared spectroscopy to be pure PVAc and the PS obtained was found to be free of PVAc, according to thin layer chromatography. In addition a chromatographic measurement showed that the content of the unextracted homopolymers in the purified copolymers was smaller than 2 wt% for both block and graft copolymers[7] .

The chemical composition was determined by the alkali consumption during the hydrolysis of the PVAc part of the copolymers, in the presence of water. To separate the grafted PS branches from the backbone, the graft copolymer was hydrolyzed with 1.5 N HCl in dioxane at 70°C. As a result of this hydrolysis the PVAc backbone was converted into a PVA chain which was not soluble in the hydrolysis medium, while the PS chains separated from the backbone remained soluble. Therefore, the separated PS could be readily recovered by pouring the solution into water after centrifugation of the dioxane-insoluble part.

Number-average molecular weights $\bar{M}_n$ of the prepolymers, the pure block and graft copolymers and the PS branch separated from the graft copolymer were determined by osmometry in tetrahydrofuran with High-Speed Membrane Osmometers.

RESULTS AND DISCUSSION

Block Coupling Reaction

The highest yield of block copolymers is attained when PS-COCl and PVAc-NH_2 are mixed in such a way that the molar concentrations of acyl chloride and amino groups in the mixture are the same. Although we did not perform the functional endgroup determination, the optimum weight fraction w_s of PS-COCl in the prepolymer mixture can be determined by measuring the viscosity of the reaction mixture versus w_s after coupling. The theoretical basis for determination of the optimum w_s from the viscosity change is given in Appendix. Figure 1 shows one example of viscosity change of a reaction mixture, measured in the presence of HCl preventing the prepolymers from coupling, and in the presence of TEA as a HCl acceptor.

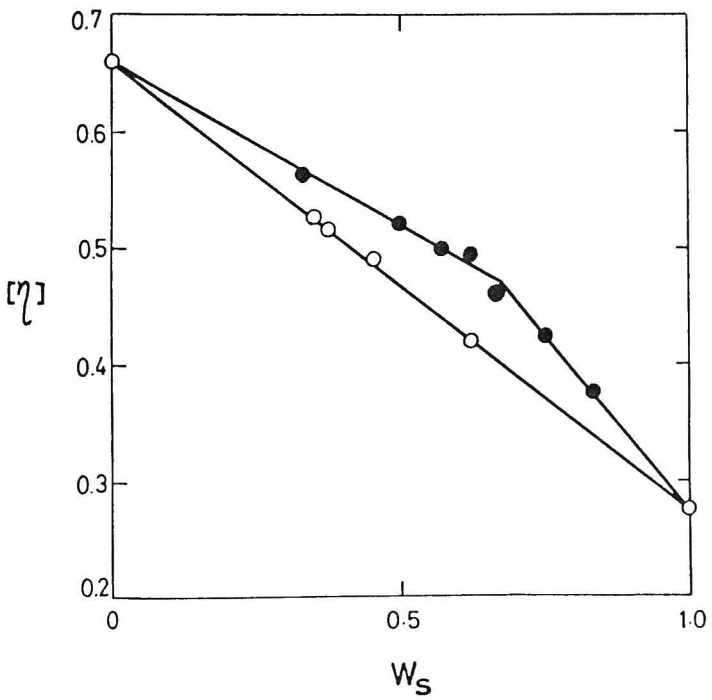

Fig. 1. Dependence of $[\eta]$ on w_s in the polymer mixture for block coupling reaction (polymer conc.= 0.833 g/dl, $\bar{M}_n$ of PS-COCl = 4.51×10^4 and $\bar{M}_n$ of PVAc-NH_2 = 7.56×10^4): (o) in the presence of HCl; (•) in the presence of TEA

The total polymer concentration is 0.833 g/dl. Intrinsic viscosities of the reaction mixture before and after the coupling reaction were assumed to be equal to the logarithms of reduced viscosities, $\ln(\eta_{rel/c})$. The molecular weights of PS-COCl and PVAc-NH_2 are 4.51×10^4 and 7.56×10^4, respectively. The viscosities increased instantaneously, upon addition of TEA, indicating that the coupling reaction takes place as a result of HCl abstraction. It is expected that the highest yield is obtained when the coupling reaction is carried out at a w_s which corresponds to the intersection of the two straight lines in Figure 1.

Table I summarizes the intrinsic viscosities and number-average molecular weights of the prepolymers used, and the optimum weight fractions w_s of PS-COCl which were determined by the viscosity measurement. The subscripts, s, a, and b refer to PS, PVAc, and the block copolymer, respectively. The block coupling reaction was carried out at the optimum weight fraction w_s under stirring for 10 min after addition of TEA, the total polymer concentration being 5.0 g/dl. Table I shows also the intrinsic viscosities and yields of the resultant block copolymers. The number-average molecular weights of the block copolymers are given in Table II, together with the styrene content of the block copolymer and the fractions of the prepolymer carrying the terminal functional group, f_a and f_s in other words, block coupling efficiencies.

TABLE I

Block Coupling Reaction between PVAc-NH_2 and PS-COCl

		BLOCK 1	BLOCK 2	BLOCK 3
PS-COCl	$[\eta]_s$	0.268	0.441	0.268
	$\bar{M}_s \times 10^{-4}$	4.51	9.38	4.51
	amount[a], g	2.0	2.0	2.0
$PVAc-NH_2$	$[\eta]_a$	0.658	0.658	0.635
	$\bar{M}_a \times 10^{-4}$	7.56	7.56	7.03
	amount[a], g	0.985	0.353	1.077
optimum w_s		0.67	0.85	0.65
Block copolymer	$[\eta]_b$	0.683	0.783	0.670
	yield, g	0.626	0.470	0.475

a) Block coupling reactions were carried out with these amounts of polymers dissolved in chloroform, the total polymer concentration being kept at 5.0 wt. %.

TABLE II

Molecular Weights of Block Copolymers and Block Coupling Efficiencies of PS-COCl and $PVAc-NH_2$

		BLOCK 1	BLOCK 2	BLOCK 3
$\bar{M}_n$ of block copolymer(10^4)	obs.	12.5	15.9	10.3
	calc.	12.1	16.9	11.5
Weight-% St	obs.	36.1	60.2	43.4
	calc.	37.3	55.5	39.2
f_a		0.385	0.631	0.301
f_s	-	0.113	0.141	0.103

The calculated values of $\bar{M}_n$ and of the styrene content in Table II are $\bar{M}_s + \bar{M}_a$ and $\bar{M}_s/(\bar{M}_s + \bar{M}_a)$, respectively. The f_s and f_a values were determined from the yield of block copolymers and their chemical composition.

The calculated values of $\bar{M}_n$ and of the styrene content of the resultant block copolymers are in satisfactory agreement with the observed values, suggesting that the coupling reaction takes place stoichiometrically. The low block efficiencies, especially f_s, may be due partly to hydrolysis of acyl chloride by traces of water.

Graft Coupling Reaction

a) Synthesis of Partially Aminoacetalized PVAc(PVAc/NH_2): As described in the experimental section, the PVAc backbone carrying amino groups randomly distributed along the main-chain was obtained by partial aminoacetalization of PVA, followed by acetylation of the remaining hydroxyl groups in the polymer. Figure 2 illustrates the influence of the mole ratio of aminoacetaldehyde diethyl acetal on the degree of acetalization of PVA obtained.
It is seen from Fig.2 that the added aminoacetaldehyde diethyl acetal has completely reacted with PVA. Acetylation of the hydroxyl groups in the aminoacetalized PVA resulted in formation of PVAc/NH_2, which is soluble in benzene and toluene.

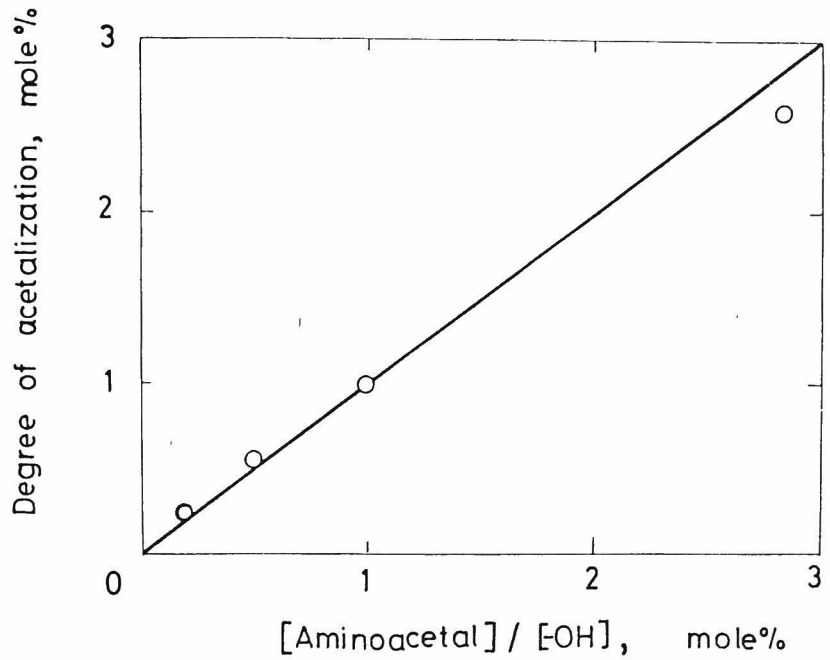

Fig. 2. Acetalization of PVA with aminoacetaldehyde diethyl acetal in aqueous solution (PVA conc. = 3.0 g/dl, $\bar{M}_n$ of PVA = 13.0×10^4, and temp. = 60°C).

We used PVAc/NH_2 containing 2.0 mole% amino group for all the coupling reactions. Since $\bar{M}_n$ of this polymer is 13.0×10^4, 30 amino groups are contained, on the average, in one PVAc/NH_2 molecule.

b) Influence of Reaction Time and Polymer Concentration on the Coupling Yield: Figure 3 shows the yield of graft copolymer in the coupling reaction carried out at a total polymer concentration of 5.0 g/dl.

The $\bar{M}_n$ values of PS-COCl used are 4.62×10^4, 9.22×10^4, and 14.3×10^4. After addition of TEA to the reaction mixtures and stirring for periods of 2 min, 1, 6, and 24 hr, hydrogen chloride was added in excess to stop the reaction. It appears that the coupling reaction comes to completion within about 2 min in all cases.

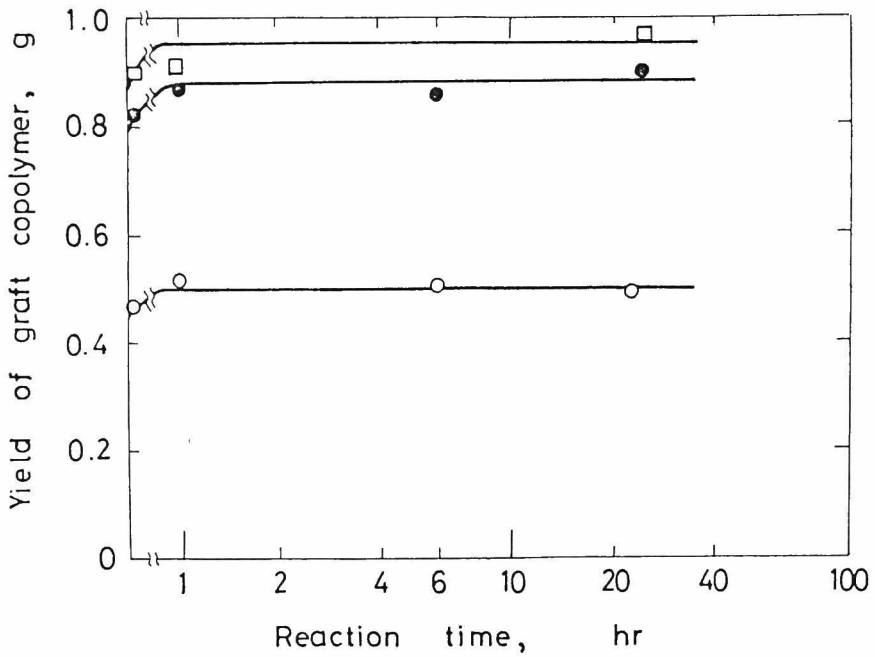

Fig. 3. Influence of reaction time on graft copolymer yield (wt. of PVAc/NH_2 = 0.30 g and total polymer conc. = 5.0 g/dl):
(o) $\bar{M}_n$ of PS-COCl = 4.62×10^4 and wt. of PS-COCl =0.60 g;
(●) $\bar{M}_n$ of PS-COCl = 9.22×10^4 and wt. of PS-COCl =1.50 g;
(□) $\bar{M}_n$ of PS-COCl = 14.3×10^4 and wt. of PS-COCl =2.00 g.

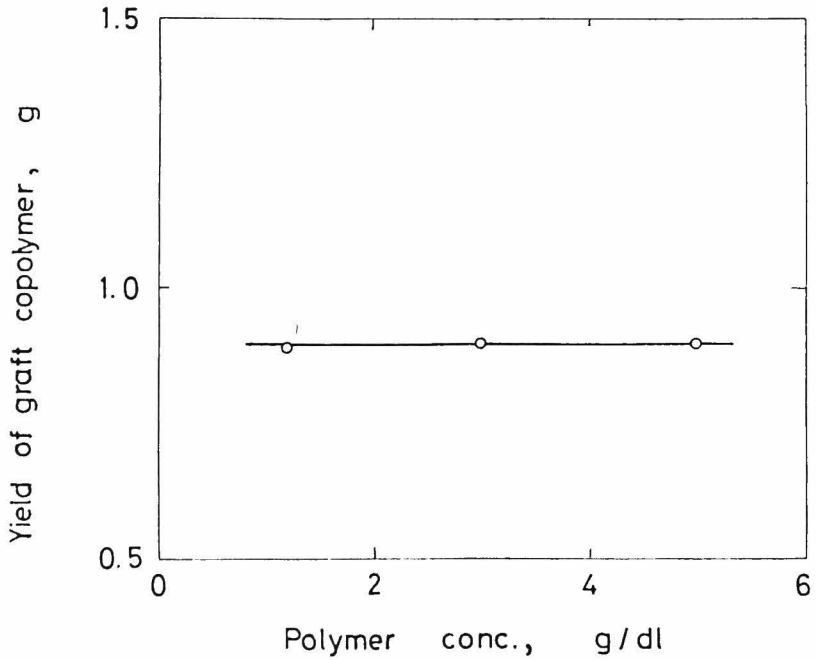

Fig. 4. Influence of total polymer concentration on graft copolymer yield (wt. of PVAc/NH_2 = 0.30 g, wt. of PS-COCl = 1.50 g and $\bar{M}_n$ of PS-COCl = 9.22×10^4).

The influence of the polymer concentration on the coupling is shown in Figure 4.
The reaction was carried out at polymer concentrations of 1.2, 3.0, and 5.0 g/dl for 1 hr with PS-COCl having $\bar{M}_n$ of 9.22×10^4. As it is seen from Figure 4, the polymer concentration has no effect on the coupling yield, at least in the concentration range studied. It is noteworthy that the reaction mixture of 5.0 g/dl appeared turbid before coupling, owing to the incompatibility between PS and PVAc, but it became clear immediately on addition of TEA.

c) Graft Coupling Efficiency: We define graft coupling efficiency of PS(or PVAc) as the weight ratio of the coupled PS (or PVAc) molecules to the whole PS (or PVAc) molecules in the feed mixture. Since the concentration of amino groups in the reaction mixture is high enough to react with all the acyl chloride groups of PS, one can expect that the graft coupling efficiency of PS-COCl has the same meaning as f_s defined in the block coupling reaction. Figure 5 shows the graft coupling efficiency of PS as a function of the PS/PVAc ratio in the feed and of the reaction time.
It is seen that the graft coupling efficiency is in the vicinity of 0.4, irrespective of the polymer mixing ratio and of $\bar{M}_n$ of PS-COCl.

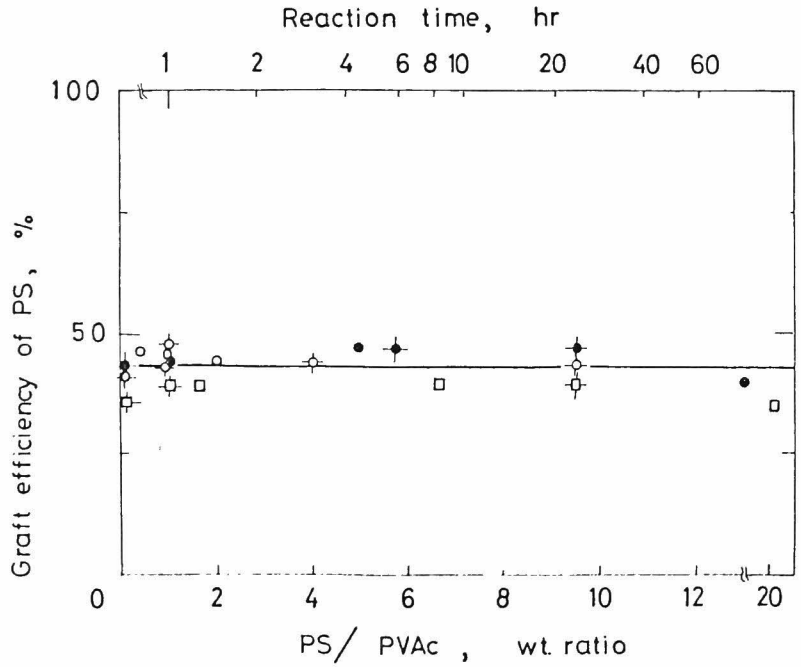

Fig. 5. Influence of polymer weight ratio in feed and reaction time on graft efficiency of PS-COCl: plots for PS/ PVAc, (o) $\bar{M}_n = 4.62 \times 10^4$, (●) $\bar{M}_n = 9.22 \times 10^4$, (□) $\bar{M}_n = 14.3 \times 10^4$; plots for time, (⊙) $\bar{M}_n = 4.62 \times 10^4$, (⊕) $\bar{M}_n = 9.22 \times 10^4$, (⊕) $\bar{M}_n = 14.3 \times 10^4$.

By applying the theoretical considerations descibed in chapter 1 to the polymerization of styrene in the presence of TCAC, we can predict that about 90 % of the PS molecules must have terminal acyl chloride groups. Therefore, the fact that the graft coupling efficiency is lower than 0.9 originate from a disappearance of acyl chloride groups by hydrolysis due to trace amounts of water in the coupling medium. This extent of disappearance seems to be smaller than that observed in the block coupling.

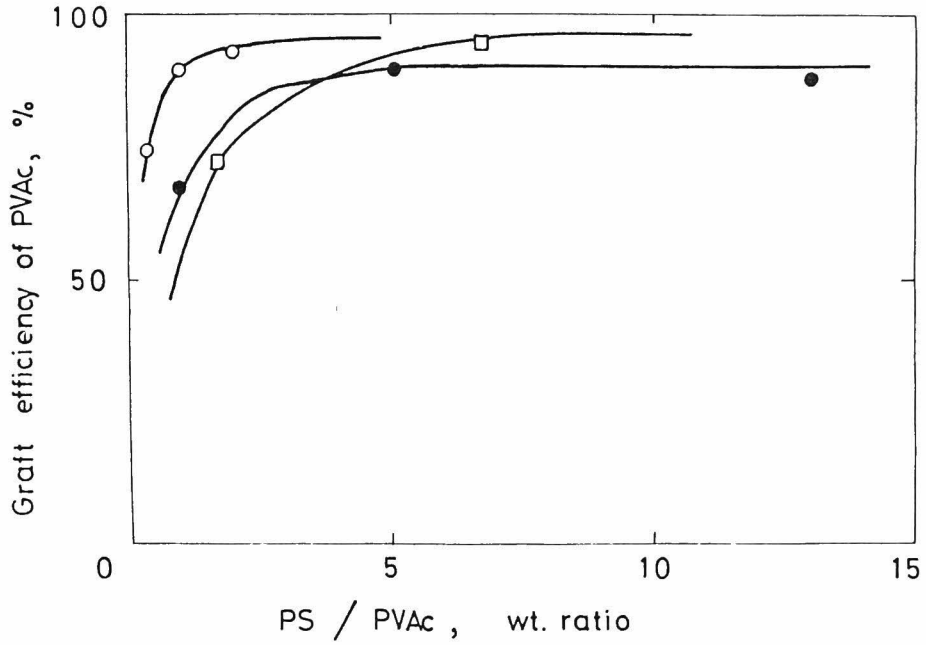

Fig. 6. Influence of polymer weight ratio in feed on graft efficiency of PVAc/NH_2: (o) $\bar{M}_n$ of PS-COCl = 4.62 x 10^4; (•) $\bar{M}_n$ of PS-COCl = 9.22 x 10^4; (□) $\bar{M}_n$ of PS-COCl = 14.3 x 10^4.

The graft coupling efficiency of backbone PVAc/NH_2, plotted against the polymer mixing ratio in Figure 6, implies that a considerable amount of PVAc carries no PS branches, when the weight ratio of PS-COCl to PVAc-NH_2 in the reaction mixture is as low as unity. This is because the average number of branches per backbone chain is very low for such mixing ratios, as expected from statistical calculations on grafting[8].

d) Preparation of Graft Copolymers with Many Branches:

Ikada and his co-workers have reported that the radiation-induced graft copolymerization generally produces graft copolymers with only one branch per backbone [9]. In contrast, the present coupling reaction is capable of grafting

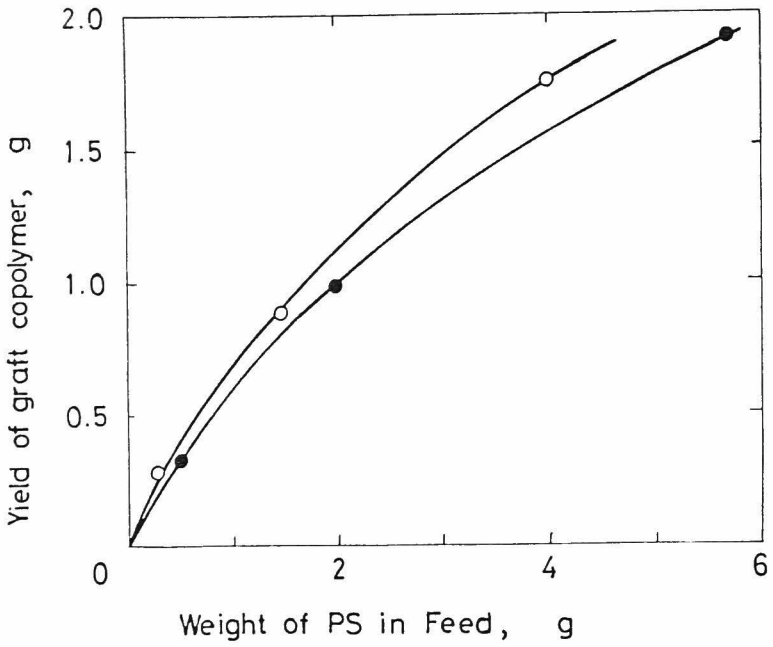

Fig. 7. Relationship between weight of PS-COCl in feed and graft copolymer yield: (o) $\bar{M}_n$ = 9.22 x 10^4; (•) $\bar{M}_n$ = 14.3 x 10^4.

many branches to the backbone polymer, merely by varying the ratio of the two prepolymers in the reaction mixture. Figure 7 shows the yield of graft copolymer in coupling reactions performed with a constant amount of PVAc/NH_2 and different amounts of PS-COCl.
The total polymer concentration in the mixture is kept at 5.0 g/dl and the time of reaction is 24 hr. The yield increases as the added amount of PS-COCl becomes larger.

The characterization results of the product are summarized in Table III.

TABLE III

Characterization of the Graft Copolymers

$\bar{M}_n \times 10^{-4}$ of starting PS	PS/PVAc, wt. ratio	Wt.-% PS in graft copolymer	$\bar{M}_n \times 10^{-4}$ Graft copolymer	$\bar{M}_n \times 10^{-4}$ Branch part	Number of branches[a]	$\bar{M}_B$[b] / $\bar{M}_{B,0}$[c]
9.22	1.00	40.6	36.1	14.7	1.60	1.65
"	5.00	67.0	55.8	37.8	4.10	1.42
14.3	1.67	46.8	42.7	20.0	1.40	1.75
"	6.65	66.9	47.4	31.7	2.11	1.21
"	20.0	84.0	103	87.0	5.78	1.25

a) Per graft copolymer molecule. b) $\bar{M}_n$ of backbone part. c) $\bar{M}_n$ of starting PVAc (= 13.0×10^4).

TABLE IV

Comparison of the Length of the Original and Separated PS's

	$\bar{M}_n \times 10^{-4}$	$[\eta]$[a]	$\bar{M}_n \times 10^{-4}$	$[\eta]$[a]	$\bar{M}_n \times 10^{-4}$	$[\eta]$[a]
Starting PS	14.3	0.617	9.22	0.387	4.62	0.260
Grafted PS	15.8	0.718		0.397		0.272

a) In chloroform, 25 °C.

The number of branches per backbone chain was calculated by dividing the sum of $\bar{M}_n$ of the branch part by $\bar{M}_n$ of one branch which was assumed to be equal to $\bar{M}_n$ of the starting prepolymer. This assumption is supported by the result described in Table IV, where [η] of the starting PS is compared with that of a PS branch separated from the graft copolymer.

If the high molecular weight fraction of PS-COCl remained uncoupled, [η] of the PS branch would become lower than that of the starting PS, but the observed [η] has a reverse trend, as is seen in Table IV. Accordingly the difference in [η] may be ascribed to the loss of the low molecular weight fraction of the separated branch polymer during the recovery procedure. It is noticed in Table III that $\bar{M}_n$ of the backbone PVAc in the graft copolymer is higher than that of the starting $PVAc/NH_2$. This suggests that a polymer chain of higher molecular weight has a higher possibility to participate in the grafting than that of lower molecular weight[9].

The number of branches per starting PVAc molecule against the PS/PVAc ratio in the reaction mixture is plotted in Figure 8.

The good linearity of the plot leads to the conclusion that the PS prepolymers which carry non-deactivated acyl chloride groups, all undergo the coupling reaction with $PVAc/NH_2$, irrespective of the molecular weight of the PS molecule, at least in the molecular weight range studied.

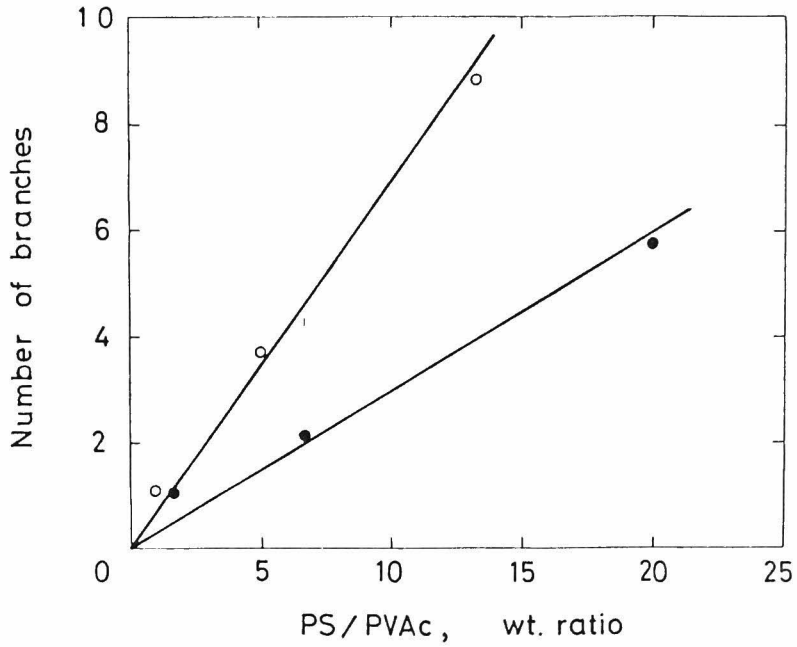

Fig. 8. Number of graft branches formed per starting PVAc molecule (total polymer conc. = 5.0 g/dl and reaction time = 24 hr): (o) $\bar{M}_n = 9.22 \times 10^4$; (●) $\bar{M}_n = 14.3 \times 10^4$.

TABLE V

Other Examples of Coupling Reaction of Partially Aminoacetalized PVAc with PS Having an Acyl Chloride Endgroup (25 °C, 24 hr , NH_2 content of PVAc = 2.0 mole%)

Code no.	$\bar{M}_n \times 10^{-4}$ of starting PS	PS/PVAc, wt. ratio	Wt.-% PS in graft copolymer	$\bar{M}_n \times 10^{-4}$		Number of branches[a)]
				Graft copolymer	Branch part	
CG-8	0.82	3.30	33.9	33.2	11.3	14
CG-1	0.94	1.50	61.3	22.9	14.1	15
CG-9	2.03	5.00	49.2	53.0	26.1	13
CG-7	8.95	25.0	79.0	53.0	41.9	4.7
CG-10	8.90	15.0	68.3	71.7	48.9	5.6
CG-2	12.3	3.0	63.1	44.3	27.9	2.3

a) Per graft copolymer molecule.

Table V summarizes the number of branches of graft copolymers prepared by coupling reaction using relatively large amounts of PS-COCl. $COCl/NH_2$ molar ratios in the reaction mixture were always kept to less than unity. It is seen that a graft copolymer having 15 branches is formed. Alkali hydrolysis of acetyl groups in the graft copolymer produced graft copolymer consisting of one PVA backbone and many branches of PS. This PVA-styrene graft copolymer was soluble in phenol, a common solvent of PVA and PS.

APPENDIX

[η] of Reaction Mixtures before and after Block Coupling

Since all the prepolymer molecules do not possess the condensable functional endgroup, the reaction mixture after the coupling contains four kinds of polymers, even if the condensation reaction between the amino and acyl chloride groups proceeds quantitatively. They are the inactive PS without the acyl chloride group, the inactive PVAc without the amino group, the active PVAc with an amino endgroup and the coupled block copolymer, provided that the molar concentration of the acyl chloride group in the reaction mixture before coupling is lower than that of the amino group. Applying an additivity rule to the solution viscosity of blend polymers, we get the following equation for the intrinsic viscosity [η] of the reaction mixture after the coupling reaction:

$$[\eta] = w_{s,i}[\eta]_s + (w_{a,i} + w_{a,a})[\eta]_a + w_b[\eta]_b \qquad (1)$$

where $w_{s,i}$ is the weight fraction of the inactive PS, $w_{a,i}$ and $w_{a,a}$ are the weight fractions of the inactive and active but unreacted PVAc, w_b is the weight fraction of the block copolymer, and $[\eta]_s$, $[\eta]_a$ and $[\eta]_b$ are the intrinsic viscosity of PS, PVAc and the block copolymer, respectively.

These weight fractions of the polymers can be written as,

$$w_{s,i} = w_s(1 - f_s) \quad (2)$$

$$w_{a,i} = w_a(1 - f_a) \quad (3)$$

$$w_{a,a} = w_a f_a - w_s f_s(\bar{M}_a/\bar{M}_s) \quad (4)$$

$$w_b = w_s f_s(1 + \bar{M}_a/\bar{M}_s) \quad (5)$$

Here w_s and w_a are the weight fractions of the whole PS and PVAc in the polymer mixture before coupling, f_s and f_a are the fractions of PS and PVAc carrying the reactive endgroups, and $\bar{M}_s$ and $\bar{M}_a$ are number-average molecular weights of PS and PVAc, respectively.

Substituting eqs. (2) - (5) into eq. (1), one obtains

$$[\eta] = [\eta]_a + (1 - f_s)[\eta]_s - (1 + \frac{\bar{M}_a}{\bar{M}_s} f_s)[\eta]_a + f_s(1+\frac{\bar{M}_a}{\bar{M}_s})[\eta]_b w_s \quad (6)$$

The above equation holds in the case of $w_a f_a/\bar{M}_a \geq w_s f_s/\bar{M}_s$, provided that the block copolymer has a constant $[\eta]$, independent of the weight fraction w_s of PS-COCl in the reaction mixture. In case that $w_a f_a/\bar{M}_a$ is smaller than $w_s f_s/\bar{M}_s$, the subscripts s and a in eq. (6) should be exchanged to give the corresponding equation. The highest degree of reaction is achieved when $w_a f_a/\bar{M}_a$ is equal to $w_s f_s/\bar{M}_s$, in other words, the concentration of acyl chloride in the reaction mixture is exactly equal to that of the amino group. Thus the intersection of the two straight lines which results from a plot of $[\eta]$ against w_s, gives the optimum w_s value where the yield of the block copolymer becomes the highest.

REFERENCES

1. "Tables of Chemical Kinetics, Homogeneous Reactions", N.B.S.,U.S.A. (1951)
2. S. N. Gupta and U. Nandi, Makromol. Chem., 176, 3179 (1975)
3. S. Matumoto and M. Maeda, Kōbunshi Kagaku 12, 428 (1955)
4. A. Yamamoto, Ph. D. Thesis, Kyoto Univ., Kyoto, Japan (1956).
5. Von O. Pfundt, Angew. Chem., 46, 218 (1933).
6. K.Kuroyanagi and I. Sakurada, Kōbunshi Kagaku, 6, 419 (1949)
7. F. Horii, Y. Ikada, and I. Sakurada, J. Polym. Sci. Polym. Chem. Ed., 13, 755 (1975)
8. Y. Ikada and F. Horii, Makromol. Chem., 175, 227 (1974).
9. Y. Ikada, F. Horii, Y. Nishizaki, T. Kawahara, and H. Uehara, Macromolecules, 8, 276 (1975).

CHAPTER 9.

Monolayers of Graft and Block Copolymers

INTRODUCTION

When graft or block copolymers are constructed of two chemically different and incompatible sequences, they may exhibit solubilizing and emulsifying properties typical of low molecular weight surfactants. For instance, if added in small proportion to a physical blend of the corresponding homopolymers, the graft or block copolymer molecule will be placed at the interface between the domains. This may be the main reason for improvement of high-impact plastics and formation of stable polymeric oil-in-oil emulsions by existence of a small amount of graft copolymers[1].

The emulsifying action of graft and block copolymers for a system of two immiscible homopolymers or low molecular weight liquids have been extensively investigated by many workers[2-7]. However, very few studies[8-12] nave been reported on colloidal, especially surface-chemical properties of graft and block copolymers, although such works are important for understanding the role of graft copolymers in multicomponent systems.

Several methods are known for exploring surface-chemical characteristics of molecules. Measurements of surface tension are widely applied to characterize surface-active agents. In this chapter, surface pressures on liquid substrates such as water and aqueous media will be determined for some graft and block copolymers in an attempt to obtain information about the molecular orientation of the copolymers at air/substrate interfaces. It was concluded that polymeric emulsions were stabilized against coagulation by graft copolymer molecules fixed as a monolayer at the interface of the emulsions [6,7]. It is expected that a further support for this conclusion will be provided by the measurement of surface pressures of graft copolymers at interfaces suitably selected.

As our purpose is to study interfacial properties of graft and block copolymers for understanding their amphiphilic properties, we will employ as materials graft copolymers with very few branches and AB type diblock copolymers. The presence of many grafted branches and multisequences in a molecule will obscure the amphiphilic properties of the copolymers.

EXPERIMENTAL

Materials

Poly(vinyl acetate)(PVAc) graft copolymers with one polystyrene(PS) grafted branch were prepared by radiation-induced graft copolymerization of styrene onto poly(vinyl alcohol)(PVA) films by a mutual irradiation method. After rough extraction of the unreacted PVA and the styrene homopolymer, the remaining polymer was acetylated to convert the PVA part to PVAc and subjected to more rigorous, alternate extraction of both homopolymers to obtain the PVAc-PS graft copolymer free from the homopolymers.

A PVAc graft copolymer with four PS branches in one molecule was prepared by a coupling reaction of PVAc possessing a small number of amino groups with PS having a terminal acyl chloride group in chloroform solution. The unreacted amino groups were completely acetylated with acetyl chloride. Both of the homopolymers were removed from the PVAc-PS graft copolymer by selective extraction. The method for preparing PVAc-PS diblock copolymers is similar to that for the graft copolymer with four grafted PS branches, except that PVAc with one amino endgroup was used for the coupling reaction instead of the PVAc having amino groups along its backbone chain.

PVA-PS graft and block copolymers were obtained by

complete hydrolysis of the corresponding PVAc-PS graft and block copolymers in dioxane for 3.5 hrs at room temperature in the presence of 1/30 N NaOH. The hydrolyzed copolymers were completely soluble in phenol which is a common solvent for PVA and PS.

Details of the preparation and characterization of these materials were described elsewhere[13-16]. Thin layer chromatography for the copolymers revealed that the content of homopolymers contaminating the copolymers was in every case below 2 wt%. Table I gives the molecular characteristics of the copolymers used for the surface pressure measurements. The A_s value given in the last column of Table I will be discussed later.

Surface Pressure Measurement

Surface pressure-area isotherms were determined using an automatic surface balance technique. The surface balance is float type (Langmuir type), and the surface pressure was sensed by a linear variable differential transformer connected to a torsion wire and recorded on an XY recorder as a function of area[17].

Stock solutions of the polymer materials were prepared by dissolving the polymers carrying a PVAc chain in benzene or the polymers carrying a PVA chain in a phenol-water(20:1) mixture to have the polymer concentration of 1.0 mg/ml.

TABLE I NUMBER-AVERAGE MOLECULAR WEIGHTS, $\bar{M}_n$, OF POLYMERS USED AND LIMITING AREAS, A_S, OCCUPIED BY POLYSTYRENE

POLYMER		STYRENE CONTENT (WT%)	$\bar{M}_n \times 10^{-4}$			A_S (m^2/mg)
			TOTAL	VAC OR VA SEQ.	STYRENE SEQ.	
STYRENE HOMOP.	S-4	100			4.0	0.13
STYRENE HOMOP.	S-10	100			9.38	0.17
STYRENE HOMOP.	S-21	100			21.1	0.13
VAC HOMOP.	V-3	0		29.5		
VA HOMOP.	A-1	0		5.90		
PVAc-PS GRAFT COP.	M3S	36.9	35.4	22.3	10.4	0.30
PVAc-PS GRAFT COP.	M8S	51.8	28.9	13.9	14.1	0.28
PVAc-PS GRAFT COP.	M9S	41.1	40.2	23.6	14.0	0.34
PVAc-PS GRAFT COP.	M10S	51.6	60.3	29.2	27.1	0.28
PVAc-PS GRAFT COP.	D-3-4[a]	67.0	55.8	18.4	9.2[b]	0.38
PVA-PS GRAFT COP.	M9S-A	53.7	26.1	12.1	14.0	0.33
PVAc-PS BLOCK COP.	B-1	37.4	12.5	7.56	4.51	0.42
PVAc-PS BLOCK COP.	B-2	55.3	15.9	7.56	9.38	0.27
PVA-PS BLOCK COP.	B-2-A	70.6	13.3	3.87	9.38	0.28

a) This graft copolymer has four grafted PS branches, but other graft copolymers one branch.
b) Mn of one PS branch.

With the use of microsyringe a measured amount of the solution was introduced dropwise onto the clean surface of substrate liquid in which the polymer was not soluble and then the film pressure was read by advancing the movable teflon float. The surface pressure measurements were carried out at 23°C, mostly using water as the substrate. When 0.2 N NaOH and 20% Na_2SO_4 aqueous solutions were chosen as the substrate, the surface pressures were determined at 20 and 25°C, respectively. The surface pressure-area plot was obtained by compressing a monolayer, so the curves in the figures developed in a right-to-left direction.

RESULTS

PVAc-PS Graft and Block Copolymers

Typical examples of dependence of surface pressure (π) on the available surface area (σ), expressed in unit of m^2/mg and for PVAc also in $\mathring{A}^2$/monomer unit, are given in Figs. 1, 2 and 3 for a VAc homopolymer(V-3), a styrene homopolymer(S-21), and a PVAc-PS graft copolymer(M9S), respectively. In the figures were given further the results of repeated compression of the monolayer after expansion to the original position. As is seen from Figs. 1 and 2, PVAc spreads out to give a thin monolayer film over a wide range of area as have

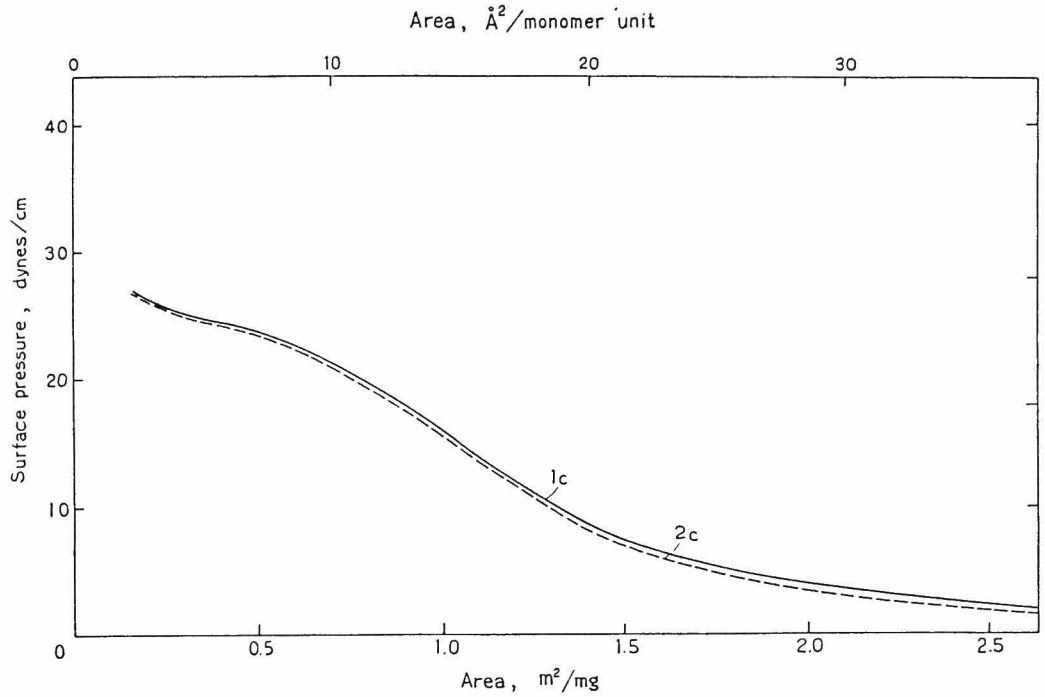

Fig. 1 Surface pressure-area isotherms for VAc homopolymer(V-3) at air/water interface observed at the first and second compressions (1c and 2c).

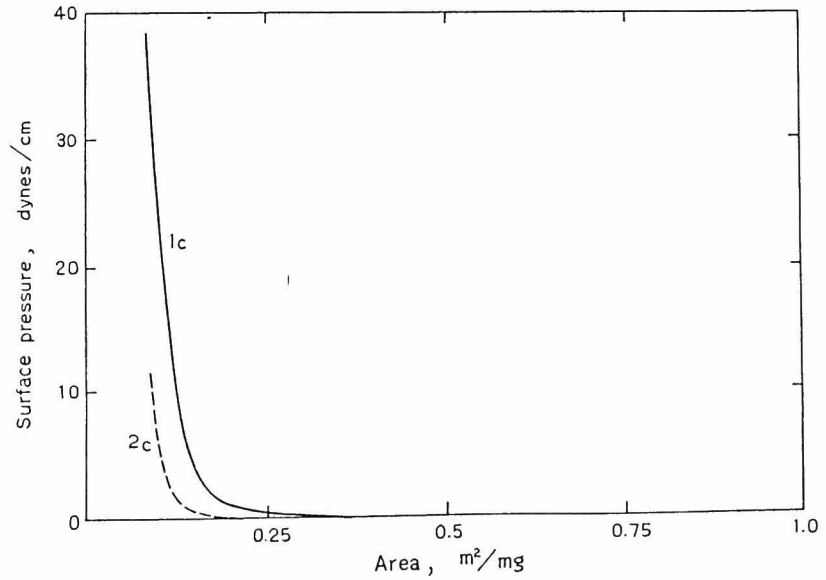

Fig. 2 Surface pressure-area isotherms for styrene homopolymer (S-21) at air/water interface observed at the first and second compressions (1c and 2c).

been reported[18,19], whereas PS shows practically no surface pressure[20,21] until it is confined to an area about 0.25 m^2/mg. It has been observed that the molecular weight of PVAc does not practically affect the pressure-area plot[19]. Apparently, the π-σ isotherms for the graft copolymer are a superposition of two plots corresponding to the homopolymers and almost reversible, whereas the isotherms for the styrene homopolymer observed at the first compression(1c) is different from those at the second compression(2c), as shown in Fig. 2. For other PVAc-PS graft copolymers we obtained similar plots as in Fig. 3 and observed no substantial difference between the graft and block copolymers. As illustrated in Fig. 4, mechanically blended homopolymers gave π-σ isotherms composed simply of two homopolymers and showed a rapid rise in π at the area identical to that of the styrene homopolymer.

Hydrolysis of PVAc-PS Graft Copolymer

Since the acetyl groups of PVAc are probably in direct contact with water, it is expected that the PVAc-PS graft and block copolymers will undergo hydrolysis when developed on an alkaline solution. Fig. 5 shows the result for a PVAc-PS graft copolymer(M9S) deposited on 0.2 N NaOH aqueous solution at 20°C. The surface pressure of the curve 1c was read one minute after addition from the benzene solution and it took 10 min. to record the curve 1c. Immediately after

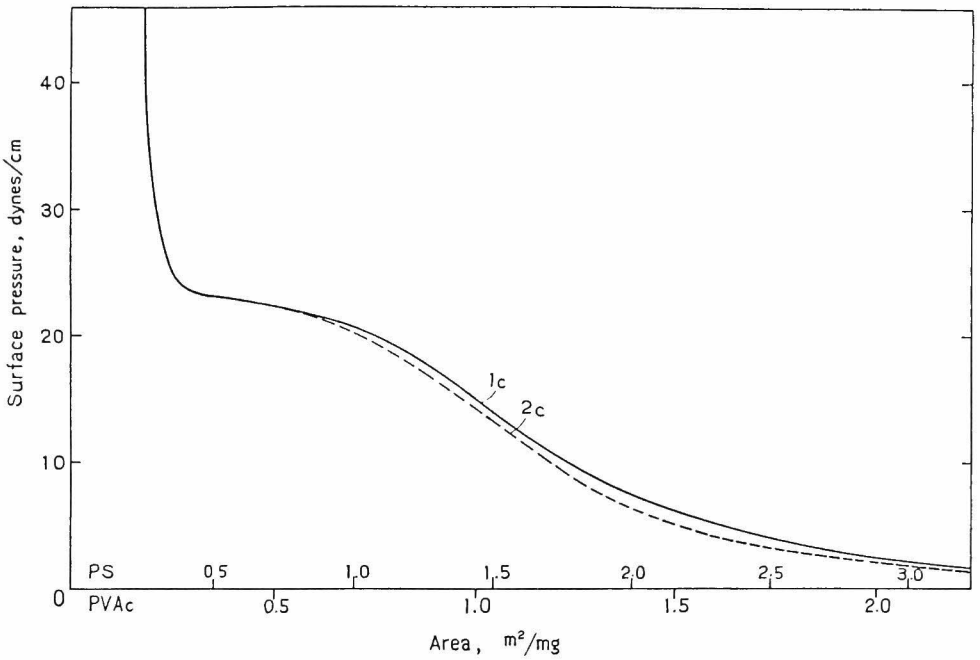

Fig. 3 Surface pressure-area isotherms for PVAc-PS graft copolymer(M9S) at air/water interface observed at the first and second compressions (1c and 2c).

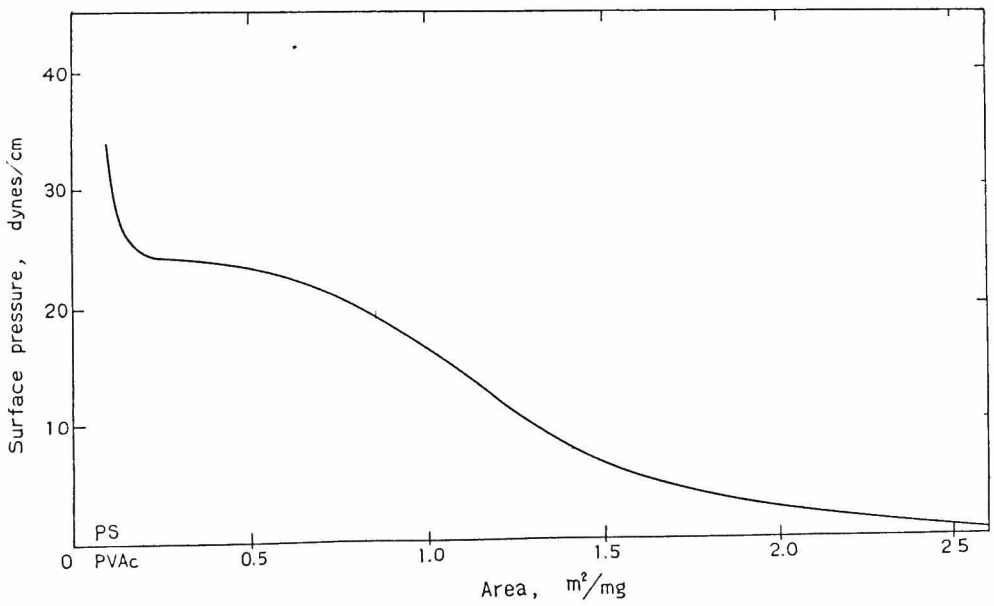

Fig. 4 Surface pressure-area isotherms for PVAc(V-3)-PS(S-21) blend at air/water interface (PVAc:PS=1:1, by wt.).

reaching the end position, the float was allowed to move back to the starting position in 5 min. Therefore, there is a 15 min. intervals between the curves 1c and 2c. Similarly, every other curve has 15 min. difference from the neighboring curve.

It is seen in Fig. 5 that the first curve is almost similar, both in shape and magnitude, to that for the copolymer on pure water (see Fig. 3), but the second and other succeeding curves show surface pressures decreasing gradually with time. On the other hand, the limiting surface area below which the surface pressure corresponding to the PS chain appears, remains constant. When a monomolecular film of VAc homopolymer was hydrolyzed at the air/0.2 N NaOH interface, we observed a result quite similar to Fig. 5 except for absence of the rapid increase in surface pressure at small areas.

Fig. 6 shows the time dependence of the surface pressure at a constant surface area of 0.5 m^2/mg (7.2 $Å^2$/monomer unit). No difference is observed for hydrolysis between the graft copolymer and the VAc homopolymer, indicating that the PS sequence of the graft copolymer does not have any effect on the hydrolysis of the PVAc chain at the interface. Under this hydrolysis condition the reaction seems to come to completion in about 150 min.

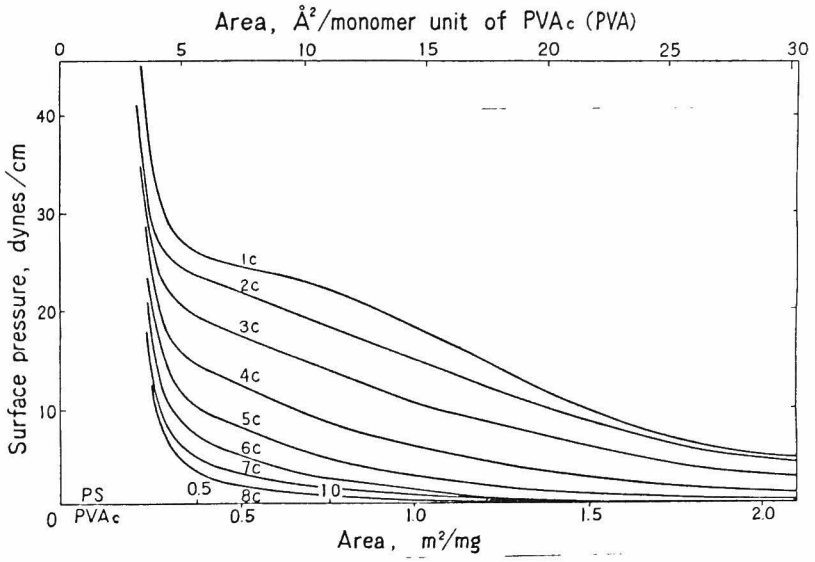

Fig. 5 Change of surface pressure-area isotherms during hydrolysis of PVAc-PS graft copolymer(M9S) at air/0.2 N NaOH aqueous solution interface with repeated compressions from 1c to 8c.

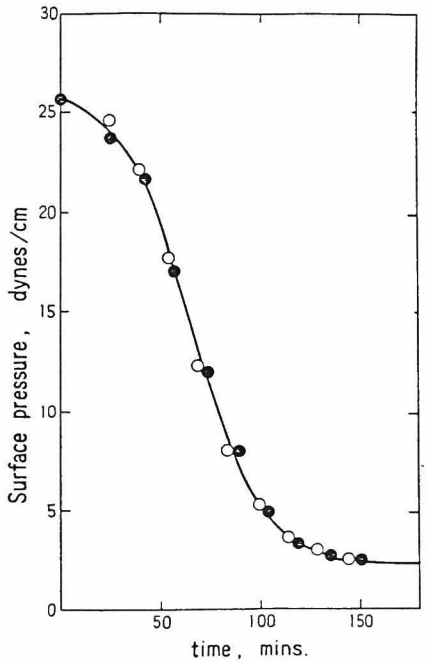

Fig. 6 Change of surface pressure at the area of 0.5 m^2/mg during hydrolysis of PVAc-PS graft copolymer(M9S) and PVAc homopolymer(V-3) at air/0.2 N NaOH aqueous solution interface.

PVA-PS Graft and Block Copolymers

According to the results shown in Figs. 5 and 6, the PVA sequence produced as a result of hydrolysis of PVAc sequence has an insignificant surface pressure, probably because the PVA chain is soluble in the aqueous medium. To confirm this, the PVA-PS graft copolymer(M9S-A) obtained from the corresponding PVAc-PS graft copolymer on hydrolysis in the dioxane solution, was deposited on pure water. The result is shown in Fig. 7, which demonstrates that the π-σ plot resembles that of the curve 8c in Fig. 5. Quite similar isotherms were also obtained when the PVA-PS graft copolymer was spread over 0.2 N NaOH aqueous solution. Fig. 8 shows the pressure-area isotherms for a PVA-PS block copolymer (B-2-A) spread on 0.2 N NaOH.

In contrast to water, concentrated aqueous solutions of Na_2SO_4 are not able to dissolve PVA. Figs. 9 and 10 give the π-σ plot on 20% Na_2SO_4 solution for PVA(A-1) and a PVA-PS block copolymer(B-2-A), respectively. It is seen that a thin film is formed in both cases on the substrate of 20% Na_2SO_4, although the surface pressures at large areas are relatively low because of a high surface tension of the PVA film. A similar result was also reported by Schick[22]. The curve 2c in Fig. 9 was recorded after completion of the first compression. One can see some weak hysteresis, in contrast to the PVAc monolayer on water. This may be attrib-

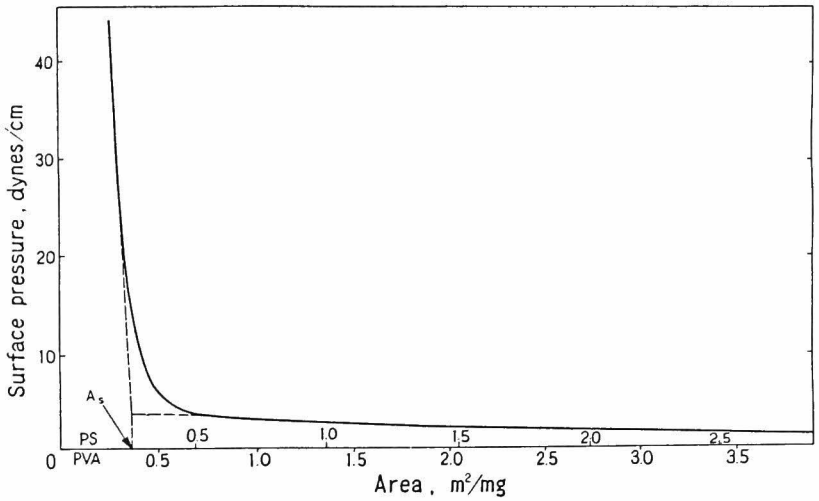

Fig. 7 Surface pressure-area isotherms for PVA-PS graft copolymer (M9S-A) at air/water interface. A_s indicates the limiting surface area for PS sequence.

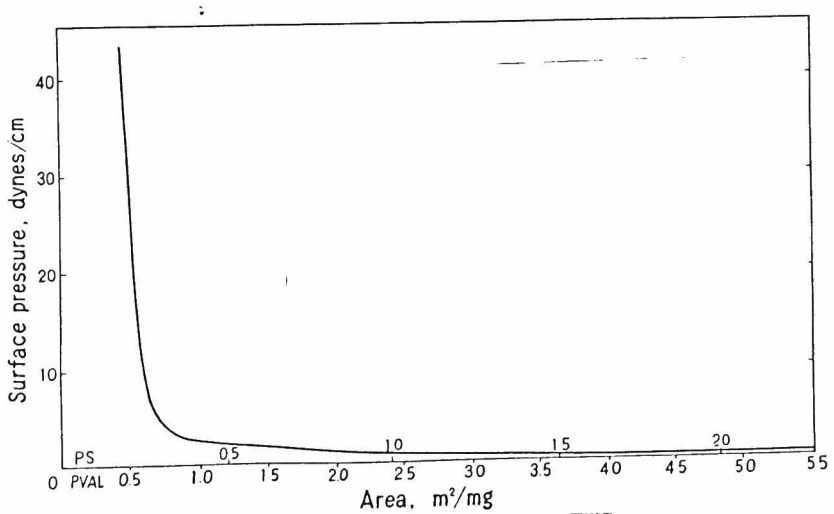

Fig. 8 Surface pressure-area isotherms for PVA-PS block copolymer (B-2-A) at air/0.2 N NaOH aqueous solution interface.

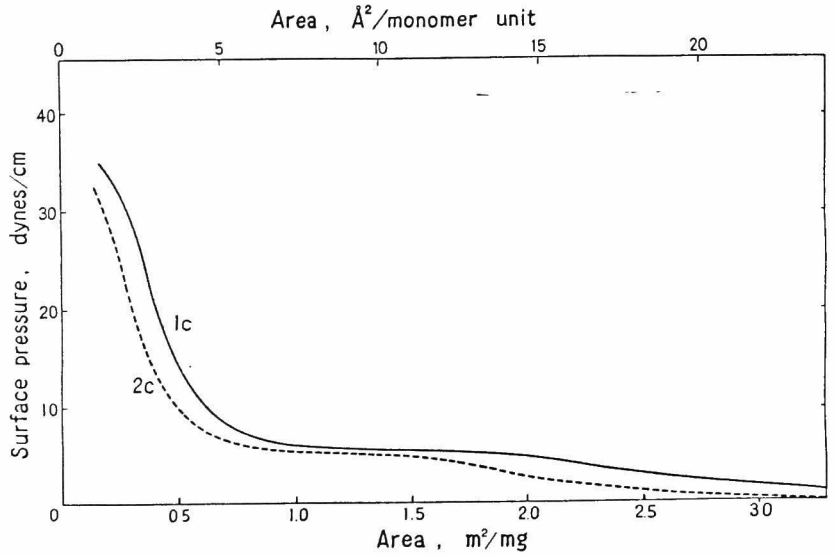

Fig. 9 Surface pressure-area isotherms for PVA(A-1) at air/20% Na_2SO_4 aqueous solution interface observed at the first and second compressions (1c and 2c).

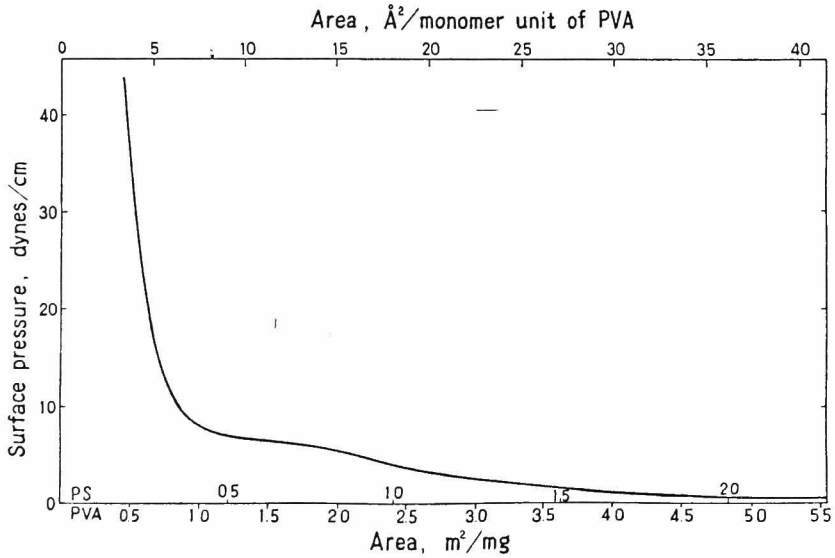

Fig.10 Surface pressure-area isotherms for PVA-PS block copolymer(B-2-A) at air/20% Na_2SO_4 aqueous solution interface.

uted to hydrogen bonds formed between hydroxyl groups of PVA at high compressions to yield a gellike film.

DISCUSSION

It is reasonable to believe from the π-σ isotherms in Fig. 1 that PVAc gives a monomolecular film of expanded liquid type at the air/water interface. In the analogy of low molecular weight compounds we use here the term "monomolecular", taking the monomer base of the polymer as a unit. On the other hand, the term "monolayer" is to be used in a wider sense, involving not only the monomolecular film but also the monolayer whose constructing unit is a tightly coiled sphere or a soluble chain of polymer. Although the nonpolar carbon skeleton of PVAc carries polar acetyl side-groups which are capable of interacting attractively with the substrate water, the PS molecule is not so polar that it cannot be spread out over the water surface as a monomolecular film. In view of the behavior at the air/water interface, PVA is quite different from the two polymers, since only PVA is soluble in water. Therefore, the graft or block copolymers consisting of these polymer sequences are expected to provide novel types of monolayer film, in contrast to the homopolymers.

Some plausible orientations of the copolymers and a physical blend of the corresponding homopolymers in films on the water are schematically represented in Fig. 11, together with that for the styrene homopolymer. As illustrated in Fig. 2, PS shows no surface pressure in a wide range of surface area until a critical surface area is reached. This implies that the PS chain seems to exist in a densed, spherical form, as Richardson directly observed by electron microscopy[23], and to aggregate into a mono- or multilayer at high compression as shown in Fig. 11(a). However, such aggregation of the spherical particles into a multilayer at high compression will be impossible if the PS chain is chemically bound

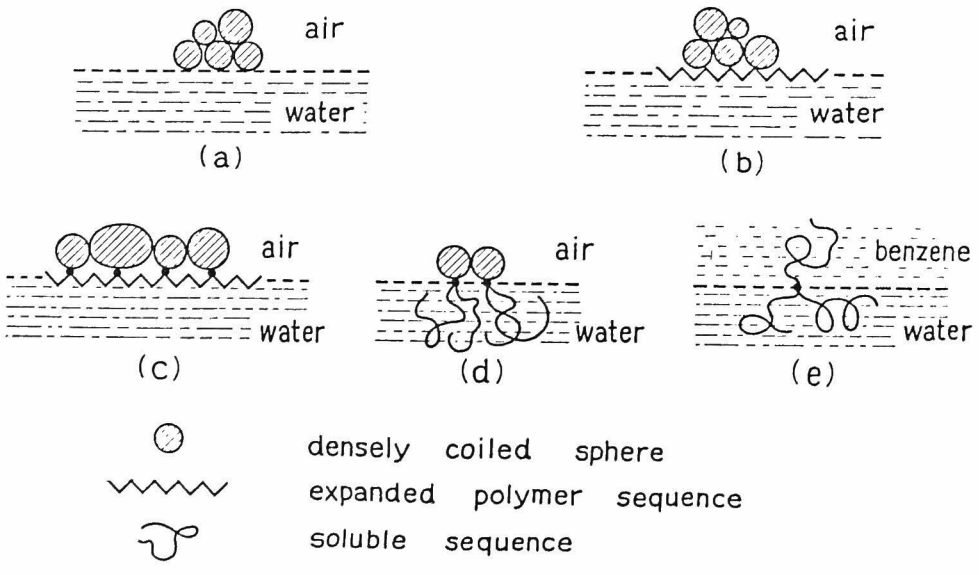

Fig.11 Schematic representation of polymer orientations at interfaces.

to a PVAc chain. In this case, the copolymer layer may have the orientation represented in Fig. 11(c), because overlapping of the PS particles will be prevented by the waved monomolecular film of the PVAc sequence. The good agreement of the surface pressure exerted by the PS sequence in the first cycle (1c) with that of the second (2c) observed in Fig. 3, supports also some contribution of the PVAc sequence linked to the PS sequence, since the surface pressure-area cycle for styrene homopolymers were no more reversible. The fact that the surface pressures in the range of large areas, originating from the PVAc chains in the copolymers, were almost identical to those for the VAc homopolymers, suggests that a phase separation may take place within the copolymer molecule at the interface, the PVAc and PS chains occupying no common domains.

The change in surface pressure accompanying the hydrolysis on the alkaline substrate can be readily explained in terms of the intramolecular phase-separation model shown in Fig. 11(c), since the PS sequence does not affect the hydrolysis of the PVAc sequence. The reactions preceding at interfaces are of special interest because of their resemblance to biological systems[24]. Unfortunately, in the present case it is not possible to estimate the rate constant for the hydrolysis, because we have not yet determined the surface pressure as a function of the chemical composition of the VAc-VA random copolymer resulting from the hydrolysis of PVAc.

There is no reason to suspect that the PVAc-PS graft copolymer molecule after the hydrolysis may have a jellyfish-type shape at the interface. This model is given in Fig. 11 (d). The hydrolyzed sequence of PVAc will be buried in the aqueous substrate, the insoluble PS sphere holding the diffusing PVA chain as an anchor. This model is also confirmed from comparison of Fig. 5 with Fig. 7. It is seen that the surface pressure of the PVAc-PS graft copolymer observed after sufficiently long hydrolysis time is similar to that of the PVA-PS copolymer, which has surface pressures exerted practically only by the PS sequence.

If this model is correct, the limiting area at which the surface pressure abruptly increases, hereafter designated as A_s, must have a correlation with two-dimensional closest packing of the PS spheres. To verify this supposition, the surface area per PS chain, S, was computed from A_s given in Table I and plotted against the molecular weight of PS sequence, $\bar{M}_{ps}$, in Fig. 12. In this figure the A_s values for the PVAc-PS graft and block copolymers were also plotted, because they were identical to those of the PVA-PS graft and block copolymers as illustrated in Fig. 5. The closest packing assumption gives the cross-sectional area occupied by the PS sphere as

$$S = \pi \left(\frac{3\bar{M}_{ps}}{4\pi\rho N_A}\right)^{2/3} \qquad (1)$$

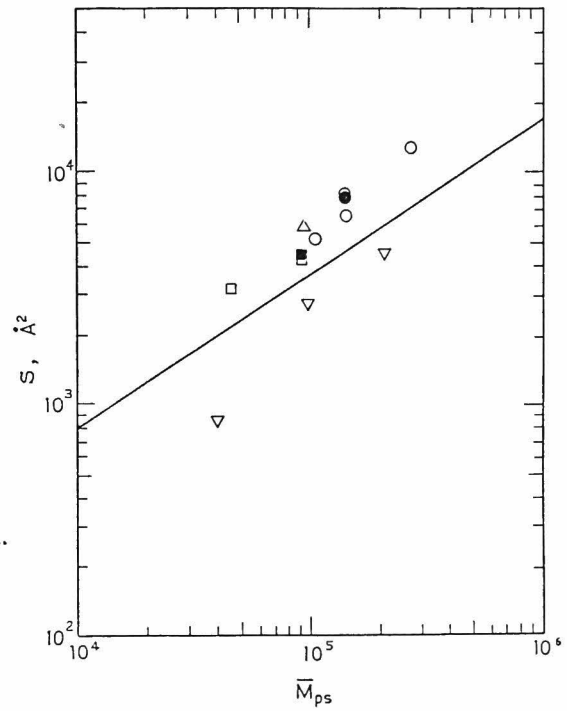

Fig.12 Plots of observed and theoretical limiting areas, S, occupied by one PS chain against its molecular weight $\bar{M}_{ps}$. (●) PVA-PS graft copolymer with one branch (M9S-A), (o) PVAc-PS graft copolymers with one branch (M3S, M8S, M9S, M10S), (△) PVAc-PS graft copolymer with four branches (D-3-4), (■) PVA-PS block copolymer(B-2-A), (□) PVAc-PS block copolymers(B-1, B-2), (▽) styrene homopolymers (S-4, S-10, S-21), and (——) theoretical curve.

where ρ is the density of PS particle and N_A is Avogadro's number. The straight curve in Fig. 12 was obtained by plotting the cross-sectional area against $\bar{M}_{ps}$ on the basis of eq.(1), assuming ρ to be equal to the density of the bulk PS (1.0 g/cm^3). The observed areas agree satisfactorily with

the estimates, if it is considered that the PS particle on water may be somewhat flattened and have the density lower than 1.0 g/cm^3. This agreement and no significant hysteresis in the π-σ plot (Fig. 3) seem to support the models about the orientation of the PVAc-PS and PVA-PS graft and block copolymers at the air/water interface, illustrated in Fig. 11(c) and (d). These observations also give a strong support for the monolayer assumption which was made to describe an emulsion stabilized by a small amount of graft copolymers[6]. It is interesting to point out that the PVAc sequence does not influence seriously the two-dimensional packing of the PS sphere, so far as the graft copolymers have very few grafted PS branches with the chain length comparable to that of the PVAc backbone. For comparison, the results for styrene homopolymers were also shown in Fig. 12, where it can be seen that the S values calculated from the observed A_s are smaller than those of the simple, two-dimensional packing. This observation provides an evidence for aggregation of spheres of styrene homopolymers into a multilayer at high compression as shown in Fig. 11(a) and (b).

There is a controversy on possibility of producing a compact particle containing only a single macromolecule. Richardson, indeed, demonstrated it to be possible by dispersing a dilute solution of polymers as fine droplets on to a suitable substrate[23]. In the case of graft or block copolymers spread on water, it seems very likely that the

soluble PVA or the expanded PVAc chain must favorably prevent the PS particle from aggregating, at least, when the copolymers are deposited on the water surface of large areas.

Spreading the PVA-PS graft or block copolymer on the substrate containing 20% Na_2SO_4 in which PVA is not soluble, is likely to result in formation of the monolayer film such as shown in Fig. 11(c), since the surface pressure to be attributed to the PVA sequence is observed in the π-σ isotherms (see Figs. 9 and 10). Thus, it may be stated that two different types of monolayer films can be produced from the PVA-PS graft or block copolymer simply by changing the substrate on which the copolymer is spread.

It is expected that a monolayer film consisting of two soluble chains, illustrated in Fig. 11(e), may be obtained from the PVA-PS graft or block copolymer if it is spread at an organic liquid/water interface. The organic liquid should be immiscible with water and be able to dissolve the PS chain. For instance, toluene and benzene satisfy this requirements. Such a monolayer will be also formed by covering with the organic liquid the water phase previously spread by the PVA-PS copolymer. This type of orientation is thought to be similar to that of graft and block copolymer molecules solubilizing and emulsifying the corresponding homopolymers[7] or low molecular weight liquids[3-5] in multicomponent systems.

REFERENCES

1. G. Molau ed., Colloidal and Morphological Behavior of Block and Graft Copolymers, Plenum Press, New York, 1971.
2. G. E. Molau, J. Polymer Sci., A, 3, 1267, 4235 (1965).
3. G. Riess, J. Kohler, C. Tournut, and A. Banderet, Makromol. Chem., 101, 58 (1967).
4. A. Banderet, C. Tournut and G. Riess, J. Polymer Sci., C, 16, 2601 (1967).
5. J. Kohler, G. Riess, and A. Banderet, European Polymer J., 4, 173 (1967).
6. Y. Ikada, F. Horii, and I. Sakurada, J. Polymer Sci., Polym. Chem. Ed., 11, 27 (1973).
7. F. Horii, Y. Ikada, and I. Sakurada, J. Polymer Sci., Polym. Chem. Ed., 11, 41 (1973).
8. T. C. Kendrick, B. M. Kingston, N. C. Lloyd, and M. J. Owen, J. Colloid Interface Sci., 24, 135 (1967).
9. G. Gabrielli and M. Puggelli, J. Colloid Interface Sci., 32, 657 (1970).
10. A. G. Kanellopoulos and M. J. Owen, J. Colloid Interface Sci., 35, 120 (1971).
11. J. L. Zatz and B. Knowles, J. Colloid Interface Sci., 40, 475 (1972).
12. A. Takahashi, T. Nobe, T. Kato, Y. Yamashita, and S. Ito, Polymer Preprints, Japan, 24, No.3, 327 (1975).

13. Y. Ikada, F. Horii, Y. Nishizaki, T. Kawahara, and H. Uehara, Macromolecules, 8, 276 (1975).
14. Y. Ikada, Y. Nishizaki, and I. Sakurada, J. Polymer Sci., Polym. Chem. Ed., 12, 1829 (1974).
15. Y. Ikada, K. Maejima, and H. Iwata, Makromol. Chem., 179, 865 (1978).
16. Y. Ikada, Adv. Polymer Sci., 29, 47 (1978).
17. M. Hatada, M. Nishi, and K. Hirota, JAERI Report 5028, 1 (1973).
18. H. E. Ries, Jr., and D. C. Walker, J. Colloid Sci., 16, 361 (1961).
19. D. J. Crisp, J. Colloid Sci., 1, 49 (1946).
20. J. Parker and J. L. Shereshefsky, J. Phys. Chem., 58, 850 (1954).
21. S. Wu and J. R. Huntsberger, J. Colloid Interface Sci., 29, 138 (1969).
22. M. J. Schick, J. Polymer Sci., 25, 465 (1957).
23. M. J. Richardson, Proc. Roy. Soc. A, 279, 50 (1964).
24. L. G. Augenstine and B. R. Ray, J. Phys. Chem., 61, 1380 (1957).

CHAPTER 10.

Grafting of Proteins onto Polymer Surfaces with the Use of Oxidized Starch

INTRODUCTION

This chapter describes the grafting of proteins to polymeric surfaces on which aldehyde groups have been introduced prior to the protein grafting.

To this end, dialdehyde starch (DAS), which is an oxidized starch having pendant aldehyde groups[1], is used as a coupling agent between the polymeric support and the protein. The supports chosen in this study are a crosslinked poly(vinyl alcohol)(PVA*) hydrogel membrane and an ethylene-vinyl alcohol copolymer(EVA) film. Both are insoluble in water. As they contain hydroxyl groups, the DAS molecules are expected to be grafted onto the polymeric substrates through acetalization between the aldehyde and the hydroxyl groups. The reaction scheme may be represented as:

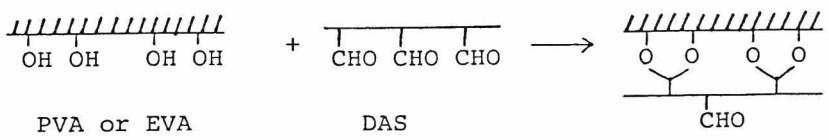

PVA or EVA DAS (1)

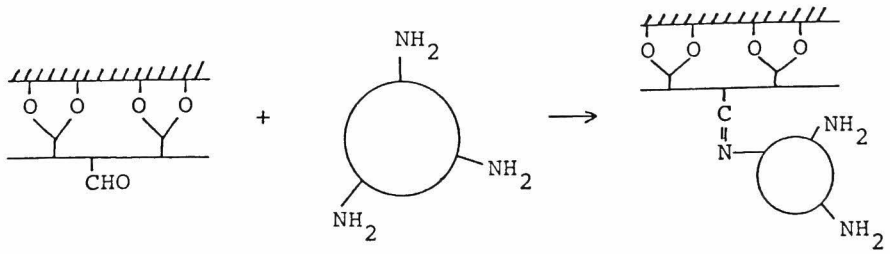

(2)

If necessary, the Schiff's base is reduced so as to be stable against hydrolysis.

EXPERIMENTAL

Grafting of DAS

DAS's with two different degrees of oxidation, 45% and 83%, were donated by The Japan Carlit Co., Ltd, Shibukawa, Gunma Pref , Japan, (DAS-45 and DAS-83). Unless otherwise specified, the oxidized starch used in this work is DAS-83 with a molecular weight of 1.1×10^4. The PVA hydrogel was prepared by radiation crosslinking of a water-swollen PVA film followed by treatment in boiling water to destroy the crystallite. Details are described by Ikada et al[2]. The EVA film, donated by Kuraray Cc., Ltd., Kita-ku, Osaka, Japan, has a composition of 67 mol% vinyl alcohol and 33 mol% ethylene unit with a thickness of 25 μm. The grafting was conducted at 50°C mostly for 4 hr in aqueous media containing 5.0 g/dl DAS and 1 N HCl as a catalyst. The graft product was washed with water and stored in water at room temperature.

Grafting of Glycolchitosan onto DAS-Grafted Polymers

Glycolchitosan(GC) for colloidal titration was purchased from Wako Pure Chemical Inductries, Ltd., Higashi-ku,Osaka, Japan, and was used without purification. The molecular

weight was over 8×10^4. The grafting was performed at 20°C for 1 hr in neutral aqueous solution of GC at 2.0 g/dl.

Grafting of Proteins onto DAS-Grafted EVA Film

The proteins chosen for the grafting were bovine serum albumin(BSA)(Povite, pure cryst.), bovine fibrinogen(Povite), Bacillus subtilis α-amylase (Type II-A Bacterial, Sigma, 4 times crystallized) and a commercial gelatin. To effect the grafting, the DAS-grafted EVA films were stirred at 30°C in aqueous solutions of each protein as follows: BSA in pure water, fibrinogen in 0.26 M NaCl, α-amylase in 0.01 M calcium acetate (buffered solution at pH 6.5), and gelatin in 0.05 M NaOH. After the grafting reaction, the films were placed in 0.013 M $NaBH_4$ at room temperature for 1 hr to reduce the residual aldehyde groups of DAS and the Schiff's bases formed. (Proteins seem not to undergo any reduction at such a low $NaBH_4$ concentration). The grafted films were stored in each solution after removal of ungrafted proteins. The amount of protein grafted was determined according to the ninhydrin method of Moore and Stein[3] after hydrolysis in 2.5 N NaOH at 100°C for 2 hr .

Measurement of Contact Angles

Contact angles of grafted films against water were measured at room temperature by the sessile drop method after washing the films. More than 5 measurements on different strips from

the same film were averaged. The deviation of each reading from the average was within ±1°. We assumed no leaching from the film any contaminants which, otherwise, would change the water contact angle.

Activity Measurement of Amylase

The enzymatic activity of grafted amylase was determined using amylose(from potato, molecular weight=$2x10^5$) and a water soluble starch(Merck) as the substrate carbohydrate. The enzyme reaction was allowed to proceed at 30°C in 0.12 M sodium acetate buffer solutions containing 2.5 mM calcium acetate followed by addition of acetic acid to stop the reaction.(When we wished to determine the reducing endgroup of the hydrolyzed amylose, the reaction was stopped by adding the Somogyi reagent.) The hydrolysis of amylose and starch was followed either by determining absorbance at 680 nm of the substrate solution to which N/3000 I_2 was added or by determining the reducing endgroups by the Somogyi[4]-Nelson[5] method. The blue value was calculated according to the definition as $(A_t/A_0)x100$, where A_0 and A_t are absorbances at the hydrolysis time of zero and t, respectively. When a procedure was used to evaluate the cyclic reactivity of the amylase, each cycle was allowed to proceed till the blue value decreased to zero.

RESULTS AND DISCUSSION

Grafting of DAS

As mentioned above, DAS is a water-soluble polymer with a large number of pendant aldehyde groups. DAS-83 may contain 110

aldehyde groups on the average in one molecule, as its number-average molecular weight is 1.1×10^4 and 83% of the α-glycols in the starting starch are oxidized with periodate.

Table I gives the results of grafting of DAS onto the crosslinked PVA hydrogel. It is seen that the grafting of DAS reduces the contact angle and brings about a slight weight increase, suggesting that grafting takes place not only on the gel surface but also in the interior of the hydrogel. This is also supported by the significant increase in the water fraction and in the size of the gel observed on addition of $NaHSO_3$ to the DAS-grafted hydrogels. Since the addition converts the aldehyde into an ionic form ($-CH(OH)-SO_3^- Na^+$), the contact angle is further decreased as given in Table I.

TABLE I

GRAFTING OF DAS ONTO PVA HYDROGEL

		NON-GRAFTED	DAS	DAS-$NaHSO_3$
DAS-45	WATER FRACTION [A]	0.678	0.696	0.740
	WT. INCREASE, %	—	4.4	5.9
	SURFACE INCREASE, %	—	-0.1	12.4
	CONTACT ANGLE, DEG.	40.5	30.1	17.0
DAS-83	WATER FRACTION [A]	0.678	0.695	0.744
	WT. INCREASE, %	—	6.4	9.4
	SURFACE INCREASE, %	—	-0.1	15.3
	CONTACT ANGLE, DEG.	40.5	30.4	8.1

A) Wt. fraction of water in water-swollen gels.

In contrast to the PVA hydrogel, the EVA film does not exhibit any detectable weight increase upon grafting of DAS. As is illustrated in Fig. 1, no distinct difference in attenuated total reflection (ATR) infrared spectra is observed between the non-grafted and the DAS-grafted EVA film. However, the water contact angle was markedly decreased on grafting of DAS. Figure 2 gives the change of contact angle with the reaction time. These findings strongly indicate that the grafting of DAS may be restricted to the surface of EVA films. It seems probable that the DAS molecules are not able to penetrate into the interior of EVA films, because the equilibrated water fraction of the water-swollen film is as low as 0.08 and the molecular weight of DAS is on the order of 10^4.

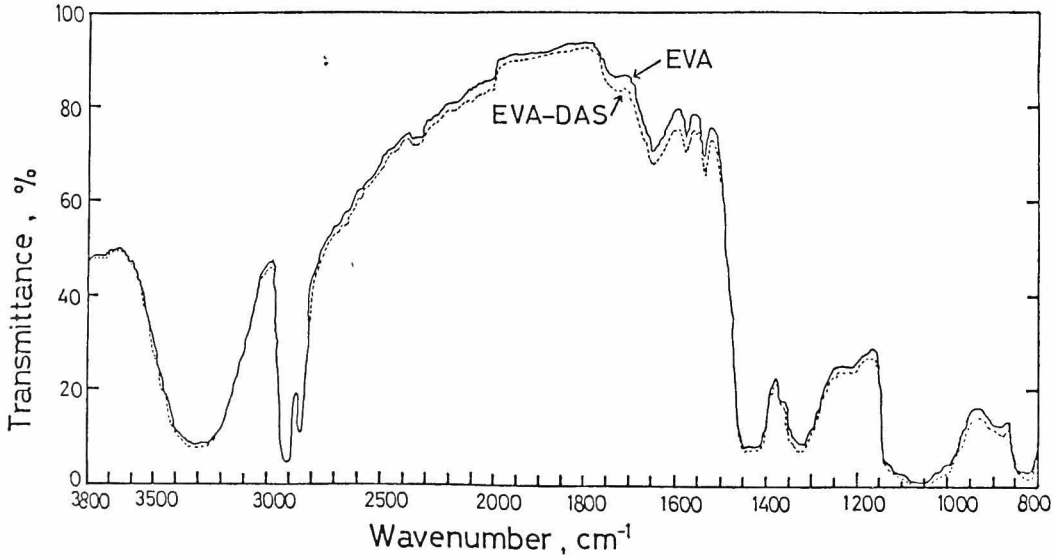

Figure 1 ATR infrared spectra of the starting EVA film and its DAS-grafted film (EVA-DAS).

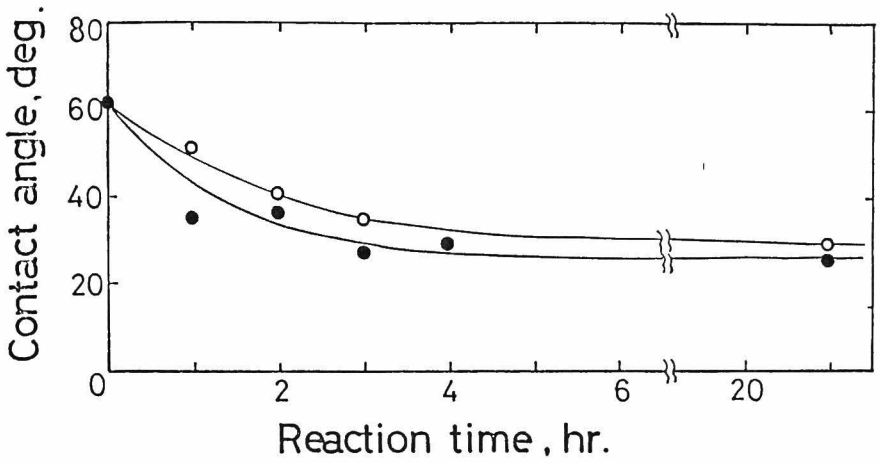

Figure 2 Change of contact angles of EVA films by acetalization with DAS ($[DAS]_0$=5.0 g/dl, [HCl]=1 N 50°C): (o) DAS-45; (●) DAS-83.

A further experiment was carried out to provide evidence for the presence of free aldehyde groups on the grafted DAS molecules. As is expected from eq. (2), the polymer possessing amino groups may be effectively coupled to the DAS-grafted surface, so far as some of the aldehyde groups remain without participating in the acetalization with the support polymer. To this end we attempted to graft GC onto the DAS-grafted substrates. GC is poly(hydroxyethylglucosamine) and is soluble in water over a wide range of pH. Figure 3 gives an X-ray photoelectron (ESCA) spectrum for the EVA film first grafted with DAS followed by grafting with GC. Clearly a peak appears at the binding energy characteristic to the nitrogen atom, which confirms the grafting of GC. If a part of the amino groups of GC remain unreacted, adhesion

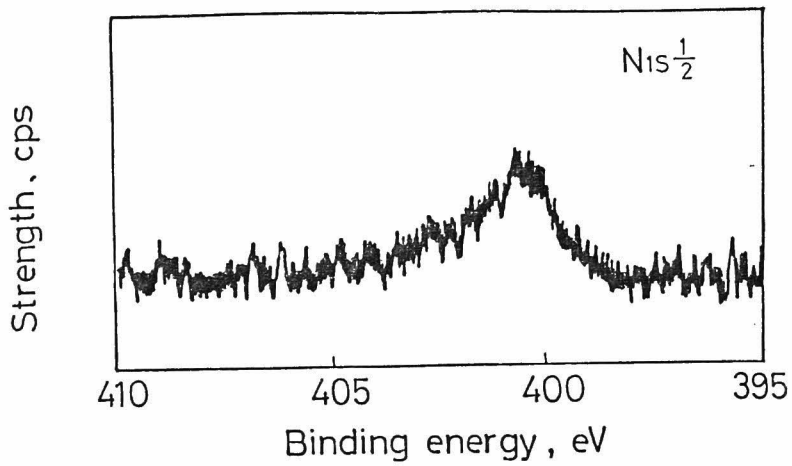

Figure 3 X-ray photoelectron spectrum of DAS-grafted EVA film grafted further with glycolchitosan.

between the DAS-grafted and the GC-grafted materials should take place through Schiff's base formation without any adhesives, when they are allowed to come into contact in the presence of water. Thus the bonding of the DAS-grafted with the GC-grafted surfaces was effected by pressing them in the presence of water under a force of 50 g/cm^2 for 0.5 hr. After drying the bonded materials were adhered to a plastic support with a cyanoacrylate adhesive to make possible the measurement of the tensile strength with Tensilon UTMII. The tensile strength of bonding is given in Table II. It is seen that the bond strength between the two surfaces is fairly high.

TABLE II

BOND STRENGTH OF ADHESION OF DAS-GRAFTED PVA AND EVA FILMS I WITH GLYCOLCHITOSAN(GC)-GRAFTED FILMS II

FILM I		CROSSLINKED PVA		EVA	
		DAS-45	DAS-83	DAS-45	DAS-83
FILM II	GC	12	12	8.0	8.8
	GC·HCL	0	0	0	0

STRENGTH (KG/CM^2)

However, it becomes virtually zero when prior to contact the GC-grafted surface is immersed in a dilute aqueous solution of HCl to convert the amino groups into the ammonium chloride form. In the case of PVA hydrogel the rupture did not occur between the two surfaces, but between the plastic support and the adhesive layer constructed for attaching the specimen to the Tensilon machine. We can say that the bonding of the DAS-grafted film to the GC-grafted film is one example of adhesion without adhesives.

Grafting of Proteins

The EVA film was utilized throughout for the grafting of proteins and the DAS-grafted films were obtained by grafting of DAS-83. As proteins having many NH_2 groups have been reported to react with DAS to form water-insoluble, crosslinked gels[6] and to react with polysaccharides oxidized with periodate[7], it was expected that the grafting of proteins onto the DAS-grafted film would also take place readily.

a) BSA

Fig. 4 shows the amount of BSA grafted onto the DAS-grafted EVA films, expressed in μg per unit area of film, which is assumed to be entirely flat. The reaction was conducted in both the absence and the presence of NaCl(0.1 M). It is clearly seen that in the absence of NaCl, BSA can be grafted to the film even at low concentrations such as 0.1 mg/ml, the grafting being complete within about 5 hrs. The adsorption to polymeric materials like poly-2-hydroxyethyl methacrylate from aqueous solutions is reported to reach an equilibrium in a similar time [8]. It is interesting to note that the grafting of BSA is strongly inhibited by the presence of NaCl. This may be intimately related to the fact that BSA has a tendency to adsorb various ions including Cl^- [9].

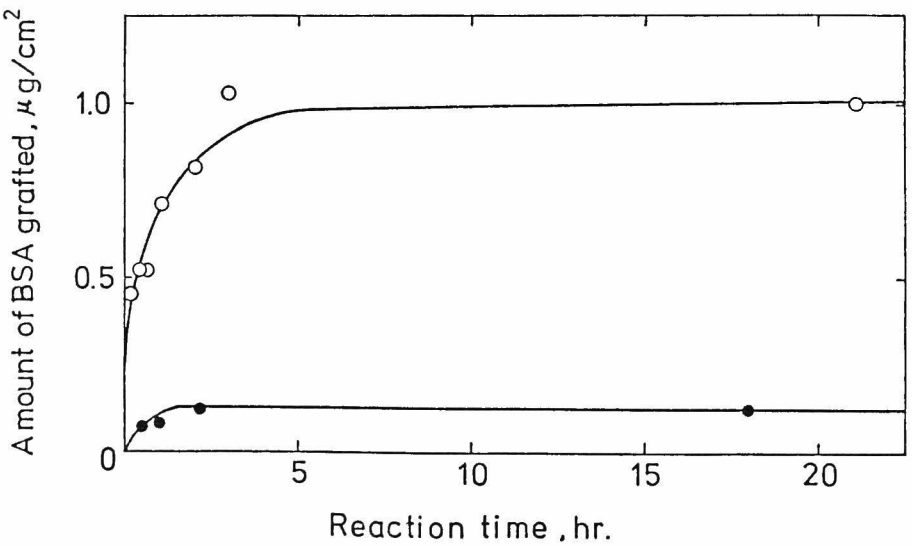

Figure 4 Grafting of bovine serum albumin (BSA) onto DAS-grafted EVA film surfaces (30°C): (o) in the absence of NaCl, $[BSA]_0$=1 mg/ml; (•) in the presence of 0.1 M NaCl, $[BSA]_0$=5 mg/ml.

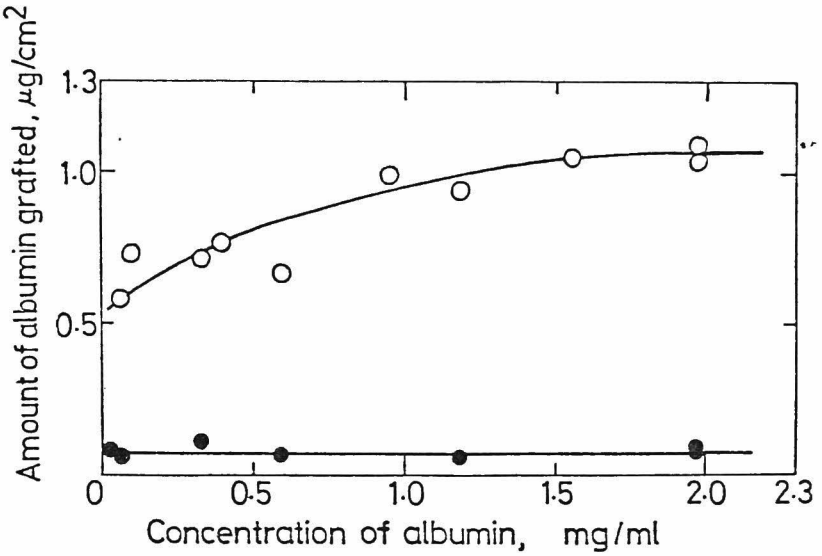

Figure 5 Grafting of bovine serum albumin (BSA) onto DAS-grafted EVA film surfaces (30°C, 43 hr): (o) CHO is not reduced; (•) CHO is reduced to CH_2OH.

The influence of BSA concentration is shown in Fig. 5 for grafting reactions carried out at 30°C for 43 hrs. It is apparent that the amount of BSA grafted is 0.5 μg per cm^2 of film at low BSA concentrations, increases gradually, and reaches a limit of about 1.1 μg/cm^2 at a BSA concentration near 2 mg/ml. Fig. 5 also shows the results of grafting onto the DAS-grafted film which had been submitted to reduction with $NaBH_4$ prior to the grafting of BSA. In this case the extent of grafting is insignificant, suggesting that the grafting of BSA onto the non-reduced, DAS-grafted film takes place as a result of the formation of Schiff's base. The adsorbability of other proteins to surface-

modified materials such as the DAS-grafted film pre-reacted with $NaBH_4$ is currently being studied in more detail.

These albumin-grafted materials are expected to exhibit good blood-compatibility [10]. Application of this albumin-grafted PVA as a biomedical material is in progress.

b) α-amylase and other proteins

Figure 6 demonstrates the results of grafting with fibrinogen, α-amylase, and gelatin carried out in 0.26 M NaCl, 0.01 M calcium acetate, and 0.05 M NaOH, respectively. NaCl was added to make fibrinogen soluble in water and calcium acetate to stabilize α-amylase in solution. As

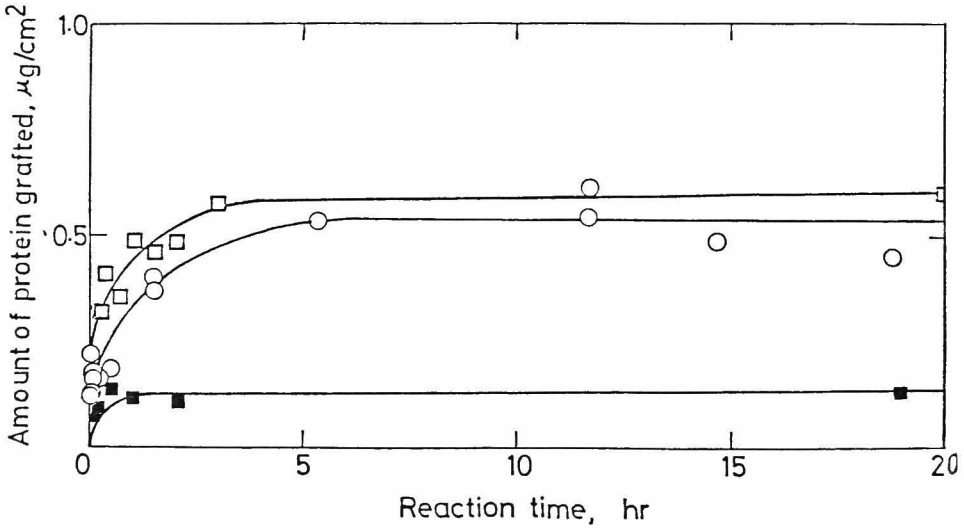

Figure 6 Grafting of various proteins onto DAS-grafted EVA film surfaces (30°C): (□) fibrinogen, 6.7 mg/ml, 0.26 M NaCl, (○) amylase, 0.2 mg/ml, 0.01 M $Ca(OAc)_2$, (■) gelatin, 5 mg/ml, 0.05 M NaOH.

gelatin reacts with DAS more readily in alkaline than in neutral solutions, the grafting of gelatin was effected in the presence of NaOH. As is seen in Fig. 6, gelatin is less reactive than fibrinogen and α-amylase. This is probably because a gelatin molecule in a random coil state occupies a much larger volume in solution than the native proteins do and hence has a low segment density. In the grafting of α-amylase and fibrinogen, which are globular proteins, the degree of grafting reaches an upper limit after about 5 hrs, similar to the grafting of BSA.

Shape and Activity of Grafted Proteins

As mentioned above, one of the most important things to be considered in the grafting of biologically active polymers is the change in their activities which might be brought about by grafting. For instance, partial denaturation of the protein would take place during the grafting reaction.

a) Surface area occupied by a grafted protein molecule

Based on the determination of the surface area occupied by a grafted protein molecule, we can obtain some information on the possibility of random coil-helix transition of globular proteins during the grafting. Table III gives the observed and calculated areas occupied by one grafted protein molecule.

TABLE III

CONTACT ANGLES(θ) AND DIMENSIONS OF GLOBULAR PROTEIN LAYERS GRAFTED ONTO DAS-GRAFTED EVA FILM SURFACES

	θ, DEG	MOLECULAR WEIGHT	LENGTH (Å)[14] / DIAMETER (Å)	AVERAGE AREA PER MOLECULE, Å^2	
				CALC.[14]	OBS.
BOVINE SERUM ALBUMIN	64.8	69000	115/40	1700[A], 4600[B]	1100 (1 MG/ML) 1500 (0.1 MG/ML)
BOVINE FIBRINOGEN	55.6	340000	475/65	4200[A], 30000[B]	9400
α-AMYLASE	37.5	48000	——	——	1500

A) END-ON COVERAGE.

B) SIDE-ON COVERAGE.

The observed value is based on the amount of protein grafted to saturation and on the assumption that the grafted molecules cover the film surface as a monomolecular layer. On the other hand, the calculated area is based on the molecular sizes of native BSA and fibrinogen as reported by Lyman et al.[11] Substantial agreement of the observed with the calculated area suggests that these proteins do not undergo any significant conformational change. As there are many possible alternations in the protein shape which do not involve complete denaturation, one cannot derive any definitive conclusion from the geometrical consideration. But it appears that the proteins are probably grafted to the film in a native state, since it is reported that the BSA molecule remains undenatured, when physically adsorbed on some polymeric surfaces[12].

As is shown in Table III, the contact angles of protein-grafted films are larger than that of the starting, DAS-grafted film (30°) except for the grafting of amylase. It is noteworthy that the BSA-grafted film exhibits a relatively high contact angle, suggesting that the film becomes more hydrophobic as a consequence of grafting of BSA. This hydrophobicity may be attributed to the hydrophobic regions that the BSA molecule is reported to have on its surface[13]. The contact angle of BSA-grafted films decreases when they are treated with a strong denaturating reagent such as guanidine hydrochloride or β-mercaptoethanol. This result is shown in Table IV. This finding also implies that BSA does not undergo any significant denaturation during grafting.

TABLE IV

CHANGE OF CONTACT ANGLES(θ) OF BSA-GRAFTED FILMS BY DENATURATION WITH GUANIDINE HYDROCHLORIDE (GU·HCL)[A] AND WITH GU·HCL AND β-MERCAPTOETHANOL (β-ME) MIXTURE[A]

	WATER	6 M GU·HCL	6 M GU·HCL + 0.1 M β-ME
$[\eta]$[B], ML/G	3.7	22.9	52.2
θ, DEG	64.8	51.9	49.6 (51[C])

A) REACTED AT 25°C FOR 13 HRS.

B) TANFORD ET AL., J. AMER. CHEM. SOC., 89, 729 (1967).

C) CONTACT ANGLE OF GELATIN-GRAFTED FILM.

b) Enzyme activity of grafted α-amylase

The change in protein properties caused by grafting can be also studied by determining the activity when an enzyme is used for the grafting. Figures 7 and 8 show the enzyme activity measured using amylose as a substrate. From Fig. 7, where number-average degrees of polymerization $\bar{P}_n$ of amylose are plotted against the enzymatic hydrolysis time, it is seen that the number of scissions of glucoside linkages is proportional to the time, with a clear indication of random scission. In Fig. 8 the blue value change is plotted against time, when the enzyme-grafted film is repeatedly used for the hydrolysis of amylose. As is seen, a noticeable decrease in the enzymatic

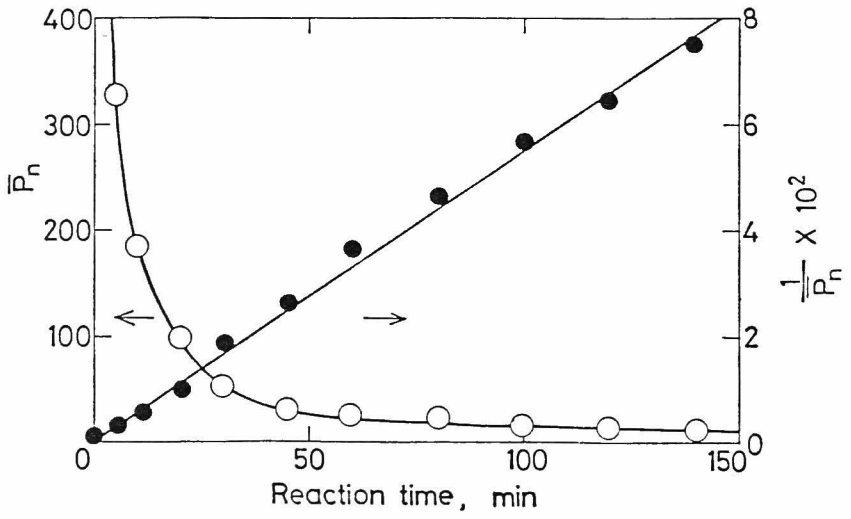

Figure 7 Change of $\bar{P}_n$ during hydrolysis of amylose by grafted α-amylase (38.5 μg/100 cm^2 film) ($[amylose]_0$=1 mg/ml, 40 ml, pH 6.9, 30°C).

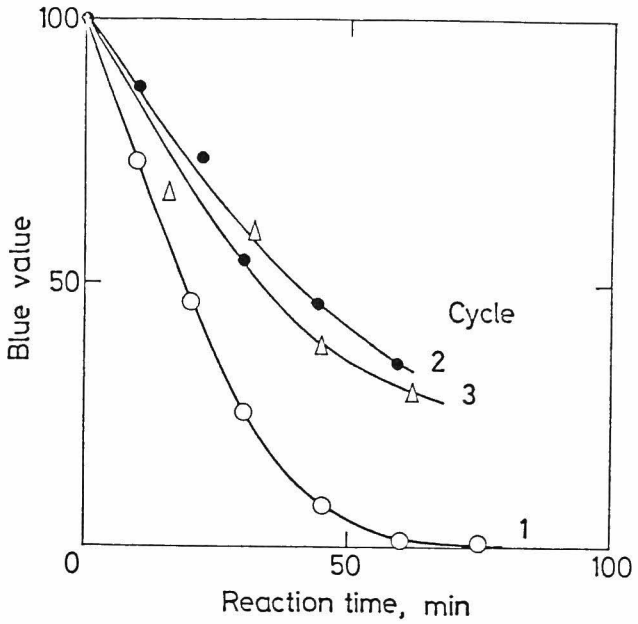

Figure 8 Effect of cycles on hydrolysis of amylose by grafted α-amylase (38.5 μg/100 cm^2 film) ($[amylose]_0$=1 mg/ml, 6 ml, pH 6.5, 30°C).

activity of amylase-grafted films is observed after the first cycle, while the decrease of activity becomes insignificant after the second cycle. This means that the film has active α-amylase molecules fixed on the surface, though the activity is unexpectedly low compared with that of the free amylase. As is shown in Fig. 9, the ratio of activity of grafted amylase to that of free amylase, relative activity, is estimated to be only 0.005. The relative activity is 0.01 when a soluble starch is used as a substrate in the enzyme reaction. The lower activity of amylase is not surprising if the kinetics of immobilized enzymes are considered[14]. It is, however, not clear to us at present, whether this low

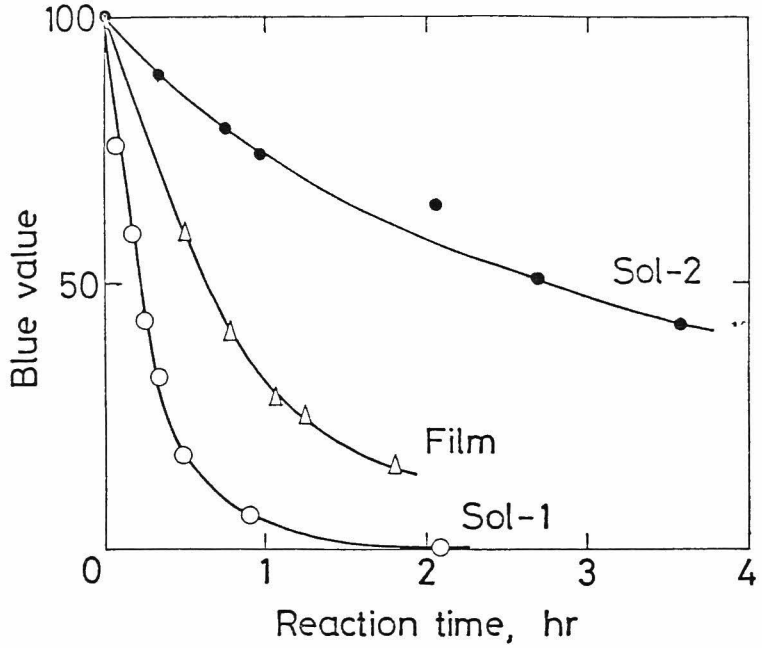

Figure 9 Hydrolysis of amylose (1 mg/ml) by α-amylase in soluble and grafted form (6 ml, pH 6.5, 30°C). Amount of enzyme added: 0.3 μg (Sol-1) and 0.03 μg (Sol-2) in soluble form, 18 μg (100 cm^2 film) in grafted form.

relative activity may be due to the high molecular weight of the substrates which hinders complex formation with the grafted enzyme molecules or to a drastic conformational change caused by the grafting reaction. Perhaps both must be taken into account. The low contact angle of water on the amylase-grafted film, shown in Table III, seems to indicate some denaturation of amylase during the grafting.

At least, however, we can say that this decrease in the relative activity is not caused by a change of the mode of enzymatic reaction. This is ascertained by the following

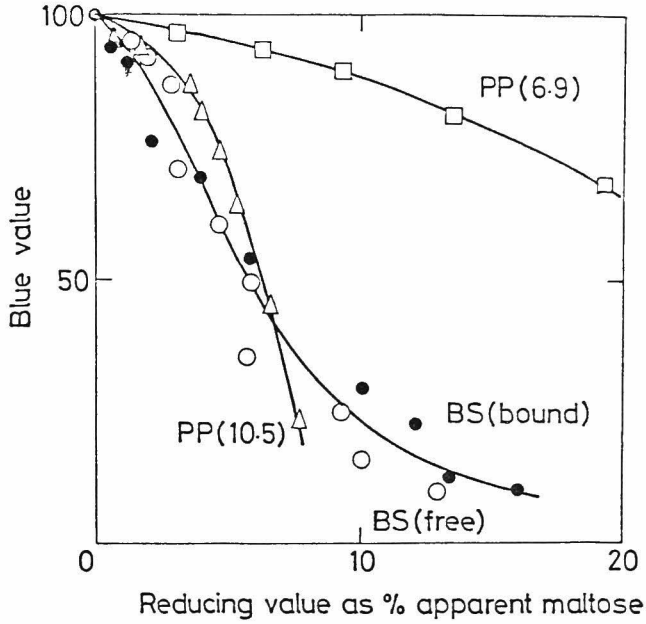

Figure 10 Comparison of the drop in blue value with the increase in reducing value for the hydrolysis of amylose by various α-amylases. (o) BS (soluble), Bacillus subtilis α-amylase in soluble form at pH 6.9, 2.5 mM Ca^{++}, and 30°C; (●) BS (grafted), Bacillus subtilis α-amylase in grafted form at pH 6.9, 2.5 mM Ca^{++}, and 30°C; (□) PP (pH 6.9), porcine pancreatic α-amylase at pH 6.9, 10 mM Cl^{-}, and 40°C; (△) PP (pH 10.5) porcine pancreatic α-amylase at pH 10.5, 10 mM Cl^{-}, and 40°C.

experiment. As French and his co-workers have demonstrated on the basis of blue values and the determination of reducing endgroups and oligosaccharides formed, the glycoside linkages in an amylose chain may be hydrolyzed either at random or in a zipper-like manner, depending on the type of α-amylase and the hydrolysis condition[15]. Figure 10 shows the result of

analyses performed according to the method of French and his co-workers. Comparison of the present work with French's, which is also given in Fig. 10, reveals that in the present case both the grafted and the free α-amylases hydrolyze the amylose chains at random. Thus it is clear that surface grafting does not alter the reaction mode of this α-amylase.

REFERENCES

1. C. L. Mehltretter, "Starch:Chemistry and Technology", R. L. Whistler and E. F. Paschall eds., Academic Press, New York and London, 1965, Vol. II, p.433.
2. Y. Ikada, T. Mita, F. Horii, I. Sakurada, and M. Hatada, Radiat. Phys. Chem., 9, 633 (1977).
3. S. Moore and W. H. Stein, J. Biol. Chem., 211, 907 (1954).
4. M. Somogyi, J. Biol. Chem., 195, 19 (1952).
5. N. Nelson, J. Biol. Chem., 153, 375 (1944).
6. F. B. Weakley and C. L. Mehltretter, Biotechnol. Bioeng., 15, 1189 (1973).
7. G. P. Royer, F. A. Liberatore, G. M. Green, W. E. Schwartz, and W. E. Meyers, Polymer Preprints, 16, No.2, 76 (1975).
8. T. A. Horbett and A. S. Hoffman, ACS Adv. in Chemistry, No. 145, 230 (1975).
9. G. Scatchard, J. S. Coleman, and A. L. Shen, J. Amer. Chem. Soc., 79, 12 (1957).
10. E. W. Salzman, J. Linden, and D. Brier, Ann. New York Acad. Sci., 283, 114 (1977).
11. J. L Brash and D. J. Lyman, J. Biomed. Mater. Res., 3, 175 (1969).
12. B. W. Morrissey and R. R. Stronberg, J. Colloid Interface Sci., 46, 152 (1974).

13. O. Laurie and J. Oakes, J. Chem. Soc. Faraday I, 72, 1324 (1976).

14. L. Goldstein, Methods in Enzymology, 44, 397 (1976).

15. J. F. Robyt and D. French, Arch. Biochem. Biophys., 122, 8 (1967).

SUMMARY

CHAPTER 1

The radical polymerization of vinyl monomers was carried out in the presence of reactive chain transfer agents possessing functional groups and the weight fractions of the resultant polymers bearing functional groups from the transfer agents were determined with a thin layer chromatographyic method. The monomer-chain transfer agent combination chosen in the present work is styrene-trichloroacetyl chloride and methyl methacrylate-2-aminoethanethiol hydrochloride. The chain transfer polymerizations were expected to produce polystyrene with an acyl chloride endgroup and poly(methyl methacrylate) with an amino endgroup in a high yield. The endgroup content of resultant polymers determined by the thin layer chromatography was in both cases in good agreement with that predicted from the polymerization kinetics, suggesting that the thin layer chromatography can be effectively applied to the endgroup determination.

CHAPTER 2

Radiation-induced radical polymerizations of styrene and vinyl acetate(VAc) were performed in the presence of additives to yield polymers possessing terminal functional groups. When either acetyl chloride(AC) or trichloroacetyl chloride(TCAc) was added to styrene, we could obtain

polystyrene carrying COCl end-groups. The attachment of the functional end-group can be explained on terms of energy transfer and radical chain transfer for the addition of AC and TCAC, respectively. Since the radical chain transfer to AC does not practically take place, it appears that any catalytic polymerization of styrene in the presence of AC cannot give polymer with such a COCl end-group. Radiation polymerization of VAc containing CCl_4 gave rise to formation of PVAc with one Cl group on one chain-end and one CCl_3 group on the other end. Hydrolysis of this PVAc resulted in formation of poly(vinyl alcohol) carrying one terminal CHO group. comparison of the observed and the theoretical rates of polymerization gave in all cases a satosfactory agreement.

CHAPTER 3

Poly(vinyl alcohol) (PVA) was oxidized by ceric ion Ce(IV) in aqueous HNO_3 medium at different temperatures and found to be degraded as a consequence of selective cleavage of the 1,2-glycol unit existing in PVA. The rate of oxidation increased with increasing temperature. The aldehyde groups formed at the ends of the degraded polymer upon oxidation, were relatively stable at 0°C. With rise of temperature, the aldehyde groups either reacted with excess of Ce(IV) to carboxylic acids, or with hydroxyl groups of PVA molecules to give acetal linkage. When the

acetalization predominated over the oxidation to carboxyl group, gelation of the reaction mixture was observed. Based on these results, a plausible mechanism of oxidation of PVA with Ce(IV) and the suitable condition to introduce the aldehyde groups or the calboxyl groups at the both ends of PVA is discussed.

CHAPTER 4

The contribution of the long-range interaction of polymer chains is theoretically evaluated on the intermolecular polymeric reaction where the rate-determining step is not a diffusion-controlled but chemical process. The derivation of rate constant is attempted for the reaction between a reactive group linked to the ℓ_1th segment of polymer 1 and the other partner reactive group linked to the m_2th segment of polymer 2 and for the reaction between polymers 1 and 2 carrying respectively a randomly distributed reactive group. In the latter case it is shown that the rate constant is closely related to the second virial coefficient. After formation of the bonding between polymers 1 and 2, the second reaction is assumed to take place between the remaining reactive groups A and B within the two linked chains. The apparent second-order rate constant of this reaction is predicted to increase with the decreasing concentration of the reactive groups.

CHAPTER 5

Inter- and intramolecular acetalizations of poly(vinyl alcohol)(PVA) carrying one or two terminal aldehyde groups were carried out in aqueous solutions as well as in dimethylsulfoxide(DMSO) solutions over a wide range of the polymer concentration. The observed rate constant for intermolecular acetalization was in both the solutions independent of the polymer concentration and not significantly different from that for the acetalization of a conventional PVA with aldol, a homologous low-molecular-weight aldehyde. The results strongly suggest that the polymer coils interpenetrate rather freely with each other in concentrated solutions even of DMSO which is a good solvent of PVA (water is almost a Θ solvent of PVA). This finding is in agreement with the theory predicting that the excluded volume effect may not be large enough to be detectable under the experimental conditions of this study. In addition, the observed OH concentration effective for the intramolecular acetalization was compatible with that predicted by the statistics of polymer chains.

CHAPTER 6

Acetalization of poly(vinyl alcohol)(PVA) carrying mostly two terminal aldehyde groups was studied in acidic aqueous solution at different PVA concentrations. The transition from sol to gel or vice versa took place at the temperature,

where an equilibrium was reached between acetalization and deacetalization. Using known rate constants for intra- and intermolecular acetalization as well as that for deacetalization, we could evaluate the extent of reaction at the sol-gel transition temperature, i. e., at the gel point. Comparison of the observed with the theoretical extent of reaction at the gel point revealed that contribution of intramolecular acetalization to the overall reaction was too large to be neglected. It was concluded that two types of intramolecular crosslinkings, both ineffective for gelation, were operative, the one producing a small ring and the other a large ring.

CHAPTER 7

ABSTRACT: A condensation coupling through acetalization is performed between hydroxyl groups on poly(vinyl alcohol)(PVA) and an aldehyde group attached to the chain end of poly(vinyl acetate)(PVAc) to produce PVA-VAc graft copolymers. The aldehyde-terminated PVAc is prepared by polymerization of VAc with monochloroacetaldehyde or monochloroacetaldehyde diethylacetal as chain transfer agent. The coupling reaction of PVAc with crosslinked porous beads of PVA, followed by extraction of ungrafted PVAc permits us to estimate the fraction of PVAc carrying the terminal aldehyde group. The observed fractions range from 0.1 to 0.5. In addition to the heterogeneous grafting onto the crosslinked beads and membrane, PVAc is grafted onto a linear PVA in dimethyl

sulfoxide(Me_2SO) which is a common solvent for both the polymers. Based on the weights of the isolated graft copolymer and of two homopolymers the number of branches in the graft copolymer is evaluated; for instance, 18 branches of PVAc with $\bar{P}_n$ of 53 are found to be coupled to the PVA backbone with $\bar{P}_n$ of 1340.

CHAPTER 8

Polystyrene (PS) and Poly(vinyl acetate) (PVAc), both carrying one terminal acyl chloride group, were synthesized by radiation-polymerization in the presence of trichloroacetyl chloride, a chain transfer agent, and the acyl chloride groups of PVAc were converted to amino groups by reacting with excess ethylene diamine. Partial acetalization of poly(vinyl alcohol) with aminoacetaldehyde followed by acetylation of hydroxyl groups in the polymer yielded PVAc having a number of pendant amino groups distributed along the main chain.

Condensation coupling reactions between the acyl chloride and amino groups were carried out in chloroform at room temperature to yield PS-PVAc diblock copolymers and PVAc-styrene graft copolymers with many branches of PS. The pure copolymers were isolated from the reaction products by extraction and then characterized by determining chemical compositions and number-average molecular weights.

CHAPTER 9

Surface pressure-area isotherms for monolayers from graft copolymers with one branch (or four) and diblock copolymers were determined at air/aqueous medium interfaces. The dependence of pressures on the area for poly(vinyl acetate) (PVAc)-polystyrene(PS) graft and block copolymers was identical to that of pure PVAc at the large areas, while a sharp increase in pressure appeared with further compression. The surface pressure of PVAc-PS graft copolymer at air/0.2 N NaOH interface decreased with time, but the critical area at which the surface pressure increased rapidly remained constant, regardless of hydrolysis time. When a poly(vinyl alcohol)(PVA)-PS graft or block copolymer was spread over water, the surface pressure originating from the PVA chain was too small to be observed, and merely that of the PS sequence appeared. It was concluded that the PS sequence was always present in a form of tightly coiled sphere at the interfaces, whereas the PVAc sequence was spread as a monomolecular film on water but diffused into the alkaline substrate as a result of the hydrolysis to PVA. Thus the PVA-PS graft and block copolymers spread on water seem to have such an interesting molecular orientation that the PVA chain "dissolved" in water is supported at the interface by the compact, monomolecular particle of PS placing on water.

CHAPTER 10

A study has been carried out on the coupling of proteins onto crosslinked poly(vinyl alcohol) hydrogel membranes and ethylene-vinyl alcohol copolymer(EVA) films previously grafted with oxidized starches having many pendant aldehyde groups. The coupling reaction of proteins is based on the Schiff's base formation between the amino groups of proteins and the aldehyde groups of the oxidized starches which have been grafted onto the substrate membrane or film through acetalization of the aldehyde of starch with hydroxyl groups of the substrate polymers.

The grafting of oxidized starches onto the EVA films seems to be restricted to the film surface, since no detectable change is observed in the weight and the attenuated total reflection infrared spectrum of the grafted films. The amount of grafted protein, determined by the ninhydrin method, reveals that, at least, plasma proteins such as serum albumin and fibrinogen are grafted to the film surface in a monomolecular layer without undergoing a marked denaturation. The α-amylase grafted onto the EVA film showed a distinct enzymatic activity in hydrolysis of amylose and starch, but the activity was very low compared with that of the ungrafted, soluble α-amylase.

LIST OF PUBLICATIONS

CHAPTER 1. Macromolecules, 10, 1364 (1977).

CHAPTER 2. in preparation.

CHAPTER 3. J. Polym. Sci., Polym. Chem. Ed., 15, 451 (1977)

CHAPTER 4. Makromol. Chem., in press.

CHAPTER 5. Macromolecules, 12, 287 (1979)

CHAPTER 6. Bull. Inst. Chem. Res., Kyoto Univ., 57, 184 (1979)

CHAPTER 7. Macromolecules, in press.

CHAPTER 8. Makromol. Chem., 179, 865 (1978).

CHAPTER 9. J. Macromol. Sci.-Phys., in press.

CHAPTER 10. J. Biomed. Mater. Res., 13, 607 (1979)

ACKNOWLEDGEMENT

The present investigation was carried out in the Department of Polymer Chemistry, Faculty of Engineering and the Institute for Chemical Research, Kyoto University from 1973 to 1979.

The author would like to express his sincere gratitude to Professor Ryozo Kitamaru and Dr. Yoshito Ikada for their constant guidance and encouragement throughout the course of this study.

The author also wishes to express his thanks to Emeritus Professor Ichiro Sakurada for his benevolent interests and constant encouragement.

Thanks are much due to Mrs. Tomoe Mita, Mr. Satoshi Nagaoka, Mr. Kazuo Maejima, Mrs. Yasuko Horii and Dr, Fumitaka Horii for their kind collaboration during the course of this investigations.

The author likes to take the opportunity to extend his hearty thanks to other investigators in this laboratory for their kind help.